Available online at www.sciencedirect.com
SCIENCE DIRECT®
Journal of Chromatography A, 1060 (2004) 77–116
JOURNAL OF CHROMATOGRAPHY A
www.elsevier.com/locate/chroma

Review

The hydrophobic-subtraction model of reversed-phase column selectivity

L.R. Snyder[a,*], J.W. Dolan[b], P.W. Carr[c]

[a] *LC Resources, 26 Silverwood Ct., Orinda, CA 94563, USA*
[b] *BASi Northwest Laboratory, McMinnville, OR 97128, USA*
[c] *Department of Chemistry, University of Minnesota, Minneapolis, MN 55455, USA*

Abstract

A recently developed treatment of reversed-phase column selectivity (the hydrophobic-subtraction model) is reviewed and extended, including its characterization of the selectivity of different column types (e.g., C_1–C_{30}, cyano, phenyl, etc.). The application of this model to retention data for various solutes and columns has provided new insights into the nature of different solute–column interactions and their relative importance in affecting sample retention and separation. Reversed-phase columns can be characterized by five selectivity parameters (***H***, ***S****, ***A***, ***B*** and ***C***), values of which are summarized here for more than 300 different columns. The selection of columns of either equivalent or different selectivity is readily achievable on the basis of their values of ***H***, ***S****, etc. The development of the hydrophobic-subtraction model, its use in characterizing the selectivity of different reversed-phase liquid chromatography (RP-LC) columns, and its application to various practical problems as described here began in 1998. The original inspiration for this project owes much to Jack Kirkland, who also contributed actively to the initial studies that laid the foundation of this model; he has since provided other important support to this project. Jack and one of the authors (LRS) have enjoyed a strong professional relationship and personal friendship for the past 35 years, and it is the privilege of the authors to dedicate this paper and the work that it represents to Jack. His contributions to HPLC column technology have extended from the mid-1960s into the present century, and it is impossible to conceive of present day HPLC practice without Jack's contributions over the years. In this and other ways, his position as a pioneer and key implementer of HPLC is widely recognized. We wish Jack well in the years to come.

Keywords: Reviews; Retention models; Hydrophobic-subtraction model; Column selectivity

Contents

1. Introduction 78
2. Theory and experimental results 79
   2.1. The hydrophobic-subtraction model 79
   2.2. Analysis of non-hydrophobic solute–column interactions 80
      2.2.1. Cation exchange interactions and Eq. (2) (κ'***C*** term) 82
      2.2.2. Steric resistance and Eq. (2) (σ'***S**** term) 82
      2.2.3. Column hydrogen-bond basicity and Eq. (2) (α'***B*** term) 84
      2.2.4. Column hydrogen-bond acidity and Eq. (2) (β'***A*** term) 84
   2.3. Development and verification of the hydrophobic-subtraction model and Eq. (2) 85
      2.3.1. Correlations for 87 type-B alkyl-silica columns 86
   2.4. Solute and column parameters as a function of solute molecular structure and column properties 86
      2.4.1. Solute hydrophobicity (η') as a function of molecular structure 86
      2.4.2. Solute "bulkiness" (σ') as a function of molecular structure 87
      2.4.3. Solute hydrogen bond basicity (β') as a function of molecular structure 89

* Corresponding author. Tel.: +1 925 254 6334; fax: +1 925 254 2386.
E-mail address: snyder0036@comcast.net (L.R. Snyder).

0021-9673/$ – see front matter © 2004 Elsevier B.V. All rights reserved.
doi:10.1016/j.chroma.2004.08.121

2.4.4. Solute hydrogen bond acidity (α') as a function of molecular structure 90
2.4.5. Molecular charge (κ') as a function of molecular structure 90
2.4.6. Column hydrophobicity ***H*** as a function of column properties 91
2.4.7. Column steric resistance ***S**** as a function of column properties 91
2.4.8. Column hydrogen-bond acidity **A** as a function of column properties 92
2.4.9. Column hydrogen-bond basicity **B** as a function of column properties 93
2.4.10. Column cation exchange capacity ***C*** as a function of column properties and mobile phase pH [12] 93
2.5. Selectivity of other column types (relative values of ***H***, ***S****, etc.) 94
2.5.1. The accuracy of Eq. (2) for other column types; additional solute–column interactions 94
2.5.2. Type-A alkyl-silica columns [11] 95
2.5.3. Columns with embedded polar groups (EPG) [31] 95
2.5.4. Columns with polar end-capping groups [31] 98
2.5.5. Cyanopropyl ("cyano") columns [32] 98
2.5.6. Phenyl columns [33] 98
2.5.7. Fluoro-substituted ("fluoro") columns [33] 99
2.5.8. Bonded-zirconia columns [11] 99
2.5.9. Polymeric alkyl-silica columns [11] 99
2.5.10. The unimportance of dipole–dipole interactions in affecting RP-LC retention 100
2.6. Values of ***H***, ***S****, etc. for other experimental conditions [12] 100
2.6.1. Effect of triethylamine added to the mobile phase [11] 100
2.7. Alternative characterizations of column selectivity 100
2.8. Possible limitations and further development of the hydrophobic-subtraction model 101
3. Applications 102
3.1. Selecting "equivalent" columns [72] 102
3.1.1. Modification of Eq. (15) as a function of the sample 104
3.1.2. Likelihood of matching different column types 105
3.2. Selecting columns of very different selectivity 105
3.2.1. Developing orthogonal RP-LC methods 106
3.2.2. Two-dimensional (2-D) separation 106
3.3. Changes in column selectivity as a function of column history 106
3.4. Gradient elution [72] 107
3.5. Quality control of columns during their manufacture 107
3.6. Peak tailing as a function of the column 107
4. Conclusions 113
5. Nomenclature 114
Acknowledgement 115
Appendix 115
References 115

1. Introduction

By the early 1990s, a general picture had emerged of reversed-phase liquid chromatography (RP-LC) with alkyl-silica columns [1,2]. Retention was attributed primarily to *solvophobic* or *hydrophobic interaction*, in which the stationary phase plays a more or less passive role and the mobile phase mainly controls separation. To the extent that hydrophobic interaction dominates the RP-LC retention process, plots of retention ($\log k$) for one column versus another should yield straight line plots with roughly unit slope and little scatter [3]. This is in fact a reasonable first approximation for RP-LC retention, as illustrated by the data of Fig. 1, where the retention of 88 solutes of widely varied structure is plotted for (a) an Inertsil ODS-3 versus (b) a StableBond C18 column. The experimental conditions used for the data presented in following Sections 1 and 2 are given in the caption of Fig. 1 (50% acetonitrile/pH 2.8 buffer; 35 °C), unless noted otherwise.

Soon after the introduction of RP-LC separation, it became apparent that the column could contribute to retention in additional ways, other than by hydrophobic interaction between solute and column. Underivatized silanols in the stationary phase can interact with retained solute molecules; thus, ionized silanols ($-SiO^-$) can retain protonated bases by cation-exchange, and neutral silanols ($-SiOH$) can hydrogen bond with proton-acceptor solutes [6]. The shape of the solute molecule can also affect sample retention, leading to so-called *column shape selectivity* [7]. Some of these (and other) contributions to column selectivity for non-ionized solute molecules have been incorporated into the *solvation equation* model [8] for RP-LC retention:

$$\log k = \underset{\text{(i)}}{C_1} + \underset{\text{(ii)}}{rR_2} + \underset{\text{(iii)}}{s\pi_2^{\text{H}}} + \underset{\text{(iv)}}{a\sum \alpha_2^{\text{H}}} + \underset{\text{(v)}}{b\sum \beta_2} + \underset{\text{(vi)}}{vV_x} \quad (1)$$

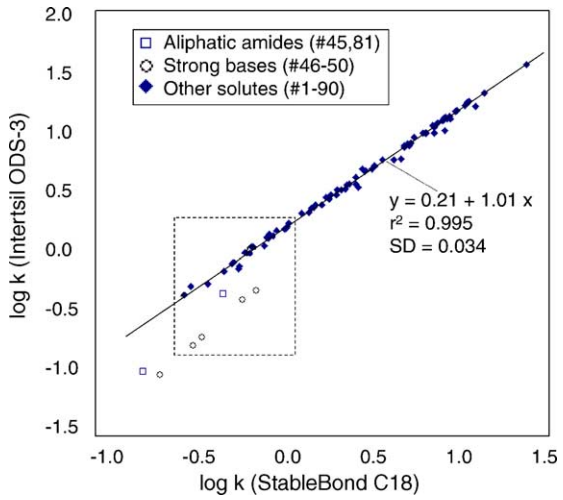

Fig. 1. Plot of log k values for an Inertsil ODS-3 column vs. values for a StableBond C18 column. *Conditions*: 50% acetonitrile/buffer; buffer is 60 mM pH 2.8 potassium phosphate; 35 °C; 2 mL/min. Sample includes solutes #1–90 of [4,5] (excluding solutes #84, 86). Data and solute numbering from [4,5].

(note a recently revised but equivalent formulation of Eq. (1), also described in [8]). C_1 is a solute-independent constant, the quantities r, s, a, b and v are determined by the choice of column and separation conditions, and R_2, π_2^H, $\sum\alpha_2^H$, $\sum\beta_2$ and V_x represent relevant properties of the solute (see Section 5 for the definitions of individual symbols). Thus, terms (ii), (iii) and (primarily) (vi) together determine the hydrophobic interaction between solute and column, term (iv) describes the effects of hydrogen bonding between acidic (donor) solutes and basic (acceptor) groups in the column, and term (v) represents the contribution of hydrogen bonding between basic solutes and acidic column groups. If separation conditions are held constant, values of r, s, a, b and v then partially characterize column selectivity. Eq. (1) ignores contributions to retention from shape selectivity, cation-exchange and related ionic interactions, and π–π complexation. While the model described by Eq. (1) has many virtues (including its applicability to an extraordinarily wide range of unrelated chromatographic and non-chromatographic phenomena), it is not accurate or precise enough to be used to predict chromatographic retention for purposes of method development, nor to enable useful comparisons of stationary phase selectivity. None the less, it has provided the initial conceptual underpinnings of the work summarized herein.

Five solute–column interactions in RP-LC are now widely recognized as significant contributors to sample retention and column selectivity [4–9]: hydrophobic interaction, shape selectivity, hydrogen bonding of acidic solutes with a basic column group or basic solutes with an acidic column group, and cation exchange with ionized silanol groups. Means for quantitatively measuring these different column properties have been proposed [6–9], but other evidence suggests that past test procedures may be of limited practical value [5,10]—as examined in Section 2.7 below. The present paper reviews the theoretical basis of a recently developed approach (hereafter the hydrophobic-subtraction model of RP-LC retention), which we believe allows a more reliable, complete and practically useful characterization of RP-LC column selectivity. We will also examine the use of this model for selecting columns of either similar or different selectivity, as well as some other applications related to column selectivity.

2. Theory and experimental results

2.1. The hydrophobic-subtraction model

The data of Fig. 1 illustrate the overall importance of a single kind of solute–column interaction (i.e., based on hydrophobicity) in determining RP-LC retention for closely related stationary phases. However, the modest (largely non-experimental-error) scatter of data in this plot also reflects contributions from other types of solute–column interactions. The hydrophobic-subtraction model of the present review assumes that we first subtract the major contribution of hydrophobicity to RP-LC retention, in order to better see remaining contributions to retention from other solute–column interactions. The further analysis of deviations from the solid curve of Fig. 1 then leads to a general equation for RP-LC retention and column selectivity [4,11]:

$$\log\alpha \equiv \log\left(\frac{k}{k_{EB}}\right) = \underset{(i)}{\eta'\boldsymbol{H}} - \underset{(ii)}{\sigma'\boldsymbol{S}^*} + \underset{(iii)}{\beta'\boldsymbol{A}} + \underset{(iv)}{\alpha'\boldsymbol{B}} + \underset{(v)}{\kappa'\boldsymbol{C}} \quad (2)$$

here k is the retention factor of a given solute, k_{EB} the value of k for a non-polar reference solute (ethylbenzene in the present treatment) on the same column under the same conditions, and the remaining selectivity-related symbols represent either empirical, eluent- and temperature-dependent properties of the solute (η', σ', β', α', κ'), or eluent- and temperature-independent properties of the column ($\boldsymbol{H}$, $\boldsymbol{S}^*$, $\boldsymbol{A}$, $\boldsymbol{B}$, $\boldsymbol{C}$). The nature of the five solute–column interactions implied by terms (i)–(v) of Eq. (2) is represented by the cartoons of Fig. 2. Thus, the various column parameters measure the following column properties: $\boldsymbol{H}$, hydrophobicity; $\boldsymbol{S}^*$, steric resistance to insertion of bulky solute molecules into the stationary phase (conceptually similar to, but not the same as, "shape selectivity" [7]); $\boldsymbol{A}$, column hydrogen-bond acidity, mainly attributable to non-ionized silanols; $\boldsymbol{B}$, column hydrogen-bond basicity, presently hypothesized to result (for some, but not all columns) from sorbed water in the stationary phase; $\boldsymbol{C}$, column cation-exchange activity, due to ionized silanols ($\boldsymbol{C}$ will therefore vary with mobile phase pH).

The parameters η', σ', etc. denote complementary properties of the solute: η', hydrophobicity; σ', molecular "bulkiness" or resistance to insertion of the solute into the stationary phase; β', hydrogen-bond basicity; α', hydrogen-bond acidity; κ', approximate charge (either positive or negative) on the solute molecule. Note that values of each solute parameter η', σ', etc. are relative to values for ethylbenzene (the reference solute for which all solute parameters are identically zero),

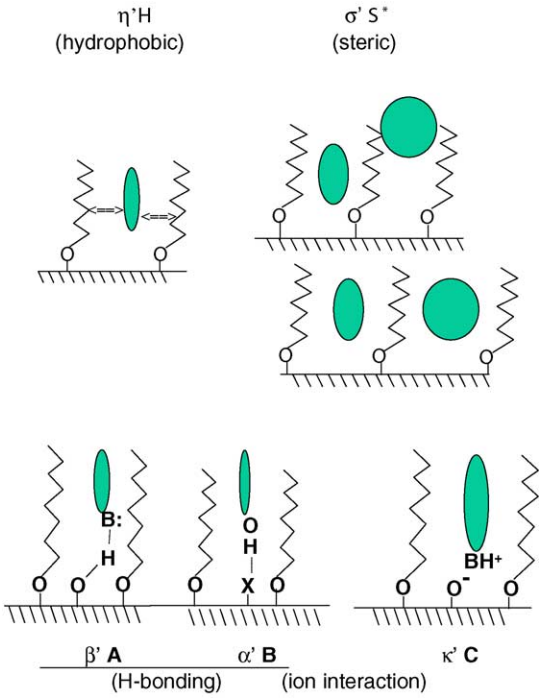

Fig. 2. Cartoon representation of five solute–column interactions of Eq. (2). "X" for $\alpha'\boldsymbol{B}$ interaction varies with column type (see Sections 2.4.9, 2.5.2 and 2.5.3). Reprinted from [5].

and the values of each column parameter $\boldsymbol{H}$, $\boldsymbol{S}^*$, etc. are relative to a hypothetical, average type-B (pure silica) C_{18} column (described in [10]). Any column, which behaves identically to the average type-B C_{18} column will have $\boldsymbol{H}$ equal to 1, and all other parameters ($\boldsymbol{S}^*$, $\boldsymbol{A}$, etc.) equal to 0. Solute–column interactions defined by terms (i) and (iii)–(v) of Eq. (2) are attractive, so that these terms are positive. Term (ii) represents a repulsive interaction, which is therefore negative [11]. The value of each term in Eq. (2) (i–v) for a given column and solute measures the change in log k for that solute, column and interaction, compared to retention of the same solute on an average type-B C_{18} column with $\boldsymbol{H} = 1$ and $\boldsymbol{S}^* = \boldsymbol{A} = \boldsymbol{B} = \boldsymbol{C} = 0$ (assuming the same mobile phase and temperature). Values of $\boldsymbol{H}$, $\boldsymbol{S}^*$, etc. in Eq. (2) are approximately the same for different separation conditions (%*B*, temperature, solvent type, etc.), except for $\boldsymbol{C}$ which varies with mobile phase pH. Values of η', σ', etc. vary with conditions.

The ensuing development of the subtraction-model and Eq. (2) in Sections 2.2–2.5 is somewhat detailed; the summary of this treatment in Table 1 may therefore be of help to the reader in following this discussion. Those primarily interested in practical applications of column selectivity may wish to skip to Section 2.4.6 and the text that follows.

2.2. Analysis of non-hydrophobic solute–column interactions

Values of k for solutes #1–90 (see [4,5] for solute identification) were measured for nine different makes of type-B C_{18} columns (e.g., Inertsil ODS-3 and StableBond C18 in Fig. 1), following which average values of log k were calculated for each solute and the nine columns. Separation conditions were held constant for this study: 50% (v/v) acetonitrile/buffer, 60 mM potassium phosphate buffer (pH 2.8), 35 °C; see [10] for details. Values of log k for each column were next correlated as in Fig. 1 with the *average* values of log k for each solute and all nine columns. Finally, deviations (δlog k) from the best-fit correlation for each column and solute were calculated as in Fig. 3. See Table 1 for details.

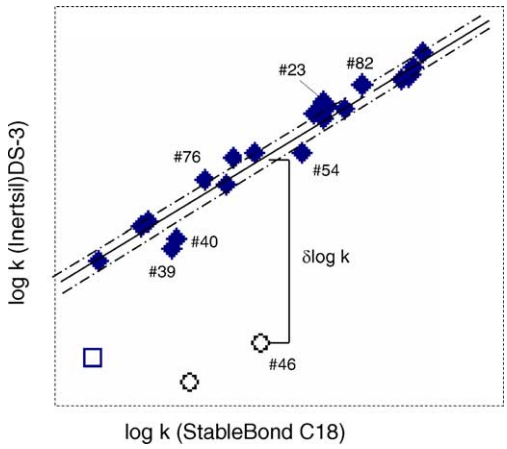

Fig. 3. Expansion of bracketed region from Fig. 1.

The rectangular region in Fig. 1 (bounded by dashed lines) is expanded in Fig. 3, so as to allow easier visualization of deviations from the best-fit line through these data. The parallel lines (–·–·–) in Fig. 3 correspond to deviations of ±0.02 units in log k from the best-fit solid line; for several solutes, it is seen that their values of log k deviate from the best-fit line by >0.02 log units (note that the experimental accuracy of these values of log k is ±0.002 log units [4]; i.e., contributing negligibly to deviations in log $k > 0.01$). These deviations for each solute can be defined as δlog k (see example for solute #46 in Fig. 3). Values of δlog k in Figs. 1 and 3 are especially large for aliphatic amides (□) and protonated strong bases (⌬), but when all nine columns of the study of [4,5] are considered, significant deviations (average S.D. > 0.02) were observed for about half of the 88 solutes of Fig. 1.

Assume next, for some solutes, that values of δlog $k > 0.02$ are determined largely by a *single* solute–column interaction *other* than hydrophobicity. For example, consider protonated strong bases, which can interact strongly with ionized silanols via cation exchange (term (v) of Eq. (2)). For any two solutes whose δlog k values are determined mainly by the same solute–column interaction (e.g., cation exchange), values of δlog k should be highly correlated. Thus, the contribution of each interaction to retention can be approximated by a product of some property of the solute (e.g., κ') and some property of the column (e.g., $\boldsymbol{C}$), so that for the strong bases (#46–50):

$$\delta \log k \approx \kappa' \boldsymbol{C} \tag{3}$$

Table 1
A summary of the development of Eq. (2), based on data from [4,5]

Section 2.2	*Identify solutes for which only one of terms (ii)–(v) are important* Calculate values of $\delta\log k$ (see Fig. 3) for each of 88 solutes and nine columns, based on plots of $\log k$ for each column vs. *average* values of $\log k$ for each solute and all nine columns (similar to Figs. 1 and 3, but with average $\log k$ values replacing $\log k$ for StableBond C18)) Select "deviant" solutes with *average* values of $\delta\log k \geq 0.02$ (as in Fig. 3) Compare values of $\delta\log k$ for each deviant solute (and all nine columns) vs. values for every other deviant solute (linear regression); group solutes that are highly correlated (four resulting groups: $\boldsymbol{S}^*$, $\boldsymbol{A}$, $\boldsymbol{B}$, $\boldsymbol{C}$)
Sections 2.2.1–2.2.4	*Estimate initial values of* $\mathbf{S}^*$, **A**, **B** *and* **C** *at pH 2.8* Calculate values of $\log\alpha \equiv \log(k/k_{EB})$ for every solute and column, where k_{EB} is the value of k for ethylbenzene and a given column; calculate corresponding values of $\delta\log\alpha$ for each solute and column from plots of $\log\alpha$, similar to plots of $\log k$ as in Section 2.2 above Preliminary values of $\boldsymbol{S}^*$, $\boldsymbol{A}$, $\boldsymbol{B}$ and $\boldsymbol{C}$ for each column are equated to the average value of $\delta\log\alpha$ for highly correlated solutes (Tables 2–5); this (arbitrarily) assumes that average values of σ', β', α' or κ' for the solutes in each selectivity group are equal to 1.00
Section 2.3	*Final application of* Eq. (2) *for nine type-B C18 columns* Preliminary values of $\boldsymbol{H}$ for each column are calculated, equal to the slope of plots of $\log\alpha$ for that column vs. $\log\alpha$ for the StableBond C18 column (solutes #1–67) Preliminary values of the solute parameters (η', σ', β', α', κ') are obtained by a multiple linear regression of values of $\log\alpha$ for each solute (#1–67) and nine columns vs. preliminary values of $\boldsymbol{H}$, $\boldsymbol{S}^*$, $\boldsymbol{A}$, $\boldsymbol{B}$ and $\boldsymbol{C}$ for the nine columns Revised values of $\boldsymbol{H}$, $\boldsymbol{S}^*$, $\boldsymbol{A}$, $\boldsymbol{B}$ and $\boldsymbol{C}$ are obtained by a multiple linear regression of values of $\log\alpha$ for each column vs. the above preliminary values of η', σ', β', α' and κ' for the 67 solutes Multiple linear regression is continued as above to obtain final ("best") values of $\boldsymbol{H}$, $\boldsymbol{S}^*$, etc. and η', σ', etc., with an agreement with Eq. (2) of ±0.8% in α (1S.D.) Values of $\log\alpha$ for a second set of solutes (#68–90) and the same nine columns were correlated (just one multiple linear regression) with the above final values of $\boldsymbol{H}$, $\boldsymbol{S}^*$, etc. to obtain values of η', σ', etc. for these additional solutes. The resulting average deviation of values of α from Eq. (2) was the same (±0.8% in α) for both sets of solutes (#1–67 and #68–90) A similar correlation of literature data for 87 solutes and five columns gave agreement with a shortened form of Eqs. (2) and (4) equal to ±2% in α
Section 2.3.1	*Extension of* Eq. (2) *to 87 type-B alkyl-silica columns* Eq. (2) was extended to 87 type-B alkyl-silica columns (C_3–C_{30}), using 16 test solutes (Table 6) whose values of η', σ', etc. are slightly changed from Step 3 because of minor changes in the mobile phase. Values of $\boldsymbol{H}$, $\boldsymbol{S}^*$, etc. for these 87 columns result, with an average standard deviation for each column that is equivalent to ±1.2% in α
Sections 2.4.1–2.4.5	*Values of the solute parameters as a function of molecular structure* Values of η', σ', etc. are compared with solute molecular structure; resulting comparisons are generally consistent with a simple physico-chemical picture (Fig. 2) for each associated solute-column interaction
Sections 2.4.6–2.4.10	*Values of the column parameters as a function of (a) column properties and (b)* **C** *as a function of mobile phase pH* Values of $\boldsymbol{H}$, $\boldsymbol{S}^*$, etc. are compared with column properties such as ligand length and concentration, pore diameter, end-capping and silica acidity; resulting comparisons are generally consistent with a simple picture for each associated solute-column interaction Values of $\boldsymbol{C}$ as a function of mobile phase pH are measured (Eq. (12))
Section 2.5	*Selectivity of columns other than type-B alkyl-silica* Eq. (2) is extended to several other column types (type-A alkyl-silica, phenyl, cyano, etc.), using multiple linear regression of values of $\log\alpha$ for each column vs. values of η', σ', etc. from Step 4 Resulting average values of $\boldsymbol{H}$, $\boldsymbol{S}^*$, etc. for each column type are compared with average values for type-B columns of similar ligand length (Table 11)

and for two strong bases 1 and 2,

$$\delta\log k_1 = \left(\frac{\kappa'_1}{\kappa'_2}\right)\delta\log k'_2 \qquad (3a)$$

where κ'_1 is the value of κ' for solute 1 and κ'_2 is the value for solute 2; (κ'_1/κ'_2) is therefore a constant for solutes 1 and 2.

An example of the correlation of values of $\delta\log k$ among the 88 solutes of Fig. 1 (solutes #1–90, except #84 and 86 as discussed below in Section 2.3) is illustrated for four solutes in Fig. 4; #46 and 48 are protonated strong bases (amitriptyline, propranol) and #35 and 72 are neutral molecules (*cis*-4-nitrochalcone, 2-nitrobiphenyl). In Fig. 4a, the correlation of $\delta\log k$ values for the two strong bases #46 and 48 (on each of nine different columns) is seen to be quite strong ($r^2 = 0.99$), whereas the correlation of the strong base #46 and neutral compound #72 in Fig. 4b is weak ($r^2 = 0.19$). We conclude that *values of* $\delta\log k$ *for these two strong bases are almost entirely the result of a single additional solute–column interaction*, which in Section 2.3 is shown to be consistent with cation exchange (or more accurately, *ion interaction*) with ionized column silanols. The similar comparison of values of $\delta\log k$ for neutral compounds #35 and 72 in Fig. 4c also results in a strong correlation ($r^2 = 0.99$), suggesting that $\delta\log k$ for these two compounds also arises from a single kind of solute–column interaction—but one different from that for the two strong bases ("steric interaction", Section 2.2.2). The final comparison in Fig. 4d for a different combination of strong base and neutral compound shows a poor correlation ($r^2 = 0.15$), as expected.

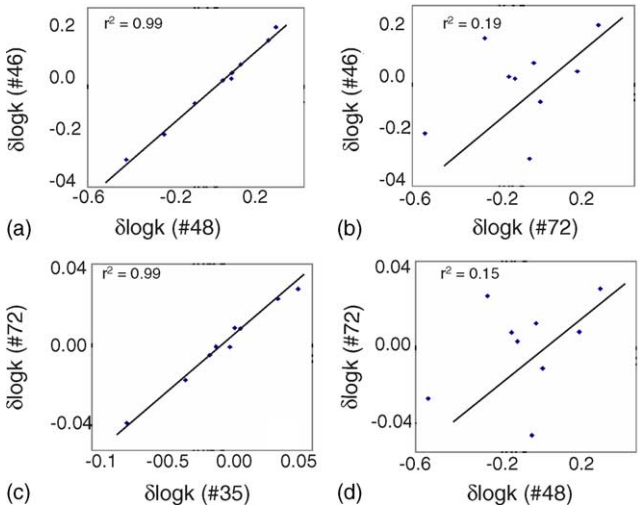

Fig. 4. Correlation of δlog *k* values for various solute-pairs and nine different C_{18} columns. Data of [4,5]; #35, *cis*-4-nitrochalcone; #46, amitriptyline; #48, propranolol; #72, 2-nitrobiphenyl. See text for details.

We should emphasize that the secondary column selectivity terms (i.e., $\sigma'\boldsymbol{S}^*$, $\beta'\boldsymbol{A}$, $\alpha'\boldsymbol{B}$, $\kappa'\boldsymbol{C}$) are obtained *not* by serial analysis of the data with subtraction of each term, but instead these four terms are obtained simultaneously and in a parallel manner, *after* a value of $\eta'\boldsymbol{H}$ is obtained and subtracted from log α (i.e., calculation of values of δlog *k* as in Fig. 3).

2.2.1. Cation exchange interactions and Eq. (2) ($\kappa'\boldsymbol{C}$ term)

Table 2 summarizes values of r^2 for the correlation of δlog *k* values for five strong bases (#46–50) and three weak bases (#51–53) [4], each of which solutes has an average value of $\delta\log k \geq 0.02$. Strong correlations among solutes with $\delta\log k < 0.02$ are less likely, because of experimental error in log *k* (±0.002, 1S.D.), plus small additional contributions from more than one solute–column interaction other than hydrophobicity. Returning to Table 2, for the five strong bases we see that the average value of r^2 is 0.995 (excluding self-correlation of solute #46 with itself, etc.); i.e., there is a consistent and pronounced correlation which suggests that the deviations of these compounds from the plot in Fig. 1 are dominated by a single type of interaction (cation exchange or ion interaction, discussed further in Sections 2.4.5 and 2.4.10). When values of δlog *k* for these strong bases are correlated with values for weak bases, the average value of r^2 is 0.82. This is reasonable, because we expect cation exchange to contribute to the retention of partly-ionized weak bases, but not as strongly as for fully-ionized strong bases (weak bases #51–53 are ≈71% protonated in this system). Because of this reduced interaction of weak bases with ionized silanols, other solute–column interactions become relatively more important, with a relative weakening of the correlation.

So far we have not considered differences in the column phase-ratio, which can arise from differences in column surface area and other column properties. The effect of differences in phase ratio alone on retention can be minimized by the use of separation factors α, in place of retention factors *k*. We can define a separation factor $\alpha = k/k_{EB}$, where ethylbenzene has been chosen as reference solute (the choice of ethylbenzene as reference solute was made on the basis of its lack of hydrogen-bonding, ionic or other polar interactions). Values of α can then be substituted for values of *k* in the above analysis of cation-exchange interaction, yielding values of δlog α instead of δlog *k*.

The average value of δlog α for the strong bases of Table 2 and a given column can be equated to the average value of $\kappa'\boldsymbol{C}$ for these five solutes and that column. We can arbitrarily define an average value of $\kappa' = 1$ for these five strong bases, which then means that $\boldsymbol{C}$ for each column is equal to the average value of δlog α for the five strong bases on that column.

2.2.2. Steric resistance and Eq. (2) ($\sigma'\boldsymbol{S}^*$ term)

The δlog *k* values of neutral compounds #35 and 72 of Fig. 4c were seen to be highly correlated. Similar, strong correlations of δlog *k* were found among these compounds and several other solutes (see Table 3). For compounds #32–40, 43, 44, 72, 73, 76–78, 88, 89 of Fig. 5 [4,5], the average value

Table 2
Solutes which exhibit cation-exchange interaction ($\kappa'\boldsymbol{C}$) with the column

Solute	Values of r^2 for correlation of different solutes							
	Fully ionized strong bases					Partly ionized weak bases		
	#46	#47	#48	#49	#50	#51	#52	#53
#46	**1.00**	**1.00**	**0.99**	**1.00**	**1.00**	0.83	0.83	0.83
#47	**1.00**	**1.00**	**1.00**	**1.00**	**0.99**	0.85	0.83	0.83
#48	**0.99**	**1.00**	**1.00**	**0.99**	**1.00**	0.83	0.81	0.79
#49	**1.00**	**1.00**	**0.99**	**1.00**	**0.99**	0.83	0.83	0.83
#50	**0.99**	**0.99**	**1.00**	**0.99**	**1.00**	0.83	0.83	0.81
#51	0.83	0.85	0.83	0.83	0.83	1.00	1.00	0.98
#52	0.83	0.83	0.81	0.83	0.83	0.99	1.00	1.00
#53	0.83	0.83	0.79	0.83	0.81	0.98	1.00	1.00

Correlation of δlog *k* values for different basic solutes of [4,5] at pH 2.8; e.g., for solutes #47 and 51 and all nine C_{18} columns, $r^2 = 0.85$. Solutes: #46, amitriptyline; 47, diphenhydramine; 48, propranolol; 49, nortriptyline; 50, prolintane; (51–53), 4-*n*-C_5, -C_6 and -C_7 aniline. Bolded values represent highly-correlated solute-pairs that are used for calculating values of $\boldsymbol{C}$, as described in the text. All solutes in this table have an average value of $\delta\log k > 0.02$.

Table 3
Solutes which exhibit steric interaction ($\sigma' \boldsymbol{S}^*$)

	Values of r^2 for correlation of different solutes																	
	#39	#40	#32	#33	#34	#35	#36	#37	#38	#72	#73	#78	#43	#77	#89	#88	#44	#76
#39	1.00	0.98	0.88	0.88	0.83	0.83	0.76	0.86	0.79	0.77	0.74	0.77	0.88	0.88	0.79	0.62	0.74	0.55
#40	0.98	1.00	0.90	0.92	0.85	0.86	0.81	0.90	0.83	0.83	0.79	0.81	0.94	0.92	0.86	0.69	0.76	0.64
#32	0.88	0.90	**1.00**	**1.00**	**0.98**	**0.98**	**0.94**	**1.00**	**0.98**	**0.98**	**0.94**	**0.98**	**0.98**	**0.98**	0.92	0.86	0.88	0.76
#33	0.88	0.92	**1.00**	**1.00**	**0.96**	**1.00**	**0.96**	**1.00**	**0.98**	**0.98**	**0.94**	**0.98**	**0.98**	**1.00**	0.94	0.86	0.88	0.76
#34	0.83	0.85	**0.98**	**0.96**	**1.00**	**0.96**	**0.88**	**0.96**	**0.94**	**0.98**	**0.94**	**0.98**	**0.94**	**0.98**	0.90	0.85	0.85	0.76
#35	0.83	0.86	**0.98**	**1.00**	**0.96**	**1.00**	**0.98**	**1.00**	**1.00**	**0.98**	**0.96**	**0.98**	**0.96**	**0.98**	0.92	0.90	0.90	0.77
#36	0.76	0.81	**0.94**	**0.96**	**0.88**	**0.98**	**1.00**	**0.96**	**0.98**	**0.94**	**0.94**	**0.94**	**0.90**	**0.92**	0.90	0.92	0.86	0.77
#37	0.86	0.90	**1.00**	**1.00**	**0.96**	**1.00**	**0.96**	**1.00**	**0.98**	**0.98**	**0.94**	**0.98**	**0.96**	**0.98**	0.94	0.88	0.88	0.76
#38	0.79	0.83	**0.98**	**0.98**	**0.94**	**1.00**	**0.98**	**0.98**	**1.00**	**0.98**	**0.98**	**0.98**	**0.94**	**0.96**	0.94	0.94	0.88	0.81
#72	0.77	0.83	**0.98**	**0.98**	**0.98**	**0.98**	**0.94**	**0.98**	**0.98**	**1.00**	**0.98**	**1.00**	**0.96**	**0.98**	0.92	0.94	0.88	0.83
#73	0.74	0.79	**0.94**	**0.94**	**0.94**	**0.96**	**0.94**	**0.94**	**0.98**	**0.98**	**1.00**	**0.98**	**0.92**	**0.94**	0.94	0.96	0.83	0.86
#78	0.77	0.81	**0.98**	**0.98**	**0.98**	**0.98**	**0.94**	**0.98**	**0.98**	**1.00**	**0.98**	**1.00**	**0.94**	**0.96**	0.90	0.92	0.86	0.81
#43	0.88	0.94	**0.98**	**0.98**	**0.94**	**0.96**	**0.90**	**0.96**	**0.94**	**0.96**	**0.92**	**0.94**	**1.00**	**0.98**	0.96	0.86	0.85	0.83
#77	0.88	0.92	**0.98**	**1.00**	**0.98**	**0.98**	**0.92**	**0.98**	**0.96**	**0.98**	**0.94**	**0.96**	**0.98**	**1.00**	0.96	0.86	0.88	0.79
#89	0.79	0.86	0.92	0.94	0.90	0.92	0.90	0.94	0.94	0.92	0.94	0.90	0.96	0.96	1.00	0.90	0.79	0.86
#88	0.62	0.69	0.86	0.86	0.85	0.90	0.92	0.88	0.94	0.94	0.96	0.92	0.86	0.86	0.90	1.00	0.77	0.90
#44	0.74	0.76	0.88	0.88	0.85	0.90	0.86	0.88	0.88	0.88	0.83	0.86	0.85	0.88	0.79	0.77	1.00	0.71
#76	0.55	0.64	0.76	0.76	0.76	0.77	0.77	0.76	0.81	0.83	0.86	0.81	0.83	0.79	0.86	0.90	0.71	1.00

Correlation at pH 2.8 of $\delta \log k$ values for selected solutes of [4,5] (shown in Fig. 5); e.g., for solutes #34 and 44 and all nine C_{18} columns, $r^2 = 0.85$. See Fig. 5 for solute structures. Bolded values represent highly-correlated solute-pairs that are used for calculating values of $\boldsymbol{S}^*$, as described in the text. All solutes in this table have an average value of $\delta \log k > 0.02$. The ordering below of these solute is (very roughly) according to values of r^2 (e.g., solutes #39 and 76 least correlated, adjacent solutes most correlated).

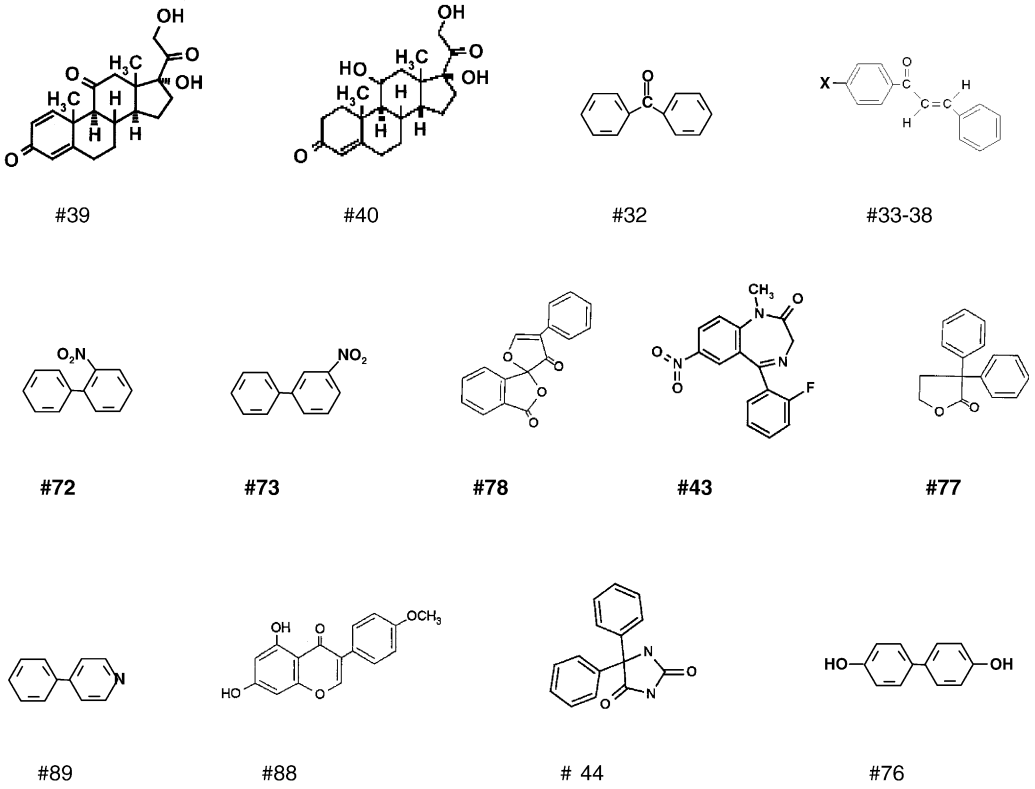

Fig. 5. Molecular structures of "bulky" solute molecules from Table 2. Solutes are arranged in approximate order of relative correlation; i.e., values of $\delta \log \alpha$ for adjacent solutes are more highly correlated (series goes from left to right, then repeats).

of $r^2 = 0.89$ (again excluding self-correlation), while for solutes #32–38, 43, 72, 73, 77, 78, $r^2 = 0.97$. Values of $\delta\log\alpha$ for the latter 12 compounds are determined mainly by a single additional (i.e. non-hydrophobic) solute–column interaction, which now appears to involve resistance to penetration of the solute into the stationary phase (steric resistance; Sections 2.4.2 and 2.4.7).

The negative average value of $\delta\log\alpha$ for highly-correlated compounds #32–38, 43, 72, 73, 77, 78 and each column can be taken as the relative steric resistance $\boldsymbol{S}^*$ of that column; i.e., a similar approach as for calculation of $\boldsymbol{C}$ in Section 2.2.1.

2.2.3. Column hydrogen-bond basicity and Eq. (2) ($\alpha'\boldsymbol{B}$ term)

A third group of solutes with values of $\delta\log k$ that are meaningfully inter-correlated are the 12 aromatic carboxylic acids (#56–67 of [4]). Table 4 summarizes values of r^2 for the correlation of various pairs of these solutes. Solutes #56–58 and 60–62 have an average value of $r^2 = 0.88$ (excluding self-correlation), suggesting that $\delta\log\alpha$ for these solutes arises largely from a single additional solute–column interaction. The value of r^2 for the remaining solutes of Table 4 equals 0.68, suggesting for these solutes a significant contribution from one or more additional (non-hydrophobic) interactions. The bottom row of Table 4 gives the approximate negative charge for each solute (or its fractional ionization in the mobile phase). It is seen that the more correlated benzoic acids (R–COOH) #56–58 and 60–62 are all less ionized (0–2% as R–COO^-), whereas the less correlated solutes in Table 4 are more ionized (8–60% as R–COO^-). This suggests that the more ionized solutes interact with the column not only by hydrogen bonding of a –COOH solute group to a basic column group (Sections 2.4.4 and 2.4.9), but also by ionic interaction; i.e., repulsion of negatively-charged ionized acids from the negatively charged stationary phase, similar (but in inverse relationship) to ion-exchange as in Section 2.1.1. Note that the fractional ionization values of Table 4 were estimated from experimental measurements of k versus pH in the present system (50% acetonitrile/pH 2.8 buffer; 35 °C [12]).

The average value of $\delta\log\alpha$ for compounds #56–58 and 60–62 and each column can be equated with the relative hydrogen-bond basicity $\boldsymbol{B}$ of that column: the same procedure as for values of $\boldsymbol{C}$ in Section 2.2.1. The origin of this column basicity appears to vary with column type (e.g., type-A versus type-B alkyl-silica, embedded-polar-group columns versus alkyl-silica, etc.); see Sections 2.4.9, 2.5.2 and 2.5.3.

2.2.4. Column hydrogen-bond acidity and Eq. (2) ($\beta'\boldsymbol{A}$ term)

A fourth group of correlated solutes is represented by three monofunctional amides: solutes #16, 45 and 81 of [4,5], as summarized in Table 5. The average value of r^2 equals 0.81, a moderate correlation which we infer to be based on a single type of solute–column interaction (hydrogen bonding of an acceptor solute with a donor column group, Sections 2.4.3 and 2.4.8), but with significant contributions from one or more other interactions (e.g., steric resistance [Section 2.2.2] is expected to vary among these three compounds). The average value of $\delta\log\alpha$ for compounds #45 and 81 (average $r^2 = 0.92$) and each column can be equated with the relative hydrogen-bond acidity $\boldsymbol{A}$ of that column, as for $\boldsymbol{C}$ in Section 2.2.1.

The derivation of (preliminary) values of $\boldsymbol{S}^*$, $\boldsymbol{A}$, $\boldsymbol{B}$ and $\boldsymbol{C}$ as above is based on specific compounds for each parameter; i.e., those compounds in the study of [4,5] whose values of $\delta\log k$ are highly correlated. This means that values of each column parameter would change to some extent if a different set of correlating compounds were used. This is of no

Table 4
Carboxylic acid solutes which interact with a hydrogen-bond acceptor in the column ($\alpha'\boldsymbol{B}$)

	Values of r^2 for correlation of different solutes											
	#56	#57	#58	#60	#61	#62	#63	#66	#67	#65	#59	#64
#56	**1.00**	**0.98**	**0.98**	**0.79**	**0.77**	**0.76**	0.96	0.79	0.76	0.92	0.61	0.64
#57	**0.98**	**1.00**	**0.98**	**0.88**	**0.88**	**0.86**	0.94	0.88	0.81	0.90	0.52	0.56
#58	**0.98**	**0.98**	**1.00**	**0.79**	**0.77**	**0.77**	0.88	0.83	0.77	0.83	0.45	0.50
#60	**0.79**	**0.88**	**0.79**	**1.00**	**1.00**	**0.98**	0.85	0.85	0.77	0.79	0.38	0.40
#61	**0.77**	**0.88**	**0.77**	**1.00**	**1.00**	**1.00**	0.83	0.85	0.77	0.79	0.38	0.40
#62	**0.76**	**0.86**	**0.77**	**0.98**	**1.00**	**1.00**	0.83	0.85	0.74	0.77	0.36	0.38
#63	**0.96**	**0.94**	**0.88**	**0.85**	**0.83**	**0.83**	1.00	0.79	0.76	1.00	0.71	0.72
#66	0.79	0.88	0.83	0.85	0.85	0.85	0.79	1.00	0.83	0.72	0.35	0.50
#67	0.81	0.77	0.77	0.77	0.74	0.76	0.83	0.66	1.00	0.72	0.37	0.41
#65	0.92	0.90	0.83	0.79	0.79	0.77	1.00	0.72	0.72	1.00	0.77	0.76
#59	0.61	0.52	0.45	0.38	0.38	0.36	0.71	0.35	0.37	0.77	1.00	0.90
#64	0.64	0.56	0.50	0.40	0.40	0.38	0.72	0.50	0.41	0.76	0.90	1.00
Negative charge[a]	0.02	0.02	0.01	0.01	0.00	0.00	0.09	0.08	0.10	0.10	0.37	0.60

Correlation of $\delta\log k$ values for selected solutes of [4,5] at pH 2.8; e.g., for solutes #57 and 62 and all nine C_{18} columns, $r^2 = 0.86$. Solutes: 56, diclofenate acid; 57, mefenamic acid; 58, ketoprofen; 59, diflunisal; (60–67), substituted benzoic acids (see [4,5] for solute numbering). Bolded values represent highly-correlated solute-pairs that are used for calculating values of $\boldsymbol{B}$, as described in the text. All solutes in this table have an average value of $\delta\log k > 0.02$.

[a] Fractional ionization of the molecule; e.g., compound #63 is an acid that is 9% ionized, so its average molecular charge is −0.09. Fractional ionization values were determined in the mobile phase, as described in Table 8 of [12].

Table 5
Amide-substituted solutes which interact with a hydrogen-bond donor in the column ($\beta'\boldsymbol{A}$)

Solute	Values of r^2 for correlation of different solutes		
	N-benzylformamide (#16)	*N*,*N*-dimethylacetamide (#45)	*N*,*N*-diethylacetamide (#81)
#16	1.00	0.66	0.86
#45	**0.66**	**1.00**	0.92
#81	**0.86**	**0.92**	1.00

Correlation of $\delta\log k$ values for selected solutes of [4,5] at pH 2.8. Bolded values represent highly-correlated solute-pairs that are used for calculating values of $\boldsymbol{A}$, as described in the text. All solutes in this table have an average value of $\delta\log k > 0.02$.

real consequence, however, as long as values of $\boldsymbol{S}^*$, $\boldsymbol{A}$, etc. are always referenced to a particular set of test solutes (as throughout the present study). If, for example, a different set of test solutes had been used, and values of $\boldsymbol{S}^*$ were therefore increased by a factor of 1.2 for all columns, the corresponding solute parameters σ' would be decreased by the same factor for all solutes, and their values of $\sigma'\boldsymbol{S}^*$ would be unchanged. Values of $\sigma'\boldsymbol{S}^*$ (as well as terms (iii)–(v) of Eq. (2)) and predicted values of α for a given compound are therefore independent of the test solutes used, as long as the reference solute (ethylbenzene) is the same.

2.3. Development and verification of the hydrophobic-subtraction model and Eq. (2)

The preceding treatment of Sections 2.1 and 2.2 has resulted in (a) the experimental identification of four solute–column interactions (in addition to hydrophobicity) that contribute to column selectivity and (b) *preliminary* values of the corresponding column parameters $\boldsymbol{S}^*$, $\boldsymbol{A}$, $\boldsymbol{B}$, $\boldsymbol{C}$ for each column. A preliminary value of column hydrophobicity $\boldsymbol{H}$ is defined as the slope of plots of $\log k$ (or $\log\alpha$) as in Fig. 1, with StableBond C18 serving as temporary reference column; i.e., $\boldsymbol{H} \approx 1.00$ for StableBond C18 (it happens also that $\boldsymbol{H} \approx 1.00$ for an average type-B C_{18} column). Values of $\log\alpha$ for each solute (#1–67 of [4]) and all nine columns were next correlated (via Eq. (2), see Table 1) with the above preliminary values of $\boldsymbol{H}$, $\boldsymbol{S}^*$, $\boldsymbol{A}$, $\boldsymbol{B}$, $\boldsymbol{C}$ (multiple linear regression with zero intercept) to yield (a) values of the corresponding solute parameters η', σ', etc. for compounds #1–67 and (b) a standard deviation S.D. of the fit. This process was repeated by correlating values of $\log\alpha$ versus the solute parameters η', σ', etc. from the preceding regression to give final values of the column parameters $\boldsymbol{H}$, $\boldsymbol{S}^*$, etc., and then repeated again versus the latter values of the column parameters to give final values of η', σ', etc. In this way, limiting (best-fit) values of both the solute and column parameters resulted, with an average S.D. for the final correlation of Eq. (2) equal to 0.004 log units (±0.9% in α; $n = 603$), which can be compared with an experimental error of ±0.002 log units [4]. For resulting best-fit values of the various column and solute parameters, see [4].

The best-fit values of $\boldsymbol{H}$, $\boldsymbol{S}^*$, etc. obtained above were subsequently applied to retention data for a second group of solutes (#68–90 of [5]) and the same nine columns. Values of η', σ', etc. for these latter solutes were obtained in this way, with a similar fit of data as for solutes #1–67 (±0.9% in α after a *single* regression; $n = 303$) [5]; i.e., no change in final values of $\boldsymbol{H}$, $\boldsymbol{S}^*$, etc. that were obtained from the use of solutes #1–67. Values of η', σ', etc. for the latter 33 solutes are given in [5]. Two solutes from this latter group gave larger deviations from Eq. (1) (±4% in α for #84 [2,4-dinitrophenol] and ±6% in α for #86 [2,4,6-trinitrophenol]), as well as unlikely values of η', σ', etc. Solutes #84 and 86 were therefore omitted from (a) the following discussion and (b) the plots of Figs. 1 and 3. We surmise that the atypical behavior of these two relatively strong acids may be related to their large negative charge and resulting ionic repulsion from the negatively charged stationary phase. The $\kappa'\boldsymbol{C}$ term of Eq. (2) has been developed primarily for ionic *attraction* (e.g., ion exchange) rather than repulsion, and the use of Eq. (2) to describe the retention of negatively charged solutes may be slightly less reliable for some solutes.

On the basis of the above correlations with Eq. (2) for solutes #1–90 and nine type-B C_{18} columns, it was tentatively assumed that all important contributions to RP-LC retention and column selectivity *for these solutes and columns* are represented in Eq. (2) [4,5]. The validity of Eq. (2) for alkyl-silica columns could be further tested [4], using data for 87 solutes (#1a–87a) and five columns from a prior study [13]. The application of Eq. (2) to the data of [13] required some modification, because (a) no acidic or basic solutes are represented in the data of [13], and (b) separation in [13] was carried out at 25 °C, versus 35 °C in [4,5]. The absence of acids and bases from the study of [13] meant that no solute had significant values of α' or κ', so that terms (iv) and (v) of Eq. (2) could not contribute to retention for compounds #1a–87a (and values of $\boldsymbol{B}$ and $\boldsymbol{C}$ could not be evaluated for the columns of [13]). The latter situation can be addressed by the use of a shortened form of Eq. (2), which is applicable for samples, which contain no acidic or basic solutes:

$$\log\alpha = \underset{\text{(i)}}{\eta'\boldsymbol{H}} + \underset{\text{(ii)}}{\beta'\boldsymbol{A}} + \underset{\text{(iii)}}{\alpha'\boldsymbol{B}} \tag{4}$$

Several solutes and one column were common to the studies of [4,5,13], which allowed a correction for the 10 °C difference in the temperatures of these two studies (by means of temperature coefficients reported in [12]).

When Eq. (4) was applied to the retention data of [13] (repeated multiple linear regression), the resulting correlation yielded S.D. = 0.008 ($n = 435$), or ±1.9% in α [4]. Thus, the

study of [13] based on 87 additional solutes and five C_8 or C_{18} columns, provides a further confirmation of Eq. (2). The slightly greater S.D. for the latter study (±1.9% versus 0.8%) may be due to the inclusion of two type-A columns in the study of [13], for which Eq. (2) has been shown to be less accurate (Section 2.5.2). Values of η', β' and α' at 25 °C for these 87 solutes are given in [4] and referred to in Section 2.4. Values of the solute parameters η', σ', etc. for a total of 150 different solutes of widely varied structure were obtained in this way [4,5].

Although the above analysis of the data of [4,5,13] (as summarized in Table 1) differs in some respects from that described in [4], the use of repeated (iterative) regression in order to obtain final best-fit values of the parameters of Eqs. (2) or (4) largely eliminates any difference in final values of these parameters or the S.D. of the fit. We have chosen the present (essentially equivalent) analysis in place of that reported in [4], because it appears more straightforward and intuitive.

2.3.1. Correlations for 87 type-B alkyl-silica columns

The above analysis for nine type-B C_{18} columns was subsequently extended to 87 type-B columns with different ligand lengths: C_3–C_{30}, but mainly C_8 and C_{18}. Sixteen test-solutes from the original sample were used for this and subsequent studies of column selectivity, as detailed in [10]. Because of minor changes in the mobile phase for these subsequent measurements, slightly different values of the final solute parameters (η', σ', etc.) resulted for the 16 test-solutes (Table 6). The average S.D. for the correlation of $\log\alpha$ for all 87 columns was 0.005 (±1.2% in α; $n = 1392$). Details are given in [10], including a detailed procedure for the measurement of the column parameters $\boldsymbol{H}$, $\boldsymbol{S}^*$, etc., based on the test solutes and conditions of Table 6.

2.4. Solute and column parameters as a function of solute molecular structure and column properties

There are several reasons for examining (a) values of η', σ', etc. versus solute molecular structure and (b) values of $\boldsymbol{H}$, $\boldsymbol{S}^*$, etc. as a function of column properties. First, such a study should allow further insight into the physico-chemical nature of RP-LC retention and selectivity, and a better understanding of the nature and relative importance of associated solute–column interactions. Second, the latter relationships (a and b) must make sense, if in fact Eq. (2) is a realistic description of solute retention and column selectivity. Therefore, such a study of the parameters of Eq. (2) provides a further test of the physico-chemical reality of Eq. (2). Third, generalizations of this kind can in some cases allow useful estimates of solute or column parameter values for a given separation, for use in practical applications of Eq. (2) (Sections 3.1.1 and 3.2). Finally, changes in $\boldsymbol{H}$, $\boldsymbol{S}^*$, etc. for (a) different batches of nominally equivalent columns or (b) as a function of column history can be used to infer reasons for such changes in column selectivity and thereby lead to means for minimizing such changes (Section 3.3).

2.4.1. Solute hydrophobicity (η') as a function of molecular structure

The $\eta'\boldsymbol{H}$ term of Eq. (2) reflects the major contribution to RP-LC retention (hydrophobicity). In the absence of other contributions to retention, Eq. (2) becomes:

$$\log k = \log k_{EB} + \eta'\boldsymbol{H}$$

or

$$\eta' = -\left(\frac{\log k_{EB}}{\boldsymbol{H}}\right) + \left(\frac{1}{\boldsymbol{H}}\right)\log k = a + b\log k \qquad (5)$$

where a and b are constant for a given column and the present separation conditions. For a Symmetry C18 column and so-

Table 6
Solute parameters used for the measurement of values of $\boldsymbol{H}$, $\boldsymbol{S}^*$, etc. for different columns

Solute[a]	η'	σ'	β'	α'	κ'
Acetophenone	−0.744	0.133	0.059	−0.152	−0.009
Benzonitrile	−0.703	0.317	0.003	0.080	−0.030
Anisole	−0.467	0.062	0.006	−0.156	−0.009
Toluene	−0.205	−0.095	0.011	−0.214	0.005
Ethylbenzene	0	0	0	0	0
4-Nitrophenol	−0.968	0.040	0.009	0.098	−0.021
5-Phenylpentanol	−0.495	0.136	0.030	0.610	0.013
5,5-Diphenylhydantoin	−0.940	0.026	0.003	0.568	0.007
cis-Chalcone	−0.048	0.821	−0.030	0.466	−0.045
trans-Chalcone	0.029	0.918	−0.021	−0.292	−0.017
N,*N*-dimethylacetamide	−1.903	0.001	0.994	−0.012	0.001
N,*N*-diethylacetamide	−1.390	0.214	0.369	−0.215	0.047
4-*n*-Butylbenzoic acid	−0.266	−0.223	0.013	0.838	0.045
Mefenamic acid	0.049	0.333	−0.049	1.123	−0.008
Nortriptyline	−1.163	−0.018	−0.024	0.289	0.845
Amitriptyline	−1.094	0.163	−0.041	0.300	0.817

See discussions of [10,30] for experimental procedure and separation conditions (50% acetonitrile/pH 2.8 buffer; 35 °C).

[a] The retention of thiourea (equal to t_o) is also required for these conditions, for the calculation of values of k; similarly, the retention of berberine at pH 2.8 and 7.0 is required for the calculation of $\boldsymbol{C}$ at pH 7.0 (Eq. (12)). A total of 18 solutes is therefore involved.

lutes #1–67, the correlation of η' versus $\log k$ gives $\eta' = -0.92 + 0.92 \log k$; $r = 0.996$, S.E. = 0.05; i.e., in agreement with the form of Eq. (5). Other columns in the study of [4] yield similar correlations, supporting the conclusion that values of η' correlate well with values of $\log k$, and η' therefore corresponds to solute hydrophobicity. RP-LC retention has previously been used as an approximate measure of solute hydrophobicity [14,15], based on relationships similar to Eq. (5) for a given column (where $\boldsymbol{H}$ is constant):

$$\log k = c + dP_{o/w}$$

or

$$P_{o/w} = \left(\frac{1}{d}\right)(\log k)\left(\frac{c}{d}\right) \quad (6)$$

here c and d are constants for a given column and separation conditions, and $P_{o/w}$ is the octanol–water partition coefficient [14]. Comparing Eqs. (5) and (6), it can be concluded that values of η' are linearly related to values of $P_{o/w}$, further confirming the equivalence of values of η' and a quantity $P_{o/w}$ that is widely used as an approximate measure of compound hydrophobicity.

2.4.2. Solute "bulkiness" (σ') as a function of molecular structure

2.4.2.1. Correlations with molecular shape and length. The solutes of Table 3 (#32–40, 43, 44, 72, 73, 76–78, 88, 89) have values of $\delta \log k$, which are well correlated with each other. An examination of the structures of these compounds (Fig. 5) suggests similar molecular shape as a common factor among these correlating solutes. Thus, each compound is built around a common structural entity (I),

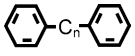

(I)

where $0 \le n \le 3$, and the two rings of (I) need not be fully unsaturated (e.g., #39, 40). Thus, molecular shape is suggested as a possible factor in the retention of each of the latter compounds. These solutes are also characterized by larger values of length to width, compared to other compounds (solutes #1–90 of [4,5], excluding the solutes of Fig. 5).

The following discussion supports a dependence of values of σ' on molecular size and shape, with additional contributions from highly-polar functional groups within the solute molecule. Thus, molecules of similar size, shape and functionality are predicted to have similar values of σ', which is observed for several groups of structurally-related compounds (Table 7; average standard deviation of σ' values for these "similar" solutes equal ± 0.04 σ'-units). Values of σ' also correlate moderately with solute molecular length L, as seen in Fig. 6 for the neutral solutes #1–45 of [4]. In Fig. 6, molecular length L is approximated by the number of atoms (excluding hydrogen) in the longest connected series that does not double back on itself (see [5] for details on the calculation of L).

Table 7
Similar values of the solute parameter σ' for solutes of near-identical size, shape and functionality

Solutes	Structure	Average σ'	S.D.
#40a, 42a	Dihalomethanes	−0.21	0.07
#68–70a, 77a	*p*-Halotoluenes, dichlorobenzene, *p*-xylene	−0.18	0.05
#63–66a, 72a	Monohalobenzenes, toluene	−0.15	0.05
#46, 49	Amitriptyline, nortriptyline	0.05	0.01
#56, 57	Diclofenate acid, mefenamic acid	0.33	0.10
#68,69	1,2- and 1,3-Dinitrobenzene	0.47	0.01
#72,73	2- and 3-Nitrobiphenyl	0.77	0.04
#39, 40	Steroids	0.97	0.01
Average			0.04

Data of [4,5].

Values of σ' can be estimated for any solute via the correlation of Fig. 6 for neutral solutes #1–45 of [4]:

$$\sigma'(\text{predicted}) = -0.90 + 0.155L \quad (r^2 = 0.79; \quad \text{S.D.} = 0.20) \quad (7)$$

Thus, σ' would have a value of about −0.9 for a hypothetical solute (of zero length), which experiences no steric repulsion from the stationary phase. The *difference* $\delta\sigma'$ between experimental and predicted (Eq. (7)) values of σ' can be defined:

$$\sigma'(\text{expt.}) - \sigma'(\text{predicted}) \equiv \delta\sigma' \quad (8)$$

Values of $\delta\sigma'$ can be compared with solute structure to infer molecular contributions to σ' *other* than those arising from solute length alone. Positive values of $\delta\sigma'$ mean larger values of σ' and greater steric resistance to (and exclusion from) the stationary phase (and vice versa for negative $\delta\sigma'$). For the neutral solutes plotted in Fig. 6, an examination of values of $\delta\sigma'$ does not suggest any consistent contribution of molecular shape (other than length) or functionality to σ'. Similarly, 87 neutral compounds from [13], including substituted benzenes and homologous series of varying molecular length, yield an

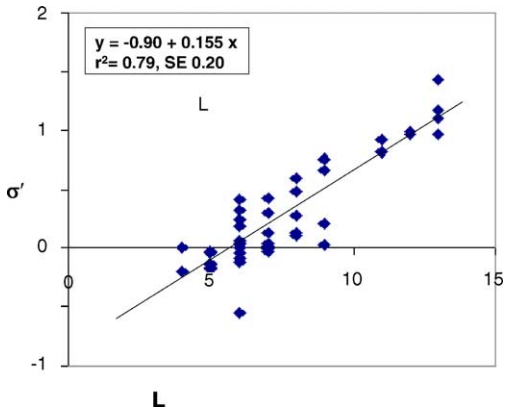

Fig. 6. Correlation of values of σ' with molecular length L for neutral solutes #1–45 of [4]. Reprinted from [5].

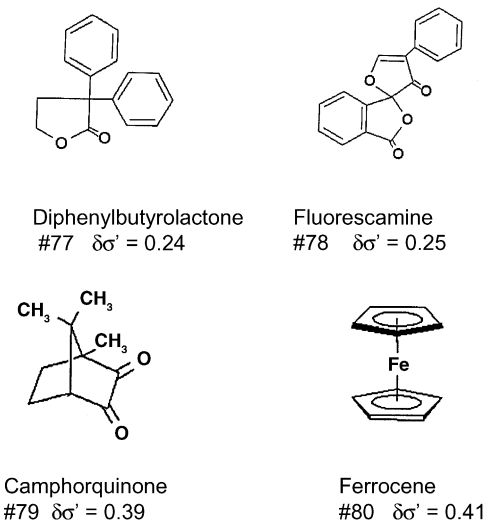

Fig. 7. Structures of neutral molecules with large values of $\delta\sigma'$; i.e., molecules that are "bulky" in three dimensions. See text for details.

average value of $\delta\sigma'$ equal to 0.00 ± 0.27. Values of σ' for homologs increase by ≈0.17 unit per $-CH_2-$ group [5].

2.4.2.2. Correlations with solute molecular "thickness" and hydrophilicity. There is some indication that increased three-dimensional "thickness" of a solute molecule (as opposed to length or width alone) leads to larger values of $\sigma'$and therefore larger values of $\delta\sigma'$, mainly for the case of very "thick" molecules. Although biphenyls are non-planar and therefore moderately "thick", values of $\delta\sigma'$ are close to 0 for this class of compounds [5]: for biphenyls not substituted in the 2-position, $\delta\sigma' = -0.01 \pm 0.23$; for biphenyls substituted in the 2-position, $\delta\sigma' = 0.10 \pm 0.33$ (1S.D.). The much greater non-planarity of 2-substituted biphenyls leads to only slightly larger values of σ'. Four compounds described in [4,5] are even "thicker" or more "three-dimensional" (Fig. 7), and the average value of $\delta\sigma'$ for these solutes is 0.32 ± 0.08. Thus, molecules that are thicker appear to have somewhat larger values of σ', apart from molecular length.

Values of σ' also appear to be affected by whether the solute is ionizable (e.g., an acid or a base), or substituted by hydrophilic groups such as –OH. Thus, for ionizable solutes #46–67 of [4], average values of $\delta\sigma'$ are -0.67 ± 0.28 (1S.D.) for the strong bases (#46–50), -0.75 ± 0.40 for the weak bases (#51–55), and -0.50 ± 0.35 for the weak acids (#56–67). While the scatter in values of σ' for each of these groups of solutes (S.D. of ±0.3–0.4 σ'-units) is greater than found for the neutral compounds of Fig. 6 (S.D. = 0.2), it is apparent that acids and bases have σ' values that are significantly lower than values for neutral solutes (by an average of 0.6 units). Seven alcohols from [13], as reported in [4], also have a hydrophilic end-group and smaller values of $\delta\sigma'$ (i.e., $\delta\sigma' = -0.4 \pm 0.2$ [1S.D.]).

2.4.2.3. A model of steric resistance ($\sigma'\boldsymbol{S}^*$). The above observations for σ' versus solute structure suggest an analogy with retention versus structure in size-exclusion chromatography (SEC [16]); namely, decreased retention for solutes with increased molecular length. In the latter form of chromatography (illustrated in Fig. 8a, "SEC"), retention is determined by the access of solute molecules to particle pores—longer molecules have larger hydrodynamic ("Stokes") diameters *d* and are excluded from narrower pores, those with diameters less than *d*. (In SEC, the solute has greater translational freedom in large pores than in small pores, so that a solute can access a greater fraction of the volume in a large pore than in a small pore. The accessible volume is known as the "free volume" and represents an entropic contribution to the free energy of a solute [17].) The exclusion of long molecules from small pores by an SEC retention process does not altogether prevent retention when the molecule is attracted to the stationary phase in RP-LC [18], but it is expected to reduce retention because of the latter entropic effect. A similar explanation for steric resistance in RP-LC (based on the dependence of σ' on solute molecular structure) is that the *spaces* between the alkyl ligands of the stationary phase provide the same restricted access to solute molecules that is provided in SEC by *pores* within the particle (see Fig. 8a, "$\sigma'\boldsymbol{S}^*$"). An important distinction between these two retention processes in Fig. 8a is that particle pores are rigid, whereas the spaces between ligands are less so.

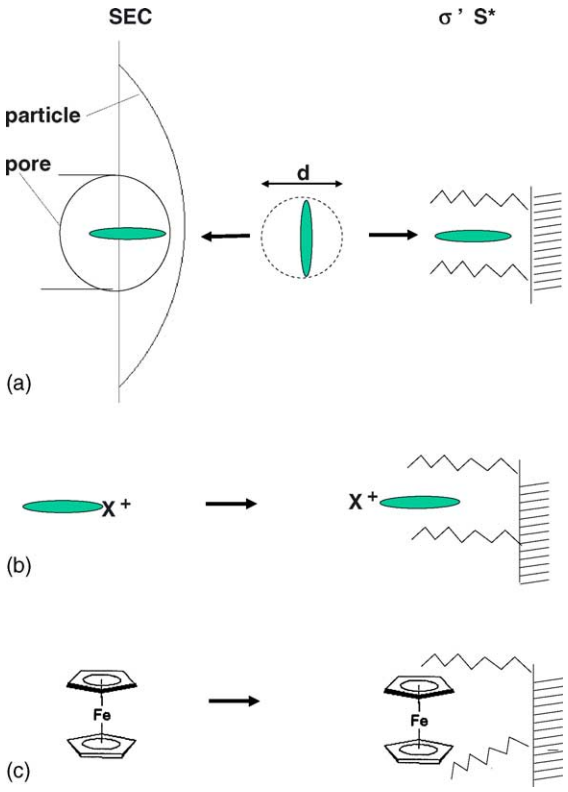

Fig. 8. Pictorial representation of steric resistance for different solute molecules and a comparison with size exclusion chromatography (SEC). See text for details. Reprinted from [5].

The acidic or basic solutes and alcohols noted above possess a terminal hydrophilic group that prefers to reside out-

side the hydrophobic stationary phase, resulting in a decrease in solute penetration into the stationary phase (with an accompanying decrease in steric resistance, and smaller values of σ'; Fig. 8b). Fig. 8c similarly illustrates the role of solute "thickness" in RP-LC retention. Molecules that are sufficiently "thick" will experience greater resistance (more constraint) in penetrating the stationary phase, and this resistance will increase for less penetrable stationary phases. To summarize, steric selectivity and the $\sigma'\boldsymbol{S}^*$ term of Eq. (2) can be described in terms of the ease of penetration of solute molecules between the ligands of the stationary phase. Solute molecules whose size and shape result in a greater constraint by surrounding alkyl ligands will experience greater steric interaction effects, resulting in larger values of σ'.

2.4.2.4. Steric resistance contrasted with "shape selectivity". "Shape selectivity" refers to the preferential retention of planar versus non-planar polycyclic aromatic hydrocarbons on some columns versus others [7]. This has been attributed to the presence of narrow openings or "slots" in the stationary phase that restrict the access of (thicker) non-planar molecules. Rigid stationary phases with narrow "slots" exhibit greater shape selectivity and are more likely to result from a synthesis that uses di- or tri-functional silanes (yielding cross-linked or "polymeric" phases with higher bonding density), rather than the more common monofunctional silanes (which result in less-rigid, "monomeric" phases). Shape selectivity can be characterized by a widely used test [19] that measures the separation factor $\alpha_{\mathrm{TBN/BaP}}$ for tetrabenzonaphthalene (TBN) and benzo(a)pyrene (BaP). A similar test for shape selectivity has been described in terms of the separation factor $\alpha_{\mathrm{T/O}}$ (the ratio of *k*-values for triphenylene versus *o*-terphenyl [9]). Larger values of $\alpha_{\mathrm{T/O}}$ or smaller values of $\alpha_{\mathrm{TBN/BaP}}$ for a column signify increased shape selectivity and a more rigid stationary phase. If shape selectivity were equivalent to steric resistance as measured by term (ii) of Eq. (2), there should be a strong positive correlation between values of $\boldsymbol{S}^*$ and either $\log\alpha_{\mathrm{T/O}}$ or $-\log\alpha_{\mathrm{TBN/BaPO}}$. Actual correlations have been reported [5,10]:

$$\boldsymbol{S}^* = -0.04 + 0.20\log\alpha_{\mathrm{TBN/BaP}} \quad (r^2 = 0.29, n = 14) \quad (9)$$

$$\boldsymbol{S}^* = -0.04 + 0.39\log\alpha_{\mathrm{T/O}} \quad (r^2 = 0.40, n = 15) \quad (10)$$

These correlations are relatively weak, and in the wrong direction for Eq. (9). Thus, shape selectivity and steric resistance are conceptually similar, but do not appear to describe the same column property. Shape selectivity involves the combination of relatively rigid solute molecules and "polymeric" stationary phases, while steric resistance applies to more flexible solute molecules and less rigid ("monomeric") stationary phases [5]. Examples of shape selectivity have most often been reported for mobile phases that contain ≥80% of the organic solvent B. Since most RP-LC separations are carried out on monomeric columns with mobile phases of <80% B, and do not involve non-planar polycyclic aromatic hydrocarbons as solutes, steric resistance seems more likely to represent a significant contribution to column selectivity for typical separations.

Table 8
Values of RP-LC hydrogen-bond basicity β' and acceptor strength β_2 in solution for various amide solutes

Solute	β'[a]	β_2[b]
10a. *N*,*N*-dimethylformamide	0.89	0.74
13a. *N*,*N*-dimethylacetamide	0.99	0.78
11a. *N*,*N*-diethylformamide	0.49	0.76
14a. *N*,*N*-diethylacetamide	0.53	0.78
12a. *N*,*N*-dibutylformamide	0.20	0.80
47a. *N*-benzylformamide	0.10	0.63

Data of [5].
[a] Data of [4].
[b] Data of [13].

2.4.3. Solute hydrogen bond basicity (β') as a function of molecular structure

The three amides of Table 5 are each characterized by strong hydrogen-bond basicity in solution ($0.63 \leq \beta_2 \leq 0.78$; see Eq. (1)), suggesting that the $\beta'\boldsymbol{A}$ term of Eq. (2) corresponds to hydrogen bonding of basic solutes to acidic silanols in the stationary phase. Five *N*,*N*-dialkyl amides of [13] also have large values of β' (0.20–0.99) and β_2 (0.74–0.80), but—unlike the case for β_2 (values of solute H-bond basicity in the mobile phase, rather than in the stationary phase [β'])—values of β' vary markedly with the degree of steric hindrance around the amide nitrogen (Table 8). That is, values of β' (but not β_2) sharply decrease with increased crowding of the amide group by longer alkyl groups attached to the amide-nitrogen (β' for dimethyl, 0.94 ± 0.07; diethyl, 0.51 ± 0.01; dibutyl, 0.20; β_2 for same five aliphatic amides = 0.77 ± 0.02). It appears that the C_{18} (or C_8) ligands that surround stationary phase silanols greatly enhance steric hindrance in the interaction of the silanol with a solute acceptor group X. Other workers have also noted that steric hindrance around hydrogen-bonding sites can be of greater importance in the RP-LC stationary phase than in solution [20].

Fig. 9a compares values of β' versus β_2 for polar aliphatic solutes R–X which have similar alkyl substitution around the polar group X (either *n*-butyl or di-ethyl; i.e., R = C_4 in each case), and presumably similar steric hindrance. A significant correlation is observed in Fig. 9a ($r^2 = 0.85$), as expected if β' corresponds to solute hydrogen-bond basicity within the stationary phase. A similar plot is shown in Fig. 9b for corresponding aromatic solutes (C_6H_5–X). As seen in Fig. 9b versus Fig. 9a, values of β' are generally about six-fold smaller for aromatic versus aliphatic solutes; this is likely due to (a) greater steric hindrance by adjacent phenyl versus *alkyl* groups and (b) electron induction from X to the aromatic ring (thereby decreasing the basicity of X). The greater scatter of data in Fig. 9b versus Fig. 9a can be attributed to the much smaller values of β' for the aromatic solutes in Fig. 9b. The correlations of Fig. 9 are consistent with our belief that the $\beta'\boldsymbol{A}$ term of Eq. (1) arises from hydrogen bonding between

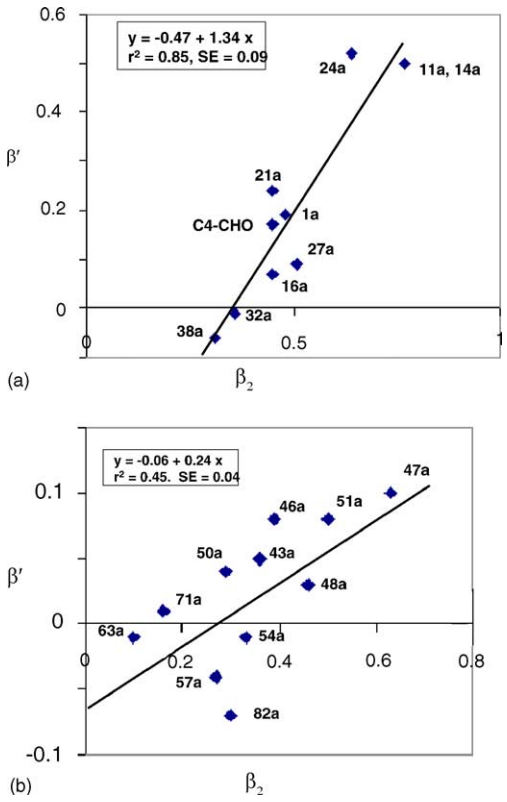

Fig. 9. Correlation of the solute parameter β' with solution values of β_2 (hydrogen bond acceptor strength from [13]). (a) Aliphatic solutes with comparable inter-molecular hindrance of the acceptor group (C_4 or diethyl derivatives); (b) aromatic solutes. Solute numbering defined in Table 7 of [4]. Reprinted from [5].

acceptor solutes and non-ionized silanols (donors) in the stationary phase.

2.4.4. Solute hydrogen bond acidity (α') as a function of molecular structure

Hydrogen bonding of acidic solutes to basic groups within the stationary phase has been reported as a minor contribution to RP-LC column selectivity [8,13], but has otherwise received little attention in the literature. Large values of α' are associated primarily with carboxylic acids ($0.36 \leq \alpha' \leq 3.10$ [5]), suggesting that these compounds can hydrogen bond to some basic group in the stationary phase, in which case a correlation of values of α' with α_2^H of Eq. (1) is expected. Table 9 compares values of α' for different groups of donor solutes with their hydrogen-donor acidity α_2^H in solution (last column of Table 9). Whereas donor strength in solution ($0.32 \leq \alpha_2^H \leq 0.6$) suggests that alcohols and phenols should also have large values of α', this is not the case ($0.1 \leq \alpha' \leq 0.2$). There is, however, a regular increase in values of α' with increasing Bronsted acidity of the solute (as reflected in solute pK_a values in water).

Steric hindrance, as in the example of Table 8 for hydrogen-bond solutes and column silanols, appears to be an unlikely explanation for the smaller α' values of phenols and especially alcohols. The preferential binding of carboxylic acids versus phenols and alcohols can be rationalized, however, if it is assumed that column hydrogen-bond basicity arises from *water* that is sorbed within the stationary phase; in this case, carboxylic acids R–COOH can hydrogen bond to water by a two-fold interaction:

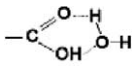

(II)

Further evidence, which supports this hypothesis, is presented in Section 2.4.9 below.

2.4.5. Molecular charge (κ') as a function of molecular structure

The RP-LC separation of protonated bases by means of alkyl-silica columns has received considerable attention in the literature, primarily because of increased peak tailing for these compounds [21]. Evidence has been reported [21,22] that suggests peak tailing is related to the interaction of protonated bases with ionized silanols in the stationary phase (at least for a mobile phase pH > 6 [23]); i.e., an ion-interaction or ion-exchange process. If the $\kappa' \boldsymbol{C}$ term of Eq. (2) is the result of ionic interaction between a charged (ionized) solute molecule and a negatively charged silanol ($-SiO^-$) in the stationary phase, there should be a correlation between values of κ' at a given pH and the fractional charge on the solute molecule: positive values of κ' for protonated bases,

Table 9
The solute parameter α' as a function of solute donor strength

Solute type	Solutes[a]	Average α'	S.D.	$\alpha_2^H(12)$
Neutral non-donors	#1–45 Except R—OH	0.02	0.12	0.00
Alcohols	#18–20, 39, 40	0.10	0.17	0.32–0.39
Phenols	#21, 22, 24–26, 75, 76, 82, 83, 88[b]	0.17	0.09	0.60
Activated —OH	#23, 87 (Vicinal diol)	0.52	0.13	
	#42	0.58		
Weak acids	#56–58, 60–63, 65–67[c]	0.88	0.33	0.59
Strong acids	#59, 64[d]	2.28	1.16	

Data of [4,5].
[a] Solute numbering given in [4,5].
[b] Solutes #84 and 86 not included, because of poor agreement with Eq. (2).
[c] Ionization ≤10% in 50% acetonitrile/pH 2.8 buffer.
[d] Ionization ≥37% in 50% acetonitrile/pH 2.8 buffer.

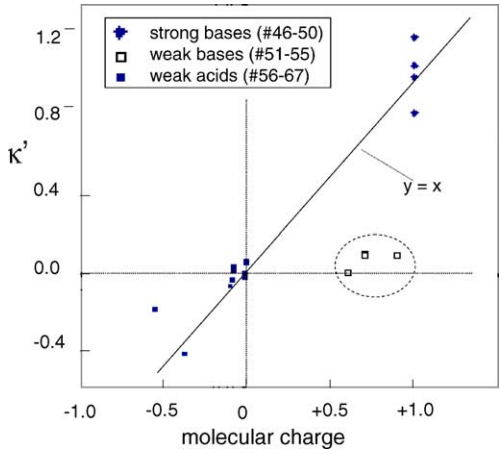

Fig. 10. Correlation of values of the parameter κ' for basic and acidic solutes (#46–67 of [4]) with the average charge on the solute molecule at pH 2.8 (as a result of varying degrees of ionization). Molecular charge is estimated from changes in retention as a function of mobile phase pH. Data of [4,12].

and negative values for ionized acids (note that the neutral solutes of [4,5] have an average value of $\kappa' = -0.01 \pm 0.03$).

As expected, a correlation between values of κ' and solute molecular charge is observed (Fig. 10, mobile phase pH 2.8), except for partly-ionized, weak bases (circled). Partly-ionized bases are retained mainly as the neutral species (for which $\kappa' = 0$), so absolute values of κ' for these compounds are expected to be lower than their absolute molecular charge (i.e., fractional ionization values). A similar reduction in $|\kappa'|$ for partly-ionized acids is not observed, perhaps because of the difference between ion–ion attraction (protonated bases) versus repulsion (ionized acids). The correlation of Fig. 10 suggests that for some type-B columns there is a negative charge on the stationary phase at pH 2.8, despite the usual assumption that very acidic silanols are largely absent from metal-free silicas [21,22], with no silanol ionization at low pH. Values of κ' for a given solute are expected to vary with its relative ionization, and therefore with mobile phase pH.

2.4.6. Column hydrophobicity *H* as a function of column properties

The column parameters ***H***, ***S****, etc. of Eq. (2) are necessarily related to properties of the column: ligand length (e.g., C_8 versus C_{18}), ligand density (μmoles/m^2), particle pore diameter (nm) and whether or not the column has been end-capped. It was suggested above that values of ***A*** and ***C*** are determined by underivatized silanols on the silica surface; values of ***A*** and ***C*** should therefore be affected by the concentration and accessibility of these silanol groups. ***A*** is further affected by the hydrogen-bond strength of these silanols, and ***C*** is a function of their relative ionization or acidity (i.e., silanol pK_a values); the latter two column properties can vary for silicas produced by different manufacturers, because of differences in the concentrations of contaminating metals and/or interactions between adjacent silanols [21,22]. Because several column properties can affect values of ***H***, ***S****, etc., in the following analysis of the dependency of these parameters on column properties we have tried to compare columns where just one column property is varied at a time. Table 10 summarizes values of ***H***, ***S****, etc. for several such column comparisons (we assume that silanol acidity will be similar in related type-B columns from the same manufacturer).

Column hydrophobicity increases with increased interaction of the solute with the alkyl ligands of the column. This suggests that ***H*** should increase for an increase in ligand density (concentration C_L) and ligand length. The curvature of narrow pores results in a closer approach of the ends of the ligands, which translates into an effectively higher average ligand density, especially for pore diameters $d_p \leq 10$ nm and C_8 or C_{18} chains [5]. Values of ***H*** should therefore increase for smaller d_p. Finally, when conventional C_{18} columns are end-capped, there is typically no more than a 3–5% increase in total carbon [24,25], so only a small increase in ***H*** should result from end-capping. Each of these predictions can be compared with the data of Table 10.

For an increase in C_L from 0.9 to 1.6 to 2.9 μmoles/m^2 (example #6 of Table 10; C_{18}, 8-nm pores), ***H*** increases from 0.76 to 0.93 to 1.13. For an increase in ligand length from C_3 to C_8 to C_{18} (examples #1–3; 8-nm pores and 2.0 μmoles/m^2), ***H*** increases from 0.60 to 0.79 to 1.01. For a decrease in pore diameter from 30 to 8 nm (examples #1–3; 2.0 μmoles/m^2, C_3–C_{18}), ***H*** increases by an average of 0.09 ± 0.01 (1S.D.). For a decrease in pore diameter from 30 to 6 nm (examples #4,5; 3.2 μmoles/m^2, C_8 and C_{18}), ***H*** increases by an average of 0.20 ± 0.01. End-capping (example #7, other column properties exactly the same) results in an increase in ***H***, but by only 0.02 units. Thus, *all of these comparisons (as well as others that can be drawn from the data of* Table 10*) are consistent with an identification of* **H** *with column hydrophobicity*.

2.4.7. Column steric resistance *S** as a function of column properties

S*, the resistance by the column to the penetration of bulky solutes into the stationary phase, should increase with column properties in the same way as values of ***H***. Thus, an increase in ligand density C_L (with increased ligand crowding) should more effectively restrict the insertion of solute molecules, resulting in larger values of ***S****. Longer ligands will be more crowded at their ends, especially for narrower-pore particles, so that ***S**** should also increase for longer ligands and smaller pores. End-capping is expected to have only a minor effect on values of ***S****. It should be kept in mind that, in contrast to ***H***, an increase in ***S**** corresponds to a *decrease* in retention (α), other factors being equal (Eq. (2)).

For an increase in C_L from 0.9 to 1.6 to 2.9 μmoles/m^2 (example #6 of Table 10), ***S**** increases from -0.04 to -0.03 to 0.06. For an increase in ligand length from C_3 to C_8 to C_{18} (examples #1–3), ***S**** increases from -0.12 to -0.08 to -0.02. For a decrease in pore diameter from 30 to 8 nm (examples #1–3; 2.0 μmoles/m^2, C_3–C_{18}), ***S**** increases by an average of

Table 10
Values of the column selectivity parameters ***H***, ***S****, etc. as a function of column properties

Column	d_p[a]	C_L[b]	*H*	***S****	***A***	***B***	***C***(2.8)	***C***(7.0)
#1 C_3[c]								
	8	2	0.601	−0.124	−0.08	0.038	−0.084	0.81
	30	2	0.526	−0.122	−0.194	0.047	0.057	0.711
(8–30 nm)			0.08	0.00	0.11	−0.01	−0.14	0.10
#2 C_8[c]								
	8	2	0.795	−0.079	0.138	0.018	0.014	1.02
	30	2	0.701	−0.085	0.002	0.047	0.146	0.82
(8–30 nm)			0.09	0.01	0.14	−0.03	−0.13	0.20
#3 C_{18}[c]								
	8	2	1.008	−0.021	0.215	−0.002	0.077	0.822
	30	2	0.906	−0.05	0.045	0.043	0.253	0.7
(8–30 nm)			0.10	0.03	0.17	−0.05	−0.18	0.12
#4 C_8[d]								
	6	3.2	0.929	−0.015	0.162	−0.017	−0.313	1.005
	30	3.2	0.739	−0.041	−0.13	0.027	0.156	0.405
(6–30 nm)			0.19	0.03	0.29	−0.04	−0.47	0.60
#5 C_{18}[d]								
	6	2.9	1.158	0.041	0.067	−0.078	0.102	0.262
	30	2.9	0.956	−0.012	−0.089	0.015	0.238	0.249
(6–30 nm)			0.20	0.05	0.16	−0.09	−0.14	0.01
#6 C_{18}[e]								
	8	0.9	0.762	−0.036	−0.216	−0.001	−0.4	0.345
	8	1.6	0.926	−0.026	−0.123	−0.004	−0.294	0.139
	8	2.9	1.132	0.059	−0.023	−0.068	−0.242	−0.161
(2.9–0.9 μmoles/m^2)			0.37	0.10	0.19	−0.07	0.16	−0.51
#7 C_{18}[f]								
Non-end-capped	9	3.17	1.03	0.029	0.388	−0.023	0.038	0.812
End-capped	9	3.17	1.048	0.057	0.007	−0.004	−0.179	0.151
End-capped–Non-end-capped			0.02	0.03	−0.38	0.02	−0.22	−0.66

Data from [10].
[a] Pore diameter (nm).
[b] Ligand concentration (μmoles/m^2).
[c] Agilent Zorbax StableBond columns of varying pore diameter and ligand length (not end-capped).
[d] Bischoff Prontosil columns #14, 17, 20, 23 of [10] (end-capped).
[e] Waters J'Sphere columns #82a–c of [10] (end-capped).
[f] Waters Symmetry C18 column described in [10].

0.01 ± 0.02. For a decrease in pore diameter from 30 to 6 nm (examples #4,5; 3.2 μmoles/m^2, C_8 and C_{18}), ***S**** increases by 0.03 ± 0.01. End-capping (example #7) results in an increase in ***S**** by 0.03 units. *Each of these comparisons appears consistent with an interpretation of* **S*** *as steric resistance by the column to the insertion of bulky solute molecules*.

2.4.8. Column hydrogen-bond acidity ***A*** *as a function of column properties*

End-capping of the column (usually by trimethylsilyl [TMS] groups) removes a substantial fraction of underivatized silanols that are left after the primary bonding (e.g., by C_8 or C_{18}) of the column. Thus, a typical 3–5% increase in total carbon as a result of end-capping a C_{18} column [24,25] corresponds to a 20–30% decrease in the total moles of unmodified silanols. End-capping also results in a decrease in silanol accessibility, because of steric hindrance between underivatized silanols and adjacent end-capping groups. Thus, end-capping is expected to strongly reduce the value of ***A*** for a column. As seen in example #7 of Table 10, this is the case: a reduction in ***A*** by 0.38 units results when the column is end-capped.

The expected variation of ***A*** with other column properties is less obvious versus that of ***H*** and ***S****. Thus, an increase in ligand concentration (e.g., C_8 or C_{18} groups) might appear to reduce the concentration of underivatized silanols, but for end-capped columns (as in example #6 of Table 10) just the opposite is true—because end-capping with the small trimethylsilane (TMS) group results in a higher fraction of derivatized silanols than bonding by C_{18} groups [25]. That is, the portion of the silica surface not initially bonded by C_{18} will be more extensively reacted by TMS groups. In example #6, an increase in C_L from 0.9 to 1.6 to 2.9 μmoles/m^2 for this end-capped column results in an increase in ***A*** from −0.22 to −0.12 to −0.02, as anticipated from the corresponding increase in the number of underivatized silanols.

Other factors being equal, it might appear that an increase in ligand length should render the surface silanols less acces-

sible to retained solutes, with a reduction in values of ***A***. The columns of examples #1–3 of Table 10 are not end-capped, and values of C_L are constant (2.0 μmoles/m^2), so the effect of ligand length on values of ***A*** can be deduced from these data. For both the 6- and 30-nm-pore columns, an increase of ligand length leads to a consistent and counter-intuitive *increase* in ***A***; the increase in ***A*** for C_8 versus C_3 is 0.20 ± 0.01, and for C_{18} versus C_8 the increase in ***A*** is 0.06 ± 0.03. For similar reasons, it would seem that values of ***A*** should be larger for larger-pore columns, based on increased silanol accessibility. Again, an opposite trend of ***A*** with pore diameter is observed: for an increase from 8- to 30-nm pores (examples #1–3), the change in ***A*** is −0.11 (C_3), −0.14 (C_8) and −0.17 (C_{18}).

To summarize, for a column in which the relative concentration of underivatized silanols is lower (as a result of end-capping and/or changes in C_L), values of ***A*** are also lower, as predicted. For less obvious reasons, changes in ligand length and pore diameter which seem likely to promote silanol accessibility lead instead to a decrease in values of ***A***. Possibly the different bonding chemistries involved in the preparation of C_3, C_8 and C_{18} columns, as well as pore diameter per se, in some way affect the hydrogen-bond acidity of remaining underivatized silanols (silanol acidity may be more important than silanol accessibility in affecting ***A***). However, an alternative possibility that we prefer is that electron-donor solutes that interact with non-ionized silanols are stabilized ("pulled" further into the stationary phase) as a result of increased hydrophobic interaction; i.e., as a result of longer ligands and/or reduced pore diameter). The interaction of the solute with a silanol group should thereby be strengthened, corresponding to an increase in the value of ***A***. The latter effect would also contribute to the above increase in ***A*** for increased ligand concentration.

2.4.9. Column hydrogen-bond basicity *B* as a function of column properties

The origin of column hydrogen-bond basicity (acceptor strength) has received little attention in the literature, although silica silanols and siloxane groups represent possible basic sites within the stationary phase. For example, it has been proposed that hydrogen-bonding of one silanol by another results in increased basicity for the proton-donating silanol [26]. If either silanol or siloxane groups are responsible for column basicity, end-capping of a column should result in a pronounced decrease in ***B***, because of steric hindrance by the end-capping groups to interaction of the solute with adjacent silanol or siloxane groups (similar to the above reduction in ***A*** after end-capping). End-capping would also sterically block any end-capped silanols, which should further reduce ***B*** if silanols are the entity responsible for column hydrogen-bond basicity.

As seen in example #7 of Table 10, end-capping instead leads to a small *increase* in ***B*** (+0.02 units). Likewise, if a single basic site in the column were responsible for its hydrogen-bond basicity, values of α' for phenols and alcohols should be comparable to values of α' for carboxylic acids, whereas this is not the case (Section 2.4.4 and Table 9). A possible explanation that addresses the latter two observations is that *water* sorbs into the stationary phase and is responsible for column hydrogen-bond basicity. If this is the case, values of ***B*** should increase with increasing concentrations of water in the stationary phase, while the concentration of sorbed water should *decrease* with increasing column hydrophobicity ***H***. Therefore, if column hydrogen-bond basicity is due to sorbed water, values of ***B*** should correlate inversely with values of ***H***. For 87 type-B alkyl-silica columns reported in [10], an approximate correlation of the predicted form was found:

$$\boldsymbol{B} = 0.131 - 0.141\boldsymbol{H}; \quad r^2 = 0.61; \quad \text{S.D.} = 0.015 \qquad (11)$$

A cross correlation was also carried out between all other pairs of column parameters (***H*** versus ***S****, ***A*** versus ***B***, etc.) for the same 87 columns, with $0.01 \leq r^2 \leq 0.18$. Only the correlation between ***H*** and ***B*** (Eq. (11)) is statistically significant, which in turn requires interpretation. Individual examples of this inverse dependence of ***B*** on ***H*** can also be seen in the data of Table 10. If water is responsible for the interaction of hydrogen-bond acids with the column, this also explains the much stronger interaction of acids versus phenols (Section 2.2.4). Because end-capping does not result in a significant decrease in values of ***B***, it appears that stationary phase water, if it contributes to hydrogen-bond basicity, is *not* bound to silanols at the silica surface

Despite the above experimental evidence, which suggests water as the source of column hydrogen-bond basicity, at present we regard this hypothesis as speculative and much in need of further confirmation. However, whatever the source of hydrogen-bond column basicity, it does represent a significant contribution to column selectivity. Some columns, other than type-B alkyl-silica, appear to involve basic, hydrogen-bonding retention sites other than stationary phase water (Sections 2.5.2 and 2.5.3).

2.4.10. Column cation exchange capacity *C* as a function of column properties and mobile phase pH [12]

Alkyl-silica columns normally possess a negative charge that results from the ionization of underivatized silanol groups: $-\text{Si}-\text{OH} \rightarrow -\text{Si}-\text{O}^- + \text{H}^+$. As mobile phase pH increases, silanol ionization and the negative charge on the column increase, as therefore should values of ***C***. Newer columns made from pure silica (type-B) are somewhat less acidic than are older, less pure columns (type-A), so their ionization and values of ***C*** should be reduced compared to type-A columns. The dependence of the column negative charge on column type and mobile phase pH is illustrated in Fig. 11, which shows experimental plots of the negative charge on two different columns (one type-A, the other type-B) as a function of pH. Because values of ***C*** are believed to be proportional to the charge on the column, ***C*** should increase with mobile phase pH in similar fashion as in Fig. 11.

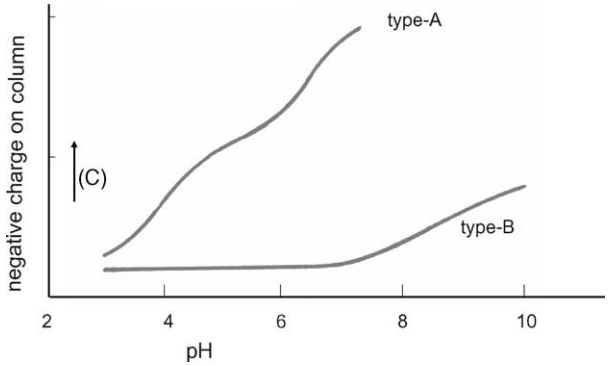

Fig. 11. Silanol ionization as a function of mobile phase pH and silica type [27]. See text for details. Adapted from [11].

Values of ***C*** at pH 2.8 (***C***(2.8)) can be obtained from Eq. (2) in the same way as for other column parameters that are measured at pH 2.8. Values of ***C***(7.0), the value of ***C*** at pH 7.0, are determined from the change in retention of the quaternary ammonium compound berberine at pH 2.8 and 7.0, with other conditions the same (50% acetonitrile/60 mM phosphate buffer; 35 °C):

$$\boldsymbol{C}(7.0) = \boldsymbol{C}(2.8) + \log\left(\frac{k_{7.0}}{k_{2.8}}\right) \quad (12)$$

where $k_{7.0}$ and $k_{2.8}$ refer to values of k for berberine at pH 7.00 and 2.80, respectively. The derivation of Eq. (12) [12] is based on the fact that $\kappa' \approx 1.0$ for fully ionized, mono-basic solutes, plus the assumption that only the $\kappa'\boldsymbol{C}$ term of Eq. (2) changes with pH (due to the changing ionization of the column as in Fig. 11). The use of a quaternary ammonium test solute in Eq. (12) was suggested by the earlier work of Neue et al. [28].

From Fig. 11, it can be anticipated that values of ***C***(7.0) will be generally larger than values of ***C***(2.8), and this is usually observed. For 87 type-B alkyl-silica columns (C_3–C_{30}), the average values of ***C*** at 2.8 and 7.0 were 0.04 ± 0.18 and 0.23 ± 0.31, respectively. Similarly, values of ***C*** should be greater for type-A versus type-B columns, which is also the case: for an average type-A column (C_8, C_{18}), ***C***(2.8) = 0.74 ± 0.57; ***C***(7.0) = 1.14 ± 0.56 ([11]; $n = 38$). In some cases, ***C***(7.0) < ***C***(2.8) for a given column, which may be attributable to differences in the ionic strength of the buffers used to measure ***C***(7.0); i.e., for the same phosphate-buffer concentration in the mobile phase (30 mM), phosphate ionization and ionic strength is greater at pH 7, which should reduce any ion-exchange interaction between berberine and ionized silanols. Ion-pairing of protonated solute with the anionic buffer may also be a factor [29].

Finally, it should be noted that what has been referred to above as the "ion-exchange" behavior of protonated bases in RP-LC is unlikely to represent a complete description of the interaction of these compounds with column $-SiO^-$ groups. For example, it has recently been proposed [29] that mobile and stationary phase ion-pairing can play a significant role in the retention of protonated bases in RP-LC. We therefore prefer to ascribe the $\kappa'\boldsymbol{C}$ term of Eq. (2) to "ion interaction" rather than "ion exchange".

2.5. Selectivity of other column types (relative values of ***H***, ***S****, etc.)

The preceding discussion is largely based on results for alkyl-silica columns made from high-purity (basic or type-B) silica. Eq. (2) has also been used to characterize several other kinds of column for RP-LC separation, as described below.

2.5.1. The accuracy of Eq. (2) for other column types; additional solute–column interactions

Eq. (2) has now been applied to almost 200 type-B alkyl-silica columns ranging from C_1 to C_{30}, most of which are either C_8 or C_{18}. The measurement of values of ***H***, ***S****, etc. for these columns has employed the 16 test solutes and corresponding solute parameters of Table 6 plus the experimental conditions and procedure described in [10] (50% acetonitrile/pH 2.8 buffer; 35 °C); the agreement of these retention measurements for type-B alkyl-silica columns with Eq. (2) and the values of η', σ', etc. of Table 6 is ±1% in α (avg. S.D.). The inter-laboratory repeatability of values of ***H***, ***S****, etc. determined in this way has also been confirmed [30] (***H***, ±0.003; ***S****, ±0.001; ***A***, ±0.022; ***B***, ±0.001; ***C***(2.8), ±0.010; ***C***(7.0), ±0.019 [avg. S.D.]), equivalent to a ±1% uncertainty in predicted values of α. Specifications have also been defined for the required accuracy of the experimental conditions used (temperature, %-acetonitrile and pH) [30].

Eq. (2) can be applied to other column types, by assuming that the test-solute parameters of Table 6 for type-B alkyl-silica columns apply for any column. Experimental values of α for these 16 test solutes and a given column can then be fit to the latter solute parameters by a single multiple linear regression, to yield values of ***H***, ***S****, etc. for that column. This extension of Eq. (2) to alternative column types generally results in poorer correlations; i.e., average errors in α > ±5% (1S.D.). Poorer agreement with Eq. (2) *could* be the result of additional solute–column interactions not represented in Eq. (2), as indeed proposed below for the case of phenyl and fluoro columns (Sections 2.5.6 and 2.5.7).

For all but fluoro and bonded-zirconia columns, however, it appears that the major reason for the poorer agreement with Eq. (2) is a consequence of the values of η', σ', etc. assumed for the 16 test solutes of Table 6 (which are average values derived for type-B alkyl-silica columns). Thus, the application of Eq. (2) to very different columns (with very different values of ***H***, ***S****, etc.) represents an extrapolation of Eq. (2)—with an increased uncertainty commonly associated with extrapolation. The latter hypothesis is confirmed by the observation that values of S.D. (for the application of Eq. (2) to the various column types studied) correlate with absolute differences in values of ***H***, ***S****, etc. for a given column ver-

sus average values for type-B, alkyl-silica columns ($\boldsymbol{H}_b$, $\boldsymbol{S}^*_b$, etc.):

$$\text{S.D.} = -0.006 - 0.001|\boldsymbol{H} - \boldsymbol{H}_b| + 0.030|\boldsymbol{S}^* - \boldsymbol{S}^*_b| + 0.041|\boldsymbol{A} - \boldsymbol{A}_b| + 0.311|\boldsymbol{B} - \boldsymbol{B}_b| + 0.010|\boldsymbol{C} - \boldsymbol{C}_b| \quad (r^2 = 0.923;\ \text{S.D.} = 0.008) \quad (13)$$

Eq. (13) has been found applicable for most RP-LC columns (type-A and -B alkyl-silica, cyano, phenyl, and columns with a polar group that is either embedded or used for end-capping; see [31,32] and summaries in [11,33].

The correlation of Eq. (13) suggests that smaller S.D. values will result for columns other than type-B alkyl-silica, if slightly different values of η', σ', etc. are assumed for each column type. The accuracy of Eq. (2) for a given column type other than type-B alkyl-silica can therefore be improved by iterative multiple linear regression, so as to derive best values for *both* solute and column parameters for each column type (rather than assuming that the values of η', σ', etc. in Table 6 apply for all columns). With this approach for different column types, agreement with Eq. (2) generally improves to acceptable levels (±1–3% in α), with resulting change in values of η', σ', etc., *but negligible change in values of the column parameters* **H**, **S***, *etc.* [11,31–33]. Therefore, values of $\boldsymbol{H}$, $\boldsymbol{S}^*$, etc. (summarized in Appendix A for all columns) were derived for each column type by means of the values of η', σ', etc. in Table 6 (single multiple linear regression). Acceptable (best-fit) agreement with Eq. (2) could not be obtained in the case of fluoro or bonded-zirconia columns (Sections 2.5.7 and 2.5.8), because too few columns of these types were available ($3 \le n \le 5$; a minimum of eight columns appear to be required for the derivation of reliable values of η', σ', etc. for a given column type). Higher values of S.D. than predicted by Eq. (13) suggest that solute–column interactions other than those represented in Eq. (2) may be important for both fluoro and bonded-zirconia columns.

2.5.2. *Type-A alkyl-silica columns [11]*

"Acidic" or type-A alkyl-silica columns are made from less pure silica that is contaminated by metals such as Al(III) and Fe(III). As a result, the underivatized silanols of type-A columns are more acidic, resulting in increased silanol ionization as a function of pH (Fig. 11), and presumably increased hydrogen-bond acidity. Most type-A columns are also based on older, less efficient bonding processes. As a result, the ligand concentration C_L for type-A columns is typically about 30% lower than for (more recently introduced) type-B columns [11]. These differences in column properties for type-A versus type-B columns account for most of the average differences in selectivity for type-A versus type-B columns.

Correlations of retention data for 38 type-A alkyl-silica columns and the test solutes of Table 6 with Eq. (2) [11], using values of η', σ', etc. from Table 6, resulted in an average S.D. = 0.032 (±8% in α). Further regression to obtain best-fit values of the column and solute parameters (and minimum average S.D.) yielded a final fit with Eq. (2) of ±3% in α, suggesting that no solute–column interactions other than those described by Eq. (2) are important for type-A columns.

Average values of $\boldsymbol{H}$, $\boldsymbol{S}^*$, etc. for C_{18} type-A versus type-B columns are compared in Table 11. Values of $\boldsymbol{H}$ and $\boldsymbol{S}^*$ for type-A columns are seen to be lower than for type-B columns (by −0.15 and −0.07 units, respectively), which can be attributed to generally lower values of C_L for type-A columns. Similarly, values of $\boldsymbol{A}$, $\boldsymbol{C}$(2.8) and $\boldsymbol{C}$(7.0) are much higher for type-A columns (by 0.19, 0.72 and 0.96 units, respectively), as predicted from the greater acidity of type-A columns. The average value of $\boldsymbol{B}$ for type-A columns is higher (0.06 units), which results from two separate effects. Values of $\boldsymbol{B}$ tend to correlate negatively with $\boldsymbol{H}$ (Eq. (11)), which means that the smaller values of $\boldsymbol{H}$ for type-A columns should result in larger values of $\boldsymbol{B}$. However, this is only part of the story. Fig. 12a shows a plot of values of $\boldsymbol{B}$ versus $\boldsymbol{H}$ for *type-B* alkyl-silica columns. The inverse correlation described by Eq. (11) is evident, and the dashed lines correspond to values of ±2.5S.D. As expected, virtually all the data points fall within the dashed lines of Fig. 12a. In Fig. 12b, a similar plot is shown for 38 *type-A* alkyl-silica columns, with the dashed lines of Fig. 12a superimposed. Thirteen type-A columns (enclosed in the dashed circle of Fig. 12b) deviate from Eq. (11) by more than 2.5S.D., and *all* of these deviations are positive. This suggests some additional contribution to $\boldsymbol{B}$ for these particular type-A columns, possibly related to the contaminating metals associated with type-A silica. The latter possibility is strengthened by the fact that all seven columns (half of the circled outliers in Fig. 12b) from two manufacturers (Jones, #12a–14a [Apex columns]; Supelco, #21a–24a [Supelcosil LC columns]), are included among the deviating type-A columns. This is consistent with the likely use of the same or similar silica by an individual manufacturer. *To summarize, we propose that carboxylic acids can interact with exposed metals present as part of the type-A silica surface, leading to their increased retention on some type-A columns* (note that carboxylic acids are able to interact strongly with multiply charged metal ions by chelation).

Values of $\boldsymbol{H}$, $\boldsymbol{S}^*$, etc. for different type-A columns tend to be more variable than for type-B columns as a group [11]. It is therefore more difficult to replace a type-A column with an equivalent type-A column (i.e., with similar values of $\boldsymbol{H}$, $\boldsymbol{S}^*$, etc.) from a different source—compared to the similar replacement of a type-B column by a type-B column from an alternative source [11]. The greater variability of type-A columns is likely a consequence of (a) the use of less optimized (and more variable) processes for column manufacture prior to 1990 [34] and (b) the greater variability of older silicas from manufacturer to manufacturer (e.g., varying silica purity).

2.5.3. *Columns with embedded polar groups (EPG) [31]*

Columns of this type have a polar functional group that is inserted ("embedded") within an alkyl ligand that is at-

Table 11
Comparison of the average selectivity of different column types

Column	H[b]	S^*	A	B	C(2.8)	C(7.0)
Type-B						
C_8	0.83	−0.01	−0.16	0.02	0.02	0.31
C_{18}	1.00	0.01	−0.07	−0.01	0.05	0.17
Type-A						
C_{18} [11]	0.84	−0.06	0.12	0.05	0.78	1.13
Difference[a]	−0.15	−0.07	0.19	0.06	0.72	0.96
Polar group embedded [31]	0.68	0.00	−0.54	0.17	−0.65	0.13
Difference[b]	−0.26	−0.01	−0.43	0.17	−0.69	−0.09
Polar group end-capped [31]	0.94	−0.02	−0.01	0.01	−0.14	0.27
Difference[b]	0.00	−0.03	0.10	0.01	−0.18	0.05
Cyano [32]	0.41	−0.11	−0.58	−0.01	0.07	0.67
Difference[c]	−0.28	−0.12	−0.22	−0.03	0.02	0.47
Phenyl [32]	0.60	−0.16	−0.23	0.02	0.16	0.74
Difference[d]	−0.23	−0.15	−0.07	0.00	0.14	0.43
Fluoroalkyl [33]	0.7	−0.03	0.1	0.04	1.03	1.42
Difference[d]	−0.13	−0.02	0.26	0.02	1.01	1.11
Fluorophenyl [33]	0.63	0.14	−0.26	0.01	0.55	1.1
Difference[e]	0.03	0.30	−0.03	−0.01	0.39	0.36
Bonded-zirconia [11][a]	1.03	−0.01	−0.43	0.05	2.08	1.98
Difference[a]	0.03	−0.02	−0.36	0.06	2.03	1.81
Polymeric alkyl-silica [11][f]	0.94	0.04	0.42	−0.02	0.69	1.38
Difference[f]	0.10	0.10	0.30	−0.07	−0.09	0.25

Data of [10,11,31–33]. See discussion of Section 2.5. In each case, comparisons between alkyl-silica and other columns are made for columns with similar ligand lengths.

[a] Vs. C_{18} type-B column.
[b] Vs. average of C_8 and C_{18} type-B columns.
[c] Vs. $C_{4.5}$ type-B column (see [32] for details).
[d] Vs. C_8 type-B column.
[e] Vs. Phenyl column.
[f] Vs. C_{18} type-A column.

tached to the silica particle. Commonly used embedded polar groups include hydrogen-bond acceptors such as amide, urea and carbamate, making EPG-columns more “basic”. EPG-columns therefore exhibit significant differences in selectivity versus non-EPG columns [35–40], which has encouraged their use in RP-LC method development when a change in separation selectivity is required (as well as for other reasons). The selectivity of EPG-columns is expected to vary with the nature of the polar group, and whether that group is embedded (present section) or used to end-cap the column (following Section 2.5.4).

Correlations with Eq. (2) and the test solutes of Table 6 for 21 EPG-columns (including the four polar-end-capped columns of Section 2.5.4) resulted in an average S.D. = 0.057 (±14% in α), using values of η', σ', etc. from Table 6. Further regression to obtain best-fit values of the column and solute parameters yielded a final fit with Eq. (2) of ±3% in α, suggesting no significant solute–column interactions other than those described by Eq. (2).

A comparison of selectivity for EPG-columns versus type-B alkyl-silica columns is shown in Table 11. Columns with an embedded polar group are generally much less hydrophobic (smaller H) than non-EPG columns (−0.26 units), due to the polarity of the embedded group. The basic polar group also appears to interact with silanols so as to reduce their acidity; as a result, average values of A (−0.43 units) and C(2.8) (−0.69 units) are much reduced relative to alkyl-silica columns. Values of C(7.0), on the other hand, are more similar for both EPG- and non-EPG-columns, which might reflect the inability of a limited number of embedded polar groups to completely neutralize silanol activity when the silanols are extensively ionized (at pH 7).

Values of B for EPG-columns are significantly higher (+0.17 units) than for non-EPG-columns, presumably because of the hydrogen-bond interaction of donor solutes such as carboxylic acids or phenols with the basic polar group of the column. In Fig. 12c, a plot similar to that of Fig. 12b for type-A alkyl-silica columns is shown for EPG-columns. All but three of the embedded-polar-group columns have values of B that fall above the error limits for type-B columns. We infer from this relationship that in most cases values of B for EPG-columns arise from a source of column basicity other than sorbed water; i.e., the basic embedded polar group. Polar-end-capped columns (circles in Fig. 12c) fall within the error limits for type-B columns, suggesting that the basicity of these columns results mainly from sorbed water—not the polar end-capping group. The three EPG columns (#16b–18b [Synergi Hydro-RP; Prevail amide; Inertsil ODS-EP]) in Fig. 12c whose values of B resemble that

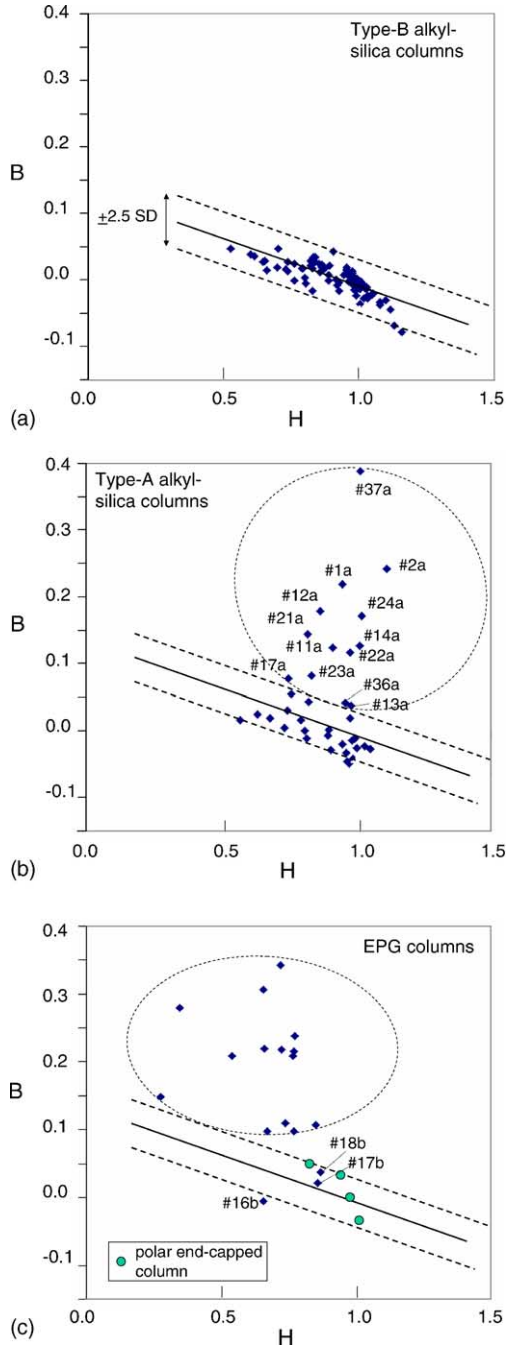

Fig. 12. Column hydrogen-bond basicity ***B*** as a function of column hydrophobicity ***H***. (a) Type-B alkyl-silica columns; (b) type-A alkyl-silica columns; (c) EPG-columns. Straight lines in (b, c) taken from (a). For column numbering, see [11,31]. See text for details. Reprinted from [31].

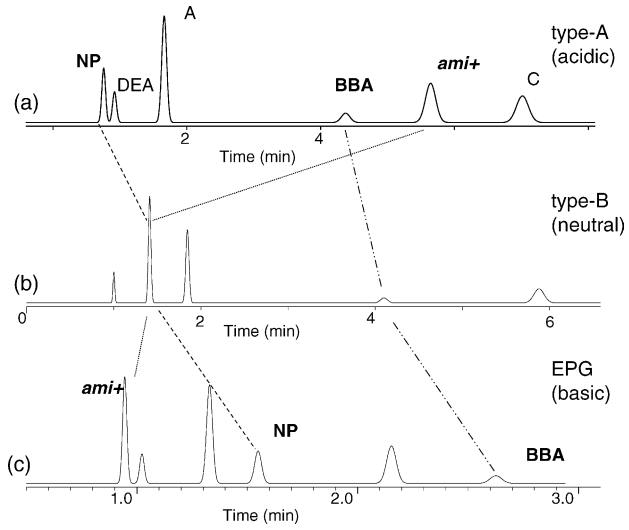

Fig. 13. Relative retention as a function of column type. (a) Allsphere ODS1 (type-A); (b) Ace C18 (type-B); (c) Bonus RP (EPG). Sample: **NP**, 4-nitrophenol; DEA, *N*,*N*-diethylacetamide; A, acetophenone; **BBA**, 4-*n*-butylbenzoic acid; **ami**$^+$, amitriptyline; C, *cis*-chalcone. Experimental conditions as in Fig. 1. Reprinted from [31].

of type-B alkyl-silica columns all have atypically low values of ***B***, due to either a less basic polar group (ether or hydroxy, see the following discussion), or a lower concentration of the polar group.

B-values for polar embedded columns presumably reflect the hydrogen-bond basicity and relative concentration of the embedded polar group:

$$\begin{aligned}&\text{ether}\,(\boldsymbol{B} = -0.01, \text{least basic}) < \text{hydroxy}\,(\boldsymbol{B} = 0.05)\\ &< \text{carbamate}\,(0.09 \le \boldsymbol{B} \le 0.10) < \text{PEG(glycol)}\,(\boldsymbol{B} = 0.15)\\ &< \text{urea}\,(0.23 \le \boldsymbol{B} \le 0.30)\\ &\approx \text{amide}\,(0.22 \le \boldsymbol{B} \le 0.37, \text{most basic})\end{aligned} \quad (14)$$

Column #17b (Prevail amide) in Fig. 12c also has an amide group, but its much lower value of $\boldsymbol{B} = 0.02$ suggests that the concentration of accessible amide groups in this column is quite low, or the amide groups are for some reason less accessible.

A few studies of EPG columns [35,39,40] have noted their selective retention of phenols, relative to retention on non-EPG columns. Because of the pronounced hydrogen-bond basicity of EPG-columns, this is expected. The hydrogen-bond acidity of phenols (as measured by their best-fit α' values) is considerably larger for EPG-columns (avg. $\alpha' = 0.7$) than for type-B alkyl-silica columns (avg. $\alpha' = 0.2$), presumably because the basic, embedded polar group interacts via a single hydrogen-bond with *both* phenols and carboxylic acids, versus the double (and therefore stronger) interaction of a carboxylic acid molecule with water (Section 2.4.5). Similarly, the average α' value for several alcohols increases from 0.1 for type-B alkyl-silica columns to 0.3 for EPG-columns. Thus, alcohols, phenols and carboxylic acids all behave as stronger hydrogen-bond acids toward EPG-columns than for type-B alkyl-silica columns, and will be selectively retained compared to other solutes. This is partly illustrated in the separations of the same sample on three different columns in Fig. 13. The type-A C_{18} column of Fig. 13a (Allsphere ODS1) is more acidic and less basic (smaller ***B***) compared to the type-B C_{18} column in Fig. 13b (Ace C18), while the

EPG-column of Fig. 13c (Bonus RP) is more basic (larger ***B***) and less acidic. The one phenol in this sample (nitrophenol, "**NP**") and the one carboxylic acid (4-*n*-butylbenzoic acid, "**BBA**") are each seen to be more retained on the type-B column than on the more acidic type-A column, and their relative retention increases further on the EPG-column. The relative retention of the strong base amitriptyline (**ami**$^+$), on the other hand, changes in the opposite direction in going from "acidic" column (a) to "basic" column (c)—as predicted for the decrease in values of ***C*** in going from column (a) to (c) (note the average values of ***C***(2.8) for these three column types in Table 11).

2.5.4. Columns with polar end-capping groups [31]

Polar functional groups can also be used to end-cap alkyl-silica columns, in contrast with the embedding of polar groups within the alkyl ligands (Section 2.5.3). As summarized in Table 11, columns of this kind show much less change in selectivity, compared to corresponding alkyl-silica columns. The reason for the small effect of an end-capping polar group on column selectivity is uncertain, although the relative concentration of polar-end-capping groups is likely smaller when compared to that of embedded polar groups. Thus, when conventional alkyl-silica columns are end-capped, there is typically no more than a 20–30% increase in the total moles of ligand bonded to the silica [31]. Another factor may be the polar end-capping group used, which is usually not specified by the manufacturer. As noted in Section 2.5.3, different polar groups vary in their effect on column basicity (values of ***B***). The combination of a less basic end-capping group with a lower concentration of that group could explain the lower values of ***B*** for polar-end-capped columns. Polar end-capping groups may also be less accessible than embedded groups, because of their relative position within the stationary phase (i.e., attached directly to the silica surface).

2.5.5. Cyanopropyl ("cyano") columns [32]

The ligand in a cyano column typically consists of a short alkyl linker terminated by a nitrile group (e.g., $-C_3-C\equiv N$). Compared to C_8 or C_{18} columns, cyano columns are less commonly used—in part because of concerns about their stability and reproducibility. Nevertheless, pronounced differences in retention and selectivity have been reported for cyano versus alkyl-silica columns [41–45]. A common observation is that cyano columns are less retentive (i.e., more polar) versus C_8 or C_{18} columns. In order to achieve comparable retention (e.g., $1 \leq k \leq 10$) on a cyano versus a C_8 or C_{18} column, a weaker mobile phase (decrease in mobile phase strength, %*B*) is usually necessary; e.g., 30% acetonitrile/buffer (cyano column) versus 50% acetonitrile/buffer (C_8 column). Consequently, when "practical" separations on a cyano versus a C_8 or C_{18} column are compared, differences in separation selectivity can result from changes in *both* the column (i.e., cyano versus C_8) *and* the mobile phase (e.g., 30% *B* for cyano, versus 50% *B* for C_8). The effect of the weaker mobile phase on selectivity (solvent-strength selectivity [46]) can be more important than differences in column selectivity for some samples [41,42].

Correlations of retention data for 11 cyano columns and the test solutes of Table 6 with Eq. (2) resulted in an average S.D. = 0.034 (±8% in α). Continued regression to obtain best-fit values of the column and solute parameters (and minimum average S.D.) yielded a final fit with Eq. (2) of ±1% in α, suggesting that no solute–column interactions other than those described by Eq. (2) are significant for these columns. Cyano columns are compared with type-B alkyl-silica columns of similar alkyl length in Table 11. Cyano columns have much smaller values of ***H*** (−0.28 units), presumably due to the polarity of the nitrile group. Values of $\boldsymbol{S}^*$ are also smaller (−0.12 units), which may result from the dipole repulsion of aligned cyano groups, resulting in a stationary phase that is more ordered and accessible. Values of ***A*** are also smaller (−0.22), perhaps due to (a) an interaction of cyano groups with non-ionized silanols, or (b) a similar (but reversed) effect as proposed to explain the increase in values of ***A*** with ***H*** for type-B alkyl-silica columns (Section 2.4.8). Values of ***B*** and ***C***(2.8) are little different (−0.03 and 0.02, respectively), while values of ***C***(7.0) are much larger (+0.47 units) for cyano columns. Dipole–dipole interactions between polar solute molecules and a cyano column appear generally unimportant (Section 2.5.10).

2.5.6. Phenyl columns [33]

As for the case of cyano columns, phenylpropyl or phenylhexyl columns are less commonly used for RP-LC separation. The selectivity of phenyl columns has been studied by several groups [41,42,47–51] and found to differ from that for alkyl-silica columns. Correlations of retention data for 11 phenyl columns with Eq. (2) [33] resulted in an average S.D. = 0.025 (±6% in α). Further regression to obtain best-fit values of the column and solute parameters (and minimum average S.D.) yielded a final fit with Eq. (2) of ±1% in α, suggesting that no solute–column interactions other than those described by Eq. (2) are significant for these columns. However, this has been shown *not* to be the case for all samples; π-acids such as aromatics (especially polycyclic and/or polynitro aromatics) are preferentially retained by π–π interaction on phenyl versus alkyl-silica columns (note that no strong π-acids are included in the test solutes of Table 6). The π-basicity of the stationary-phase phenyl group appears to be similar for most phenyl columns, leading to about the same increased relative retention of π-acids for all phenyl columns; i.e., no additional term for π–π interaction is required in Eq. (2) for comparisons of column selectivity among different phenyl columns. The enhanced retention of π-acids varies with the organic solvent in the mobile phase as: tetrahydrofuran (least) < acetonitrile < methanol (most). It should be noted that what we have just ascribed to π–π interaction may also be due in smaller part to stronger dispersion interactions for phenyl versus (less polarizable) C_8 columns; see the related discussion of fluoro-columns in Section 2.5.7 and [33].

Phenyl columns are compared with alkyl-silica columns in Table 11. The reduced hydrophobicity of phenyl versus alkyl groups leads to smaller values of $\boldsymbol{H}$ (−0.23 units), while values of $\boldsymbol{S}^*$ are also smaller (−0.15 units)—possibly because the phenyl groups are more ordered, as suggested above for column cyano groups. Values of $\boldsymbol{A}$ are moderately reduced (−0.07 units), perhaps for similar reasons as in the case of cyano columns (Section 2.5.5). Values of $\boldsymbol{C}$ are larger for phenyl columns (+0.14 to 0.43 units), for no apparent reason.

2.5.7. *Fluoro-substituted ("fluoro") columns [33]*

Per-fluorinated alkyl or phenyl ligands are the basis of so-called fluoro columns. Fluoro-column selectivity has been studied by several groups [52–57], with the observation that solutes of lower refractive index (and lower molecular polarizability) are relatively more retained on fluoro-alkyl columns, compared to retention on a C_8 or C_{18} column (as predicted by solubility parameter theory [53]). This is illustrated in Fig. 14, where retention on a fluoroalkyl column is compared with the average retention of each solute on four C_8 columns. Polyaromatics ("PAH", –·–·–) are seen to be less retained on the fluoro-alkyl column than substituted benzenes (Ar–X, —), while aliphatic solutes (R–X, - - -) are more retained. Fluoro-substituted aromatics (Ar–F, · · ·) have even larger values of k on the fluoro column. This behavior has been attributed to differences in solute–column dispersion interactions for fluoro-alkyl columns, as a result of the much lower polarizability of fluoro-alkyl columns. Thus, compounds and columns of similar polarizabilty should interact preferentially, with increased relative retention of less polarizable solutes on fluoro-alkyl columns. The selectivity pattern shown in Fig. 14 for a fluoro-alkyl column bears a superficial (but inverted) resemblance to phenyl column selectivity, which is consistent with the greater polarizablity and refractive index of phenyl versus alkyl ligands. However, other observations [33] suggest that varying dispersion interactions play a less important role in determining the selectivity of phenyl columns.

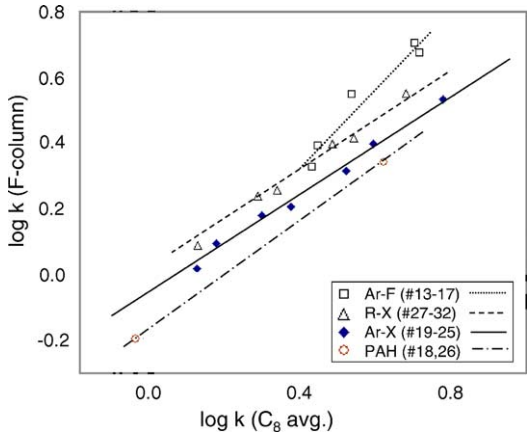

Fig. 14. Comparison of retention on a fluoro-alkyl column with the average retention for each solute on four C_8 columns. See [33] for details. Reprinted from [33].

Because of the importance of differential dispersion interactions in retention on fluoro columns, and because such interactions are not taken into account in Eq. (2) (which is largely based on data for aliphatic phases), the correlation of retention on fluoro columns with Eq. (2) is poor: for five fluoro columns, an average S.D. = 0.059 (±15% in α) was found. Further regression to obtain best-fit values of the column and solute parameters was not possible, because of the small number of fluoro columns studied. However, other features of retention on fluoro columns [33] confirm the importance of dispersion interactions in affecting column selectivity and suggest that a best fit to Eq. (2) might still yield a poor correlation ($\gg$±3% in α).

Because of the importance of differential solute–column dispersion interactions that are not recognized in Eq. (2), values of $\boldsymbol{H}$, $\boldsymbol{S}^*$, etc. for fluoro columns may have less physicochemical significance than for other kinds of columns. Nevertheless, Table 11 compares values of these column parameters for both fluoro-alkyl and fluoro-phenyl columns with C_8 columns, as a rough guide to the relative selectivity of fluoro columns. Noteworthy is the much larger value of $\boldsymbol{S}^*$ for perfluorophenyl (PFP) columns, which also exhibit much greater shape selectivity (as measured by values of $\alpha_{T/O}$ [57]).

2.5.8. *Bonded-zirconia columns [11]*

These columns consist of a polymeric stationary phase (polybutadiene or polystyrene) that is coated onto a porous zirconia particle. Bonded-zirconia (ZrO_2) columns are stable over a pH range of at least 1–13 and at temperatures >200 °C, making them uniquely useful for separations at extremes of temperature or pH. The zirconia surface differs in important ways from silica, which results in strong Lewis interactions with oxyanion solutes [58,59], analogous to the strong interaction of cations with the type-A silica surface.

Correlations of retention data with Eq. (2) for three ZrO_2-columns gave very poor agreement (avg. S.D. = 0.16 or ±41% in α), and this cannot be attributed entirely to differences in values of $\boldsymbol{H}$, $\boldsymbol{S}^*$, etc. compared to an average type-B alkyl-silica column [11]. Average values of $\boldsymbol{H}$, $\boldsymbol{S}^*$, etc. for ZrO_2-columns are compared with values for type-B C_{18} columns in Table 11. Values of $\boldsymbol{A}$ are relatively low compared to C_{18} columns (difference in $\boldsymbol{A} = -0.4$), while values of $\boldsymbol{C}$ are extraordinarily high (avg. difference in $\boldsymbol{C} = 2.0$). These values of $\boldsymbol{A}$ and $\boldsymbol{C}$ for bonded-zirconia columns are consistent with what we know about this stationary phase [59]; i.e., an absence of proton-donor silanols and the ability of phosphate (in the buffer) to strongly adsorb to the zirconia surface with creation of a large negative charge on the column. As noted above for other column types, values of $\boldsymbol{A}$ generally increase with values of $\boldsymbol{C}$, which contrasts with the situation for ZrO_2-columns.

2.5.9. *Polymeric alkyl-silica columns [11]*

Commonly used alkyl-silica columns are mainly monomeric; i.e., made with monofunctional bonding reagents such as chlorodimethyloctadecylsilane. Polymeric

alkyl-silica ("polymeric") columns are made from di- or trifunctional silanes such as dichloromethyloctadecylsilane; as a result, polymeric columns are usually more heavily bonded (larger C_L values). Polymeric columns tend to be more stable, but less reproducible from batch to batch [46]. Values of ***H***, ***S****, etc. have been determined for three polymeric, type-A, C_{18} columns [11] and found to show a similar agreement with Eq. (2) as for other type-A columns. Table 11 compares polymeric and type-A columns in terms of selectivity, showing larger values of ***H*** and ***S**** for the polymeric columns, as expected from their heavier bonding. Observed differences in average values of ***A*** and ***C*** may not be significant, because only three polymeric columns were studied, and silica acidity can vary widely among type-A columns.

2.5.10. The unimportance of dipole–dipole interactions in affecting RP-LC retention

It is logical to assume that solute molecules with large dipole moments should be preferentially retained (by dipole orientation) on columns such as cyano, which have a ligand group with a large dipole moment. Similarly, RP-LC retention is generally governed by solute hydrophobicity, which is often regarded as inversely related to solute "polarity". However, solute RP-LC "polarity" and dipole moment are not directly related in this fashion. Thus, plots of log *k* for a cyano versus a C_8 column, using solutes with varying dipole moments but only minor differences in steric interaction (σ'), hydrogen bonding (β', α') or cation exchange (κ') behavior, show only small deviations (small values of δlog *k*), with no correlation of resulting δlog *k* values with solute dipole moment [32]. That is, dipole–dipole interactions between solute and column do not appear to play a significant role in determining stationary phase selectivity in RP-LC. Since dipole orientation is important in solution, its reduced importance in the stationary phase is likely the result of increased steric hindrance, as well as much more limited orientation possibilities for a cyano group that is tethered to the silica surface. Eq. (2) predicts that more "polar" solutes will be relatively more retained than "non-polar" solutes on more polar columns (columns with smaller values of ***H***), despite the generally reduced retention of all solutes on more polar columns (assuming similar values of σ', β', α' and κ' for the solutes compared).

*2.6. Values of **H**, **S***, etc. for other experimental conditions [12]*

Experimental studies leading to the development of Eq. (2) have for the most part involved the same experimental conditions: isocratic separation with a mobile phase of 50% acetonitrile/buffer, where the buffer is 60 mM pH 2.8 phosphate, at a temperature of 35 °C. If a change in conditions results in the same change in log *k* for each of the solutes of Table 6 on *different* columns, values of ***H***, ***S****, etc. determined for one set of conditions (e.g., 50% acetonitrile/buffer) will be applicable for other conditions as well; however, the solute parameters (η', σ', etc.) will vary with mobile phase composition and temperature. We have already noted that a change in pH can affect values of ***C*** (Section 2.4.10, Eq. (12)). Apart from pH, however, a change in conditions appears to have little effect on values of ***H***, ***S****, etc. [12]. Thus, for changes in %*B* (40% versus 50% acetonitrile/buffer), temperature (45 °C versus 35 °C), and solvent type (methanol or tetrahydrofuran partially replacing acetonitrile), changes in log *k* with conditions for a wide range of solutes tend to be quite similar for a given solute and different type-B C_{18} columns, especially when values of ***H***, ***S****, etc. for these columns are more similar. Thus, when trying to match the selectivity of two columns based on similar values of ***H***, ***S****, etc. (determined using 50% acetonitrile/buffer at 35 °C), we can to a first approximation ignore differences in separation conditions, as long as the same conditions are used for the two columns which are compared. This becomes less true when separation conditions are quite different from those used to determine values of ***H***, ***S****, etc. (50% acetonitrile/buffer; 35 °C); see the further discussion of [12].

2.6.1. Effect of triethylamine added to the mobile phase [11]

In the past, triethylamine (TEA) was often added to the mobile phase as a means of suppressing the effect of column silanol activity and minimizing the tailing of basic compounds [60]. With the more frequent use today of less acidic, type-B columns, TEA is less commonly employed. Nevertheless, the effect of TEA on column selectivity is of interest for various reasons, including the continued use of older, type-A columns for separations that were developed several years ago. Two studies of the effects of TEA addition on column selectivity have been reported [11,60]. For mobile phases of higher pH (e.g., pH > 7), TEA can be present in both the neutral and ionized form. In this case, non-ionized TEA can be taken up by the stationary phase with a lowering of values of ***H*** due to the polarity of the TEA molecule. Values of ***A*** and ***C*** are also decreased, due to the association of TEA with both ionized and neutral silanols. For more acidic mobile phases (e.g., pH < 5), TEA will be present exclusively as the protonated molecule, in which case the only possible interaction of TEA with the stationary phase is its attachment to ionized silanols by ion exchange. This can result in a pronounced lowering of values of ***C*** for type-A alkyl-silica columns (e.g., by as much as 0.5 unit at pH 2.8), but little change in other column selectivity parameters [11].

2.7. Alternative characterizations of column selectivity

The measurement of values of ***H***, ***S****, etc. as described here is only the most recent of a long series of similar attempts at characterizing column selectivity. Three general approaches can be recognized: use of (a) the solvation parameter model (Eq. (1) [8]), (b) principal component analysis (PCA), cluster analysis, and related chemometric procedures [9,61–64], and

(c) retention data for test solutes believed to measure specific solute–column interactions [6,9,65–68].

We have previously compared the hydrophobic-subtraction model (Eq. (2)) with the conceptually similar solvation parameter model [4,5]. Because the solute parameters of Eq. (2) are derived empirically, and because Eq. (2) recognizes two additional contributions to column selectivity ($\sigma' \boldsymbol{S}^*$ and $\kappa' \boldsymbol{C}$), Eq. (2) provides a more accurate and complete description of column selectivity than is provided by the solvation parameter model. A further limitation of Eq. (1) is its failure to recognize that steric hindrance in the stationary phase is much more pronounced than steric hindrance in the mobile phase (see Section 2.4.3. and discussion of [5]). This leads to the use of inappropriate values of $\sum\beta_2$ and possibly other solute parameters for RP-LC, with resulting errors in predictions by Eq. (1) of ±10–15% in k.

PCA is able to provide a description of column selectivity that is (in principle) similarly detailed and reliable as Eq. (2) [63], but resulting column selectivity parameters cannot be related to the known interactions between solute and column. PCA has also not been extended to allow quantitative comparisons of column selectivity as in Section 3 (based on the hydrophobic-subtraction model).

Test solutes believed to be indicative of various solute–column interactions are commonly used to describe column selectivity, but with the exception of Eq. (2) no attempt has so far been made to show that such measurements can provide a complete and reliable characterization of column selectivity. A popular set of test solutes that has been applied to almost 200 columns [68] yields the following column selectivity parameters: methylene selectivity, α_{CH_2} (roughly comparable to hydrophobicity $\boldsymbol{H}$); shape selectivity, $\alpha_{T/O}$ (comparable to $\boldsymbol{S}^*$?); hydrogen-bond acidity, $\alpha_{C/P}$ (comparable to $\boldsymbol{A}$?); ion-exchange capacity at pH 2.7 and 7.6, $\alpha_{A/P}$ (comparable to $\boldsymbol{C}$(2.8) and $\boldsymbol{C}$(7.0)?); see Section 5 for details on these individual tests of column selectivity. A comparison of the latter parameters with values of $\boldsymbol{H}$, $\boldsymbol{S}^*$, etc. for several columns shows poor or marginal correlations ($0.0 \le r^2 \le 0.4$) for $\alpha_{T/O}$, $\alpha_{C/P}$ and $\alpha_{A/P}$ at pH 7.6 with their counterparts from Eq. (2) [10]. A related observation is that end-capping is expected to strongly suppress the hydrogen-bonding activity of silanols (Section 2.4.8), but values of $\alpha_{C/P}$ show little change for otherwise similar end-capped versus non-end-capped columns (in contrast to values of $\boldsymbol{A}$).

2.8. Possible limitations and further development of the hydrophobic-subtraction model

While Eq. (2) provides a consistent and apparently useful understanding of RP-LC separation and column selectivity, it is premature to suggest that this represents a complete description for all possible samples or RP-LC separations. When the almost endless number of possible solute structures are considered, in combination with a wide range of possible separation conditions (including the column), there are likely to be separations that are less well described by Eq. (2). One example is the separation of polycyclic aromatic hydrocarbons on polymeric columns, which can be affected by so-called "shape selectivity" (which differs from "steric resistance"). A second problem arises from our attempt to represent steric resistance by a simple product-term ($\sigma' \boldsymbol{S}^*$), which should be contrasted with the known physico-chemical complexity of RP-LC stationary phases and interactions that involve steric hindrance. A third issue is that the hydrophobic interaction term $\eta' \boldsymbol{H}$ can be dissected into additional contributions to column selectivity, as already discussed for Eq. (1) and demonstrated experimentally for retention on fluoro columns (Section 2.5.7). Fourth, the form of Eq. (2) assumes that each of the five solute–column interactions are independent of each other, whereas this may not be strictly true (as in the proposed dependence of $\boldsymbol{A}$ on $\boldsymbol{H}$ in Section 2.4.8). Finally, it has been assumed that values of $\boldsymbol{H}$, $\boldsymbol{S}^*$, $\boldsymbol{A}$ and $\boldsymbol{B}$ do not vary with mobile phase pH (these parameters have been measured only for pH 2.8). With the substantial ionization of many silicas at neutral pH [12], it seems possible that values of $\boldsymbol{A}$ (which are determined by non-ionized silanols) may be somewhat reduced for pH > 6. Small, but significant changes in $\boldsymbol{H}$, $\boldsymbol{S}^*$, or $\boldsymbol{B}$ with pH are also possible but have not been explored.

The use of Eq. (2) for separations of large solute molecules (e.g., proteins, nucleic acids, synthetic polymers) raises additional questions. Sufficiently large molecules may be unable to penetrate the stationary phase, which should greatly affect the values of each of terms (i)–(v) of Eq. (2). This suggests that Eq. (2) may not be as reliable for large solute molecules as for small, for the same reason that Eq. (2) with solute parameters from Table 6 is less reliable for column types other than type-B alkyl-silica (excessive extrapolation of Eq. (2); see related discussion of Eq. (13)). While in principle the magnitude of the $\sigma' \boldsymbol{S}^*$ term would appear to be greatly increased for large molecules, actually there may be little difference in values of $\sigma' \boldsymbol{S}^*$ for large (non-penetrating) molecules of different size, because entry (or "non-entry") of the molecule into the stationary phase then no longer depends on ligand spacing; i.e., the form of Eq. (2) and the $\sigma' \boldsymbol{S}^*$ term may be inappropriate for very large molecules. (Studies of certain large molecules (polycyclic aromatic hydrocarbons [69], carotenoids [70], fullerenes [71]) are consistent with the interaction of only a small portion of these molecules with the stationary phase, as suggested by significant retention changes for relatively small differences in the structures of different solute pairs. This indicates a need for a new way of looking at the retention of such compounds [courtesy of John Fetzer, Fetzpahs Consulting, Pinole, CA]).

An understanding of possible exceptions to Eq. (2) (and of the underlying physico-chemical phenomena) should be facilitated by the further application of the "subtraction" approach used in its derivation. Thus, predictions based on Eq. (2) can be compared with experimental values of α, and differences between these two numbers can then be correlated with solute molecular structure, column properties, experimental

conditions, etc. Although a truly universal and quantitative description of column selectivity represents a distant goal at present, nevertheless it is now possible to make useful predictions of column selectivity based on Eq. (2), as detailed in the following section.

3. Applications

The convenient application of Eq. (2) to practical problems involving column selectivity requires values of $\boldsymbol{H}$, $\boldsymbol{S}^*$, etc. for a large fraction of commercially available RP-LC columns. Appendix A summarizes such values for more than 300 columns. This list is being updated continuously as part of commercial software (Column Match®, Rheodyne LLC, Rohnert Park, CA), which allows the selection of columns of either similar or different selectivity. The reproducible measurement of values of $\boldsymbol{H}$, $\boldsymbol{S}^*$, etc. has been described [10] and validated by inter-laboratory comparisons [30]. A shorter, slightly less accurate column-test procedure has also been developed that uses 8 solutes in place of the 16 solutes of Table 6 [30]; however, it is only recommended to use the shorter procedure for type-B alkyl-silica columns.

The evaluation of the present procedure for practical comparisons of column selectivity began in 2003, with its use for identifying equivalent replacement columns for a number of routine assay procedures that had been developed previously in four pharmaceutical laboratories [72]. The results of these preliminary column comparisons are summarized in Section 3.1. More recently, values of $\boldsymbol{H}$, $\boldsymbol{S}^*$, etc. are being used to select columns of very different selectivity for use in the development of orthogonal separation procedures. However, only preliminary results from the latter study were available at the time this paper was accepted for publication (Section 3.2.1).

3.1. Selecting "equivalent" columns [72]

Routine RP-LC assay procedures are often carried out over periods of months or years, as well as in different laboratories and different parts of the world. During the application of such a procedure over time, several "equivalent" replacement columns may be required in order to obtain the same separation in each run (by "equivalent" columns, we mean columns that provide separations that are acceptably similar, as judged by the person responsible for a given RP-LC assay). For various reasons, it may prove difficult or impossible to obtain a replacement column from the original source with sufficiently similar selectivity (and adequate sample resolution). In such cases, it is necessary to locate an equivalent replacement column from a different source—or a column with a different designation from the same source. During the development of a RP-LC procedure, it is also recommended that one or more back-up columns (different designations and/or sources) of equivalent selectivity be specified. The need for columns of similar selectivity as for an original column is therefore not uncommon.

A column-comparison function based on values of $\boldsymbol{H}$, $\boldsymbol{S}^*$, etc. for columns 1 and 2 has been derived [10]:

$$F_s = \{[12.5(\boldsymbol{H}_2 - \boldsymbol{H}_1)]^2 + [100\boldsymbol{S}_2^* - \boldsymbol{S}_1^*)]^2 + [30(\boldsymbol{A}_2 - \boldsymbol{A}_1)]^2 + [143(\boldsymbol{B}_2 - \boldsymbol{B}_1)]^2 + [83(\boldsymbol{C}_2 - \boldsymbol{C}_1)]^2\}^{1/2} \quad (15)$$

here $\boldsymbol{H}_1$ and $\boldsymbol{H}_2$ refer to values of $\boldsymbol{H}$ for columns 1 and 2, respectively (and similarly for values of $\boldsymbol{S}_1^*$ and $\boldsymbol{S}_2^*$, etc.). F_s can be regarded as the distance between two columns whose values of $\boldsymbol{H}$, $\boldsymbol{S}^*$, etc. are plotted in five-dimensional space, with the weighting factors (12.5, 100, etc.) determined for a 67-component sample of "average" composition. It was found [10] that if $F_s \leq 3$ for two columns 1 and 2, average variations in α should be $\leq$3% (and differences in resolution R_s will be less than 0.4 units), so that the two columns are likely to provide equivalent selectivity and separation for different samples and conditions, if the same mobile phase and temperature are used for the two columns being compared.

An example of the application of Eq. (15) is shown in Fig. 15, for the separation of a mixture of neutral, basic and acidic compounds on four different columns. Values of F_s from Eq. (15) are shown for the three columns of Fig. 15b–d, each of which is compared with the Discovery C8 column of Fig. 15a. The values of F_s for the Ace C8 (b) and Precision C8

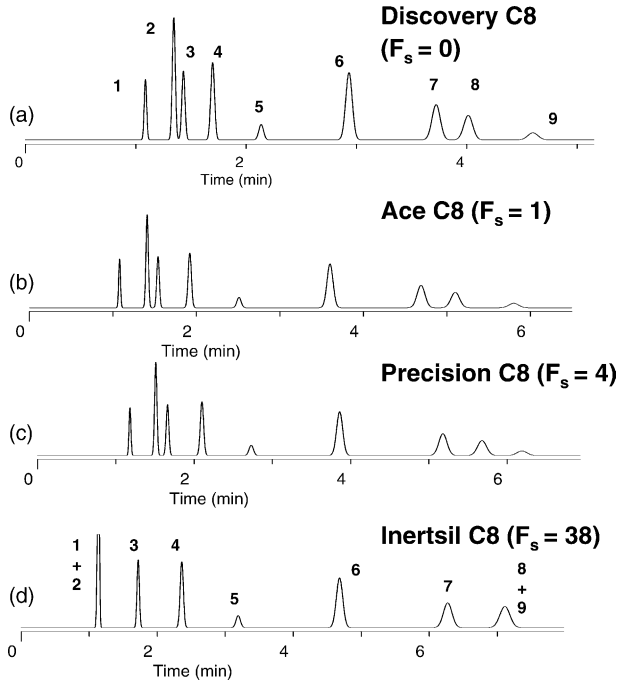

Fig. 15. Comparisons of column selectivity for a given sample and RP-LC procedure. Sample: (1) *N*,*N*-diethylacetamide; (2) nortriptyline; (3) 5,5-diphenylhydantoin; (4) benzonitrile; (5) anisole; (6) toluene; (7) *cis*-chalcone; (8) *trans*-chalcone; (9) mefenamic acid. Columns (15 cm × 0.46 cm, 5 μm particles) identified in the figure. *Experimental conditions*: 50% acetonitrile/pH 2.8 buffer; 35 °C; 2.0 mL/min. F_s values compared with Discovery C8 column (a). Reprinted from [31].

(c) columns are relatively small ($F_s \leq 4$), and separation on these columns is therefore expected to be (and is) quite similar to that for the Discovery C8 column. For the Inertsil C8 column (d), $F_s = 38$, meaning that this column has a selectivity that is very different from that of the Discovery C8 column (note the co-elution of bands #1/2 and 8/9 in Fig. 15d). Note also that minor differences in run time in the separations of Fig. 15a–c can be minimized by small adjustments in flow rate.

The sample of Fig. 15 was chosen from the 16 test-solutes (Table 6) used to measure values of $\boldsymbol{H}$, $\boldsymbol{S}^*$, etc. in Eq. (15) and is therefore not an independent demonstration of the ability of the F_s function to select equivalent columns. A better test of the utility of Eq. (15) and values of $\boldsymbol{H}$, $\boldsymbol{S}^*$, etc. for this purpose has recently been reported [72]. Twelve different routine RP-LC separations (with widely varying samples and separation conditions, including both isocratic and gradient elution) were selected from four different pharmaceutical laboratories, following which mostly successful attempts were made to select equivalent replacement columns for each separation on the basis of Eq. (15). One of these separations for a pharmaceutical drug product is illustrated in Fig. 16, where the original separation on an ACE C8 column (a) is compared with that on three other columns (b–d) with $1.3 \leq F_s \leq 248$. The separation with the Discovery C8 column (b) is seen to be reasonably similar to that in (a), as expected from a value of $F_s = 1.3$. However, separation on the Kromasil C8 and Bonus RP columns (c and d) is increasingly different, in agreement with their larger values of F_s.

Note that the chromatograms of Fig. 16 involve gradient elution, so that separation conditions differ from those used to measure values of $\boldsymbol{H}$, $\boldsymbol{S}^*$, etc. However, as discussed in Section 2.6, values of $\boldsymbol{H}$, $\boldsymbol{S}^*$, etc. are not much affected by experimental conditions other than mobile phase pH. This is especially true for columns that are more similar (smaller values of F_s), and for conditions that are not far removed from those used to measure values of $\boldsymbol{H}$, $\boldsymbol{S}^*$, etc. (50% acetonitrile/buffer; 35 °C). Another illustration of the applicability of values of F_s for changed separation conditions is shown in Fig. 17, for four cyano columns and a mobile phase of 30% acetonitrile/pH 2.8 buffer (versus use of 50% acetonitrile/buffer for the measurement of the values of $\boldsymbol{H}$, $\boldsymbol{S}^*$, etc. that were used to calculate F_s). Band spacing on the Thermo CN (Fig. 17b) and Genesis CN (Fig. 17c) columns (with $F_s = 3$ for each column) is seen to be equivalent to that on the Discovery CN column (Fig. 17a), while separation on the Luna CN column with $F_s = 41$ is noticeably different. While run times for the separations of Fig. 17a–c vary from 7 to 14 min, changes in flow rate for the individual runs can be used to equalize sample retention times while maintaining approximately the same resolution for all peaks. Alternatively, possible replacement columns can be restricted to columns with more similar values of k_{EB}, for which average retention (values of k) and run time should be more similar.

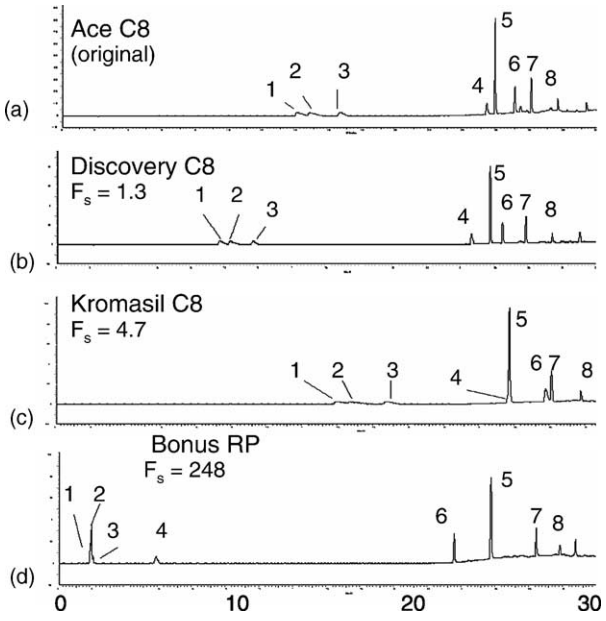

Fig. 16. Comparative separations of a pharmaceutical sample on an original column (a) and three possible replacement columns (b–d). Sample contains strong bases and carboxylic acids. Columns (15 cm × 0.46 cm, 5 μm particles) identified in the figure and values of F_s determined from the column parameters of Table 13 (obtained with 50% ACN/buffer). *Conditions*: gradient separation with solvents A and B; A is pH 2.7 buffer; B is acetonitrile; the gradient is 10/10/22/88/88% *B* in 0/5/15/25/27 min; 1.0 mL/min. See [72] and text for other details. F_s values compared with column (a). Reprinted from [72].

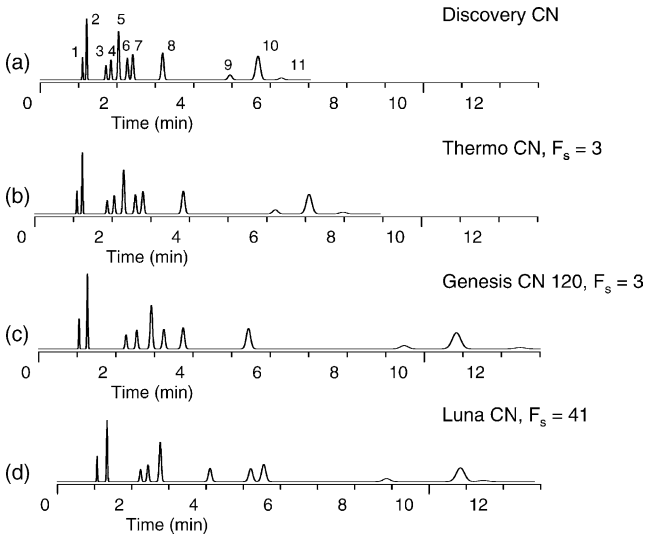

Fig. 17. Comparison of separation on cyano columns with a mobile phase of 30% ACN/buffer. Columns identified in the figure and values of F_s determined from the column parameters of Table 13 (obtained with 50% ACN/buffer). Conditions as in Fig. 1 (unless noted otherwise), with columns identified in the figure. Sample is composed of *N*,*N*-dimethylacetamide (1); *N*,*N*-diethylacetamide (2); acetophenone (3); benzonitrile (4); 5,5-diphenylhydantoin (5); 4-*n*-hexylaniline (6); amitriptyline (7); ethylbenzene (8); *cis*-chalcone (9); mefenamic acid (10); *trans*-chalcone (11). F_s values compared with column (a). Reprinted from [32].

3.1.1. Modification of Eq. (15) as a function of the sample

Eq. (15) assumes that acids, bases and/or neutrals may be present in the sample. When this is the case, values of both ***B*** and ***C*** can be important in affecting separation selectivity for that sample. If either ***B*** or ***C*** has little or no effect on the separation, however, it is useful to reduce its contribution to the final value of F_s, because resulting lower values of F_s for all columns make it more likely that a suitable replacement column (i.e., one with $F_s \leq 3$) can be found. Specifically, the possible absence of acids or fully-ionized bases leads to a re-weighting of the last two terms of Eq. (15):

$$F_s^* = \{[12.5(\boldsymbol{H}_2 - \boldsymbol{H}_1)]^2 + [100(\boldsymbol{S}_2^* - \boldsymbol{S}_1^*)]^2 + [30(\boldsymbol{A}_2 - \boldsymbol{A}_1)]^2 + [143x_B(\boldsymbol{B}_2 - \boldsymbol{B}_1)]^2 + [83x_C(\boldsymbol{C}_2 - \boldsymbol{C}_1)]^2\}^{1/2} \quad (16)$$

here x_B and x_C represent possible correction factors (with values between 0 and 1) that depend on sample composition and mobile phase pH. For example, if bases are absent from the sample, the term $x_C \approx 0$, because values of ***C*** mainly affect the retention of ionized basic solutes. For similar reasons, if carboxylic acids were absent from the sample, $x_B \approx 0$. Note that when x_B and x_C equal 1.0, Eqs. (15) and (16) become equivalent, and $F_s = F_s^*$. When a basic compound is only partly ionized, there is a much reduced contribution of ***C*** to the separation (because values of κ' decrease from about 1 to 0.1 when a basic solute becomes partly ionized [Fig. 10]). Therefore, weak bases such as anilines or pyridines have $x_C \approx 0.1$ for a mobile phase pH < 6, with $x_C \approx 0$ for pH ≥ 6. Similarly, strong bases (aminoalkyl derivatives) have $x_C \approx 0.1$ for pH ≥ 7, and $x_C \approx 1$ for pH < 6. See [72] for details. Because solute ionization at a given buffer pH (or the apparent pK_a of an acid or base) can vary significantly with %*B* or temperature, as well as with solute molecular structure, the immediately preceding estimates of x_C represent only very crude approximations at this stage in our use of Eq. (16). Eq. (15) is safer to use in this regard, although it may exclude potentially similar columns (for which $F_s > 3$) when a sample does not contain acids or fully-ionized bases. Two columns are likely to be equivalent, when $F_s^* < 3$, and the likelihood of finding an equivalent column will be greater when $F_s^* < 3$, than when $F_s < 3$.

An example from the study of [72] which illustrates the use of Eq. (16) is shown in Fig. 18, for the gradient separation of a complex mixture, which contains carboxylic acids, but no bases. Eleven components of the sample are of interest (indicated by "*"), and it was necessary to separate each of these compounds from adjacent peaks with baseline resolution ($R_s \geq 1.5$). The original separation on a Luna C18 column meets this requirement (Fig. 18a). Three other columns with $0.8 \leq F_s^* \leq 10.1$ were selected as possible replacements for the original column; the separation with each of these columns is shown in Fig. 18b–d. Virtually the same separation is obtained for the Prodigy ODS (b) and Inertsil

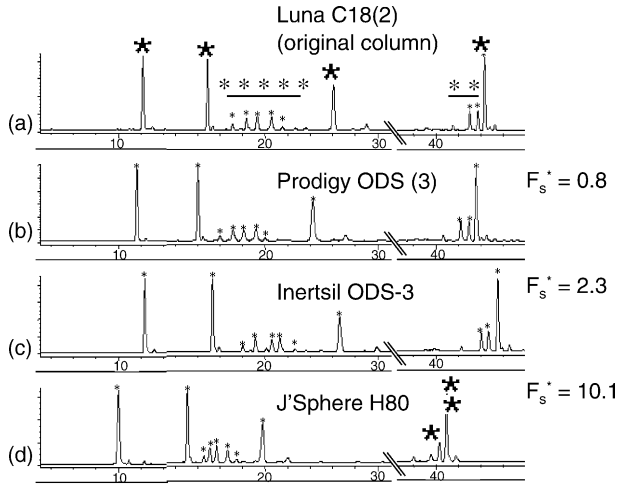

Fig. 18. Comparative separations of a pharmaceutical sample on an original column (a) and three possible replacement columns (b–d). Sample contains carboxylic acids and no bases. Columns (15 cm × 0.2 cm, 5 μm particles) identified in the figure and values of F_s^* determined from the column parameters of Table 13 (obtained with 50% ACN/buffer). *Conditions*: gradient separation with solvents A and B; A is 5% acetonitrile/pH 6.8 buffer; B is 95% acetonitrile/buffer; the gradient is 0/19/25/50/100% *B* in 0/5/28/40/60 min; 0.2 /min. See [72] and text for other details. F_s^* values compared with column (a). Additional (*) added for emphasis; reprinted from [72].

ODS-3 (c) columns, as expected from their low values of F_s^* (0.8 and 2.3, respectively). However, the J'Sphere H80 column with $F_s^* = 10.1$ does not provide equivalent separation (complete overlap of the last two bands). In another 10 separations reported in [72], one or more successful replacement columns could be identified in the same way as in Figs. 16 and 18.

Because the weighting factors in Eqs. (15) and (16) are based on an "average" sample, samples with quite different values of η', σ', etc. will respond differently to changes in ***H***, ***S****, etc., leading to somewhat decreased reliability in the use of these equations for some samples. However, Eqs. (15) and (16) are still very useful for the initial *screening* of potential columns (i.e., as a replacement for an original column). Even when predictions of column equivalency are less reliable, the number of candidate columns (with F_s or $F_s^* < 3$), which need to be experimentally tested, is greatly reduced by the use of these equations. The potentially decreased accuracy of Eqs. (15) and (16) for some samples also means that columns with values of F_s or F_s^* moderately larger than 3 are often suitable replacements, so that columns with $F_s^* < 6$ should be regarded as *possible* replacement columns.

When the critical resolution $R_s \gg 2$ for the original separation, larger changes in α may be allowable for the replacement column. As a rough rule, allowable values of F_s^* for equivalent columns can be as large as 1.5 times the critical resolution. For example, with a critical resolution $R_s = 4$ for the separation on the original column, columns with $F_s^* \leq 6$ are *likely* to be suitable replacements for the original column, and columns with $F_s^* \leq 12$ are *possible* candidates. See [72] for further details.

3.1.2. Likelihood of matching different column types

We have noted (Section 2.5.2) that type-A alkyl-silica columns are more variable in terms of values of $\boldsymbol{H}$, $\boldsymbol{S}^*$, etc. than are type-B columns, so that the frequency of different columns of equivalent selectivity is much lower for type-A columns. One study (Table 10 of [33]) has summarized the relative frequency of equivalent columns for different column types. Type-A alkyl-silica, embedded-polar-group, and fluoro columns are each more variable in terms of their values of $\boldsymbol{H}$, $\boldsymbol{S}^*$, etc., so that finding an equivalent replacement column of this type is less likely. On the other hand, type-B alkyl-silica, cyano and phenyl columns are more easily matched (within each group) in terms of selectivity. The frequency of matched columns increases for all column types, when acids and especially bases are absent from the sample (x_B and $x_C = 0$ in Eq. (16)). The likelihood of finding a replacement column also increases when values of $\boldsymbol{H}$, $\boldsymbol{S}^*$, etc. are available for a larger number of columns of that type (Appendix A lists values of $\boldsymbol{H}$, $\boldsymbol{S}^*$, etc. for almost 200 C_8 and C_{18} columns, but a smaller number of other column types).

3.2. Selecting columns of very different selectivity

During RP-LC method development, a need for a change in separation selectivity is often encountered [46]. Similarly, in some cases there is a requirement for so-called *orthogonal separations*, where a very different separation selectivity can be used to check for the appearance of sample components which were not present (or were overlooked) during method development, and which may overlap another peak in the original method. In these and other cases, a major change in column selectivity may be required; values of F_s or $F_s^* \gg 3$ can be used to select columns of different selectivity. The examples of Figs. 15d–18d are suggestive of the latter possibility.

Values of η', σ', etc. reported in [4,5] for 150 different solutes also provide a basis (in some cases) for estimating *very* approximate values of these parameters as a function of solute molecular structure (Sections 2.4.1–2.4.5). In principle, values of these solute parameters for two compounds that overlap in an initial separation could be used to select a second column that is more likely to separate the two compounds in question. Thus, if the compounds appear to have significantly different values of σ', a second column with a very different value of $\boldsymbol{S}^*$ should be chosen. This approach to separating previously overlapped peak-pairs has not been evaluated experimentally at the time the present paper was accepted, and further study may be required for its effective implementation.

The values of $\boldsymbol{H}$, $\boldsymbol{S}^*$, etc. of Table 11 can be used to compare the *average* selectivity of different RP-LC column types in terms of their F_s values (Eq. (15)), as summarized in Table 12. For example, type-B C_8 and C_{18} columns tend to be rather similar, with an average $F_s = 6$ for two such columns. This does not mean that every C_8 and C_{18} column has a similar selectivity, just that there is often not a large difference in selectivity for C_8 versus C_{18} columns (especially columns of similar designation from the same manufacturer; e.g., Symmetry C8 and C18). Similarly, polar-end-capped columns ("PE" in Table 12) are not too different from type-B C_8 ($F_s = 16$) or C_{18} ($F_s = 14$) columns, as was noted in Section 2.5.4. For the largest *average* change in selectivity, assuming a type-B C_{18} column as the original column, a bonded zirconia column (ZrO_2, average $F_s = 172$) or a fluoroalkyl column (F-alk, average $F_s = 85$) is most likely to result in a large change in selectivity. Since the F_s values of Table 12

Table 12
A comparison of average column selectivity by column type

	F_s								
	C_8-B[a]	C_{18}-B[a]	C_{18}-A[b]	EPG[c]	PE[d]	CN[e]	Phenyl[f]	F-alkyl[g]	F-phenyl[h]
C_8-B[a]	6								
C_{18}-A[b]	62	64							
EPG[c]	65	61	122						
PE[d]	16	14	77	51					
CN[e]	21	18	64	66	27				
Phenyl[f]	21	19	54	73	30	15			
F-alkyl[g]	82	85	21	143	98	83	74		
F-phenyl[h]	44	47	31	104	60	48	44	45	
ZrO_2[i]	170	172	110	228	186	168	161	89	129

Values of F_s at pH 2.8 for the various column types of Table 11 (Eq. (15)). Note that values of F_s for two columns of the same type (e.g., type-B C_{18}) can differ by much more than the average F_s value for two columns of different type.

[a] Type-B C_{18} or C_8 column.
[b] Type-A C_{18} column.
[c] Embedded polar group column.
[d] Polar end-capped column.
[e] Cyano column.
[f] Phenyl column.
[g] Perfluoroalkyl column.
[h] Perfluorophenyl column.
[i] Bonded zirconia column.

will change with mobile phase pH or sample composition (i.e., absence of acids or bases), the comparisons of column selectivity in Table 12 represent no more than very approximate guidelines. Actual values of F_s for two columns are much more reliable predictors of column similarity (small F_s) or orthogonality (large F_s). Whenever a new column is selected for a change in selectivity or the development of an orthogonal separation, it is unlikely that the same conditions used previously for the original column will result in a satisfactory separation. Generally, after a change of column, the mobile phase composition and/or temperature must be re-optimized for the sample of interest [46]. Our recommendation for achieving a satisfactory final separation on the new column is the simultaneous variation of temperature and either isocratic %*B* or gradient time, preferably with the aid of computer simulation [73].

3.2.1. Developing orthogonal RP-LC methods

We propose the following procedure for the development of an RP-LC separation, which is intended to be orthogonal to an original RP-LC method, for use in the determination of the presence of new compounds that are overlapped in the original separation. First, select a new column of different selectivity on the basis of a large value of F_s for the two columns. Second, change the B-solvent; if acetonitrile is used initially, use methanol instead, and vice versa if methanol is used initially. On the basis of data reported in [12], we estimate that the combination of these two changes in conditions will typically result in a large enough change in average values of α to result in the separation of most previously overlapped peak-pairs (but possibly with previously separated peaks now being overlapped). Finally, optimize temperature and either %*B* or gradient time for the adequate separation of the sample in the second (orthogonal) procedure as described in [73].

Several laboratories are currently exploring this simple and convenient approach for developing an orthogonal method, with some interesting preliminary results (unpublished data). Fig. 19a shows the gradient separations of a sample of the same (proprietary) drug product by the original RP-LC method (Aquasil C18 column, acetonitrile as the B-solvent). Four degradation products or impurities (peaks #1, 2, 4, 5) are observed, in addition to the drug product (peak #3) and a gradient artifact (*). An orthogonal procedure was developed (BetaMax Acid column (F_s = 196), methanol as B-solvent) and applied to these same two samples (Fig. 19b). Pronounced changes in selectivity are apparent between the original and orthogonal runs: a significant increase in the separation of peaks #1 and 2, an elution reversal of peaks #4 and 5, *and the appearance of a previously unsuspected peak #6* (overlapped by peak #3 in the original method) *in the orthogonal method*. In this example, the orthogonal separation has achieved its intended purpose: the detection of a compound that was not recognized (i.e., missed) by the original method. Further results of this ongoing study will be reported in the near future.

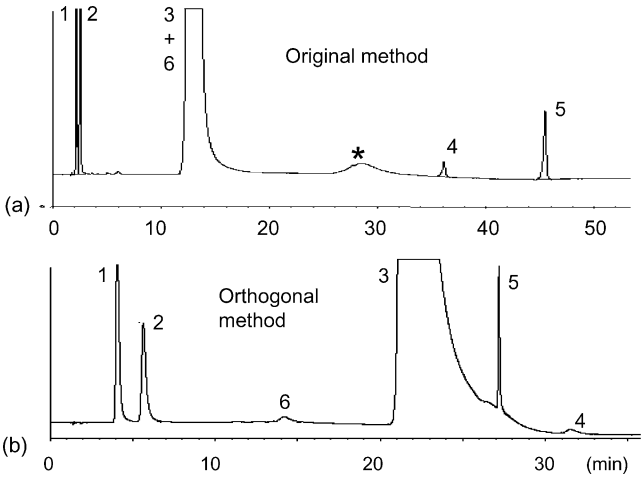

Fig. 19. Separation of a sample containing a drug-substance and related impurities and degradation products by means of the original procedure (a) and an orthogonal method developed as described in the text (b). Conditions for (a): gradient separation with solvents A and B: A is pH 2.5 buffer, and B is 10% acetonitrile/buffer; gradient of 0/0/100% *B* in 0/24.5/44.5 min; 30 °C. Conditions for (b): gradient separation with solvents A and B: A is pH 2.5 buffer, and B is 50% methanol/buffer; gradient of 0/0/16/70% *B* in 0/10/23/25 min; 23 °C. See text for details.

3.2.2. Two-dimensional (2-D) separation

Complex samples that contain a large number of sample components can prove difficult to separate by RP-LC [74], because only a certain number *n* of resolved peaks (the peak capacity PC of the separation [75]) can be accommodated within a single chromatogram. If a sample is successively separated by two orthogonal procedures (2-D separation [76]), each of which has a peak capacity of *n*, however, the possible number of resolved peaks (the peak capacity) can be as large as n^2. However, attaining the full potential of 2-D separation requires two procedures that are completely orthogonal. Because different RP-LC separations are highly correlated (cf. Fig. 1), the use of two RP-LC columns in series will have a peak capacity that lies between *n* and n^2 (usually much closer to *n* than to n^2). Larger values of PC will result for two columns that are more different in terms of selectivity; i.e., two columns with the largest possible values of F_s. Peak capacity can be increased further by the use of different conditions (temperature, mobile phase) for the two columns (as noted in Section 3.2.1 and illustrated in the example of Fig. 19).

3.3. Changes in column selectivity as a function of column history

Appendix A summarizes values of $\boldsymbol{H}$, $\boldsymbol{S}^*$, etc. for more than 300 RP-LC columns. With these data and Eq. (16), it is easy to select two or more equivalent columns, as in the examples of Figs. 15–18. However, this approach assumes that all columns of a given designation (e.g., Symmetry C18) have the same values of $\boldsymbol{H}$, $\boldsymbol{S}^*$, etc. This will very likely be

true for columns from the same production batch, and it is also *likely* to be true for type-B alkyl-silica columns from different production batches [34]. While it is often assumed that columns of the same designation but different particle size will have the same selectivity [46], this has not so far been shown to be the case.

The data of Appendix A were measured soon after these columns were received from the manufacturer (without prior use). It is well known that the selectivity of a column can change during its use for separating samples, as well as after extended flushing of the column by mobile phase [46]. For this reason, it is usually recommended that previously unused ("virgin") columns be used for method development. Likewise, the selection of a replacement column is best made from virgin columns.

It is less well appreciated that the manner in which a RP-LC column is equilibrated prior to separation can also affect column selectivity. For example, the exposure of a C_8 or C_{18} column to a pH 7 mobile phase, followed by its use at low pH, may require hours or even days before the column becomes fully equilibrated [77], so that its selectivity does not change further with time. Similarly, equilibration of the column may be slow when ion-pair reagents or other additives are part of the mobile phase, or when changing from a mobile phase that contains tetrahydrofuran to one containing methanol or acetonitrile [46].

Column selectivity can also change with time during the storage of the column in the original solvent in which it was shipped from the supplier. Unreported measurements of values of $\boldsymbol{H}$, $\boldsymbol{S}^*$, etc. as a function of time during storage suggest that many columns show a slow increase in values of $\boldsymbol{A}$ and $\boldsymbol{C}$, suggesting an increase in the accessibility, concentration or acidity of unreacted silanols. Thus, column selectivity can change with age (storage), with use (number of samples injected), and with exposure of the column (even for a short time) to a high-pH mobile phase or certain other mobile phase additives. Any of these changes can render the use of Eqs. (15) and (16) less reliable, especially for the selection of columns of similar selectivity.

3.4. Gradient elution [72]

With one, minor exception, column selectivity can be defined by values of $\boldsymbol{H}$, $\boldsymbol{S}^*$, etc. for both isocratic and gradient separation. The exception occurs for gradient elution when values of $\boldsymbol{H}$, $\boldsymbol{S}^*$, etc. for two columns are similar, but their phase ratios (as measured by values of k_{EB} for the reference solute ethylbenzene) are very different. In the case of isocratic separation that involves two columns of similar selectivity, but different values of k_{EB}, relative retention and separation on the two columns will be similar, but retention times on the column with a lower value of k_{EB} will all be smaller by a constant factor x. For isocratic separation, a simple change in flowrate for the replacement column (by the factor $1/x$) can be used to minimize such differences in retention.

In the case of gradient elution, a smaller value of k_{EB} will also result in reduced retention times t_R, but smaller values of t_R now mean that each band moves through the column in a lower local concentration of the B-solvent. This change in the concentration of the B-solvent during elution can itself affect separation selectivity ("solvent-strength" selectivity [46]), independent of column selectivity, so that "equivalent" separations may not be observed in this situation. However, it is possible to adjust retention time in gradient elution (and simultaneously eliminate solvent selectivity changes) by changes in flowrate so as to make retention times for the two columns more similar, exactly as for the case for isocratic separation; i.e., a slower flow rate in gradient elution (other conditions unchanged) will increase the retention of all peaks, and vice versa for a faster flow rate.

3.5. Quality control of columns during their manufacture

Values of $\boldsymbol{H}$, $\boldsymbol{S}^*$, etc. for individual columns can in principle be used to ensure batch-to-batch reproducibility. However, a simpler procedure is the measurement of values of k for five test solutes that can be used as surrogates for each of the five column-selectivity parameters (same mobile phase and temperature as in Table 6). Recommended test compounds are *N*,*N*-diethylacetamide (***A***), amitriptyline (***C***), 4-*n*-butylbenzoic acid (***B***), toluene (***H***), and *trans*-chalcone ($\boldsymbol{S}^*$). These five compounds elute in the order shown (*N*,*N*-diethylacetamide first) and are well separated on most type-B C_8 or C_{18} columns. Therefore, only a single test-run is required of the mixture of these five solutes. If values of α (equal $k/k_{toluene}$) are compared, small variations in column surface area will cancel, allowing a clearer picture of changes in column selectivity.

3.6. Peak tailing as a function of the column

There exists a large literature on the topic of peak tailing in reversed-phase HPLC, as summarized in [21–23] and references cited therein. Protonated basic compounds form by far the most common examples of peak tailing, and three different origins for such behavior have been suggested: (a) ion-exchange retention by a small number of ionized silanols, with consequent overloading of these silanols by small amounts of the solute (usually >1 μg of injected compound for a 15 cm × 0.46 cm column), (b) slow desorption kinetics for the retained solute, and (c) ionic repulsion of sorbed cationic solutes, with a rapid increase in tailing for sample sizes above 1 μg. For the retention of protonated bases on type-B alkyl-silica columns with low-pH, non-ion-pairing mobile phases, it now appears that ionic repulsion (c) is the dominant factor in causing peak tailing [23]. If true, this suggests that such peak-tailing should prove similar for different columns of this type; also, peak-tailing should be relatively minor for sample sizes of <1 μg, except for low-surface-area columns. For separations on both type-A

Table 13
Summary of values of column selectivity parameters for several RP-LC columns

Column[a]	***H***	***S****	***A***	***B***	***C***(2.8)	***C***(7.0)	k_{ref}[b]	Type[c]
Agilent								
Zorbax C18	1.089	0.055	0.474	0.060	1.489	1.566	10.7	C_{18}-A
Zorbax C8	0.974	−0.041	0.216	0.176	0.974	1.051	8.3	C_8-A
Zorbax Eclipse XDB-C18	1.077	0.024	−0.064	−0.033	0.054	0.088	9.1	C_{18}-B
Zorbax Eclipse XDB-C8	0.918	0.026	−0.221	−0.009	0.002	0.011	6.7	C_8-B
Zorbax Extend C18	1.098	0.05	0.012	−0.041	0.030	0.016	8.4	C_{18}-B
Zorbax Rx-18	1.076	0.04	0.307	−0.039	0.096	0.414	7.7	C_{18}-B
Zorbax Rx-C8	0.790	−0.073	0.113	0.015	0.011	0.947	5.1	C8-B
Zorbax StableBond 300A C18	0.906	−0.05	0.045	0.042	0.254	0.701	2.2	C_{18}-B
Zorbax StableBond 300A C3	0.526	−0.12	−0.194	0.047	0.057	0.711	0.7	C_3-B
Zorbax StableBond 300A C8	0.700	−0.083	0.000	0.045	0.146	0.820	1.3	C_8-B
Zorbax StableBond 80A C18	0.995	−0.029	0.262	−0.003	0.136	1.040	7.7	C_{18}-B
Zorbax StableBond 80A C3	0.601	−0.123	−0.081	0.038	−0.084	0.810	2.8	C_3-B
Zorbax StableBond 80A C8	0.793	−0.076	0.134	0.015	0.013	1.020	5.1	C_8-B
Bonus RP	0.737	0.074	−0.831	0.379	−2.800	−0.836	4.5	EPG
Zorbax SB-AQ	0.593	0.120	−0.083	0.038	−0.136	0.736	2.5	EPG
Zorbax SB-Phenyl	0.623	0.161	0.065	0.038	0.033	1.089	2.7	Phenyl
Zorbax XDB-Phenyl	0.665	0.127	−0.242	0.019	0.063	0.584	3.2	Phenyl
Zorbax SB-CN	0.502	0.108	−0.224	0.042	−0.146	1.047	1.7	Cyano
Zorbax Eclipse XDB-CN	0.456	0.068	−0.312	0.003	0.074	0.994	1.3	Cyano
Akzo nobel								
Kromasil 100-5C18	1.051	0.035	−0.069	−0.022	0.038	−0.057	12.5	C_{18}-B
Kromasil 100-5C4	0.732	0.003	−0.337	0.013	0.008	−0.004	5.0	C_4-B
Kromasil 100-5C8	0.864	0.012	−0.213	0.019	0.054	−0.001	7.6	C_8-B
Kromasil KR60-5CN	0.440	−0.135	−0.578	−0.014	0.216	1.036	2.0	Cyano
Alltech								
Adsorbosphere (C18)	0.986	−0.069	0.060	−0.050	1.492	1.679	7.7	C_{18}-A
Adsorpbosphere UHS C18	1.103	−0.004	0.402	−0.046	−0.125	0.877	18.2	C_{18}-A
Allsphere ODS1	0.730	−0.151	0.380	−0.006	0.847	1.143	4.7	C_{18}-A
Allsphere ODS2	1.001	−0.035	0.236	−0.034	0.959	1.279	8.0	C_{18}-A
Alphabond (C18)	0.789	0.102	0.062	−0.010	0.485	1.625	3.0	C_{18}-A
Econosil (C18)	0.963	−0.062	0.369	−0.040	1.025	1.338	8.2	C_{18}-A
Econosphere C18	0.816	−0.125	0.028	−0.024	1.045	1.521	5.1	C_{18}-A
Prosphere C18300A	0.903	−0.012	0.176	0.013	0.577	1.266	2.2	C_{18}-A
Alltima AQ	0.882	0.070	0.301	0.016	0.158	1.266	9.0	?
Alltima C18	0.993	−0.014	0.037	−0.013	0.093	0.391	11.5	C_{18}-B
Alltima C18-LL	0.778	0.070	−0.110	0.021	0.048	0.486	5.8	C_{18}-B
Alltima C18-WP	0.942	−0.058	0.072	−0.011	0.155	0.178	4.9	C_{18}-B
Alltima C8	0.756	0.015	−0.279	0.009	−0.062	0.288	5.493	C_8-B
Alltima HP C18	0.987	−0.026	0.059	0.011	0.190	0.193	4.9	C_{18}-B
Alltima HP C18 High Load	1.081	−0.050	0.080	−0.034	0.028	0.121	11.6	C_{18}-B
Alltima HP C8	0.834	−0.010	−0.116	0.035	0.122	0.153	3.2	C_8-B
Brava BDS C18	0.935	0.033	0.033	0.012	0.281	0.768	4.7	C_{18}-B
Platinum C18	0.807	−0.076	−0.104	−0.001	0.493	1.002	4.4	C_{18}-B
Platinum EPS C18	0.614	−0.162	0.330	0.018	0.720	1.730	2.6	C_{18}-B
Platinum EPS C8	0.418	−0.147	0.146	0.021	0.509	1.368	1.1	C_8-B
Prevail C18	0.890	−0.068	0.320	0.022	0.111	1.209	9.4	C_{18}-B
Prevail C8	0.618	−0.088	0.042	0.041	0.082	1.073	3.4	C_8-B
Prevail Select C18	0.822	0.028	−0.367	0.141	−1.056	0.455	7.5	C_{18}-B
Alltima HP C18 Amide	0.466	−0.072	−1.763	−0.259	−0.978	−0.033	3.1	EPG
Alltima HP C18 EPS	0.456	−0.164	−0.212	−0.056	0.032	0.832	1.2	EPG
Platinum EPS C18300	0.867	0.125	0.317	0.089	0.510	1.554	2.4	EPG
Platinum EPS C8300	0.584	0.113	−0.136	0.089	0.481	1.440	1.0	EPG
Prevail Amide	0.880	−0.069	0.287	0.025	0.087	1.238	9.6	EPG
Alltima HP C18 EPS	0.655	0.104	0.401	0.036	0.459	1.260	1.2	C_{18}-A
Alltima HP C18 Amide	0.497	0.026	0.357	0.124	−0.019	0.926	3.1	EPG
Prosphere 300 C4	0.689	0.015	−0.059	0.027	0.312	0.684	1.0	C_4-B
Prosphere 100 C18	0.883	0.073	0.305	0.017	0.181	1.517	6.4	C_{18}-B
Analytical Sales and Service								
Advantage 300	0.867	−0.001	0.123	0.020	0.597	1.110	1.7	C_{18}-B
Advantage Armor C18120A	0.962	−0.014	−0.076	−0.004	0.077	0.261	8.6	C_{18}-B
Armor C183um	0.964	−0.016	−0.079	−0.002	0.122	0.296	8.5	C_{18}-B

Table 13 (*Continued*)

Column[a]	***H***	***S****	***A***	***B***	***C***(2.8)	***C***(7.0)	k_{ref}[b]	Type[c]
Beckman								
Ultrasphere Octyl	0.896	−0.016	0.004	0.086	0.157	0.546	5.7	C_8-B
Ultrasphere ODS	1.085	0.014	0.174	0.068	0.279	0.382	8.7	C_{18}-B
Bioanalytical systems								
BAS MF-8954	0.979	−0.069	0.181	0.022	1.081	1.397	6.9	C_{18}-B
Bischoff								
Bischoff EU Reference Column	1.004	0.001	0.264	0.006	0.178	0.449	9.3	C_{18}-A
ProntoSIL 120-5 C18 SH	1.032	0.020	−0.105	−0.024	0.115	0.404	8.7	C_{18}-B
ProntoSIL 120-5 C8 SH	0.739	−0.062	−0.080	0.013	0.076	0.526	4.9	C_8-B
Prontosil 120-5-C1	0.413	−0.079	−0.084	0.020	0.042	0.656	1.2	C_1-B
ProntoSIL 120-5-C18 H	1.006	0.007	−0.104	−0.003	0.125	0.156	9.7	C_{18}-B
ProntoSIL 120-5-C18-AQ	0.975	−0.007	−0.082	0.004	0.137	0.224	8.1	C_{18}-B
Prontosil 120-3-C30	0.919	0.130	0.571	−0.003	0.507	1.788	6.9	C_{30}-B
Prontosil 200-5-C18 AQ	0.973	0.011	−0.057	0.006	0.125	0.288	6.3	C_{18}-B
ProntoSIL 200-5 C8 SH	0.761	−0.026	−0.194	0.024	0.125	0.238	2.8	C_8-B
ProntoSIL 200-5-C18 H	0.956	−0.002	−0.119	0.017	0.163	0.219	4.8	C_{18}-B
Prontosil 200-5-C30	0.909	0.099	0.347	0.007	0.305	1.171	4.4	C_{30}-B
Prontosil 200-5-C4	0.549	−0.064	−0.220	0.038	0.086	0.511	1.3	C_4-B
ProntoSIL 300-5 C8 SH	0.739	−0.042	−0.130	0.028	0.156	0.405	1.8	C_8-B
ProntoSIL 300-5-C18 H	0.957	−0.013	−0.088	0.016	0.239	0.250	3.2	C_{18}-B
Prontosil 300-5-C30	0.909	−0.030	0.152	0.021	0.352	1.002	2.9	C_{30}-B
Prontosil 300-5-C30 EC	0.925	0.047	−0.018	0.012	0.303	0.458	2.8	C_{30}-B
Prontosil 300-5-C4	0.471	-0.093	−0.073	0.055	0.115	0.786	0.6	C_4-B
ProntoSIL 60-5 C8 SH	0.929	−0.015	0.160	−0.019	−0.314	1.004	8.4	C_8-B
ProntoSIL 60-5-C18 H	1.155	0.041	0.060	−0.085	0.102	0.262	12.2	C_{18}-B
Prontosil 60-5-C4	0.686	−0.072	0.108	0.001	−0.056	1.201	4.1	C_4-B
ProntoSil CN	0.370	−0.114	−0.414	−0.028	0.168	0.668	0.9	Cyano
ProntoSIL 120-5-CN EC	0.427	0.053	−0.320	0.015	0.019	0.768	1.2	Cyano
ProntoSIL 120-5-C18 ace-EPS	0.815	0.009	−0.482	0.238	−0.246	0.099	8.3	EPG
ProntoSIL 120-5-C18 AQplus	0.964	−0.022	0.255	0.036	−0.106	0.631	9.1	EPG
Prontosil 120-5-C8 ace-EPS	0.554	−0.028	−0.808	0.226	−0.255	0.121	3.7	EPG
ProntoSIL 200-5-C18 ace-EPS	0.805	−0.009	−0.466	0.223	0.079	0.196	4.7	EPG
ProntoSIL 300-55-C18 ace-EPS	0.803	−0.005	−0.487	0.219	−0.001	0.190	2.9	EPG
ProntoSIL 120-5-Phenyl	0.557	0.163	−0.217	0.022	0.167	0.706	2.4	Phenyl
ProntoSIL 60-5-Phenyl	0.703	0.196	−0.005	−0.009	0.410	1.509	4.5	Phenyl
HyperSORB 120-5-ODS	0.951	0.065	0.039	−0.021	0.795	1.315	5.2	C_{18}-B
SpheriBOND 80-5-ODS1	0.700	0.190	0.367	0.010	1.453	>2.4	3.8	C_{18}-A
SpheriBOND 80-5-ODS2	1.010	0.026	0.153	−0.037	0.731	1.008	7.7	C_{18}-A
Dionex								
Acclaim C18	1.033	0.017	−0.142	−0.026	0.086	−0.003	10.0	C_{18}-B
Acclaim C8	0.857	0.004	−0.275	0.011	0.086	0.016	6.0	C_8-B
Acclaim300 C18	0.958	−0.018	−0.168	0.021	0.262	0.223	2.9	C_{18}-B
Acclaim PA C16	0.855	0.067	−0.116	0.023	−0.270	0.357	6.8	C16
Eprogen								
SynChropak RP8	0.638	−0.096	0.108	0.026	0.223	0.940	1.2	C_8-A
SynChropak RPP	0.746	−0.111	0.229	0.030	0.261	1.287	1.8	C_{18}-A
SynChropak RPP 100	0.921	−0.060	−0.063	0.127	0.229	0.320	5.4	C_{18}-A
ES industries								
Chromegabond WR C18	0.979	0.026	−0.159	−0.003	0.320	0.283	5.4	C_{18}-B
Chromegabond WR C8	0.855	0.025	−0.279	0.023	0.200	0.144	3.6	C_8-B
GL science								
Inertsil Ph-3	0.526	0.179	−0.133	0.040	0.121	0.735	2.6	Phenyl
Inertsil C8-3	0.830	−0.004	−0.265	−0.016	−0.333	−0.362	7.1	C_8-B
Inertsil ODS-2	0.994	0.032	−0.045	−0.005	−0.116	0.773	8.4	C_{18}-B
Inertsil ODS-3	0.991	0.021	−0.142	−0.021	−0.473	−0.333	10.9	C_{18}-B
Inertsil ODS-P	0.977	−0.021	0.608	−0.043	0.235	1.479	11.2	C_{18}-B
Inertsil WP300 C18	0.938	−0.015	−0.117	0.001	0.202	0.163	3.8	C_{18}-B
Inertsil WP300 C8	0.793	−0.015	−0.212	0.013	0.122	0.069	2.2	C_{18}-B
Inertsil CN-3	0.369	0.049	−0.808	0.083	−2.607	−1.297	1.1	Cyano
Inertsil ODS-EP	0.825	0.056	−1.590	0.054	−0.600	−0.049	7.2	EPG

Table 13 (*Continued*)

Column[a]	***H***	***S****	***A***	***B***	***C***(2.8)	***C***(7.0)	k_{ref}[b]	Type[c]
Grace/Vydac								
Vydac 201TP	0.900	−0.019	0.407	−0.006	0.395	1.027	2.1	C_{18}-A
GROM analytik								
GROM-SIL 120 ODS-5 ST	1.035	0.001	0.134	−0.005	0.135	0.121	10.5	C_{18}-B
GROM-SIL 120 Octyl-6 MB	0.872	−0.001	−0.007	0.029	−0.017	0.135	5.8	C_8-B
GROM Saphir 110 C18	1.055	0.002	0.085	0.000	−0.030	0.115	12.1	C_{18}-B
GROM-SIL 120 ODS-3 CP	1.029	−0.019	0.093	−0.005	0.099	0.123	10.2	C_{18}-B
GROM SAPHIR 110 C8	0.835	0.032	−0.103	0.031	−0.093	0.255	7.1	C_8-B
Hamilton								
HxSil C18	0.847	−0.073	0.302	0.014	0.230	1.055	7.0	C_{18}-B
HxSil C8	0.683	−0.074	0.088	0.028	0.067	0.856	4.4	C_8-B
HiChrom								
Hichrom RPB	0.964	−0.027	0.106	0.003	0.153	0.143	6.4	C_{18}-B
Hichrom 3005 RPB	0.944	−0.028	0.044	0.015	0.226	0.216	2.6	C_{18}-B
Higgens								
Targa C18	0.977	−0.019	−0.070	0.000	0.013	0.175	8.6	C_{18}-B
Imtakt								
Unison UK-C18	0.981	0.019	0.015	−0.011	0.110	0.070	8.9	C_{18}-B
Jones								
Apex C18	0.984	−0.037	0.010	0.037	1.245	2.311	6.1	C_{18}-A
Apex C8	0.869	−0.069	0.235	0.168	1.368	1.376	4.4	C_8-A
Apex II C18	1.009	−0.072	0.239	0.121	2.041	2.691	6.7	C_{18}-A
Genesis AQ 120A	0.961	−0.037	−0.155	0.008	0.061	0.234	9.6	C_{18}-B
Genesis C18120A	1.005	0.003	−0.068	−0.006	0.139	0.124	9.8	C_{18}-B
Genesis C18300A	0.975	0.004	−0.085	0.014	0.266	0.270	3.5	C_{18}-B
Genesis C4300A	0.615	−0.057	−0.398	0.036	0.143	0.249	1.1	C_4-B
Genesis C4 EC 120A	0.646	−0.059	−0.331	0.027	0.063	0.400	3.4	C_4-B
Genesis C8120A	0.829	−0.017	−0.082	0.017	0.055	0.300	6.2	C_8-B
Genesis EC C8120A	0.863	0.005	−0.174	0.022	0.063	0.141	6.9	C_8-B
Genesis CN 120A	0.424	−0.114	−0.681	−0.013	−0.001	0.573	1.4	Cyano
Genesis CN 300A	0.397	−0.108	−0.645	−0.009	0.025	0.397	0.5	Cyano
Genesis Phenyl	0.600	0.147	−0.378	0.035	0.128	0.584	2.9	Phenyl
Machery Nagel								
Nucleosil 100-5-C8 HD	0.865	−0.008	−0.173	0.029	0.045	0.188	6.3	C_8-A
Nucleosil 100-5-C18 HD	0.962	−0.021	−0.125	0.009	0.089	0.150	8.8	C_{18}-A
Nucleosil 100-5-C18 Nautilus	0.702	0.002	−0.482	0.268	−0.441	0.486	5.4	EPG
Nucleosil C8	0.574	−0.131	0.036	0.014	0.282	1.123	2.7	C_8-A
Nucleosil C18	0.906	−0.053	0.009	−0.033	0.321	0.730	7.3	C_{18}-A
Nucleosil ODS	0.860	−0.081	−0.008	0.014	0.453	0.984	2.7	C_{18}-A
Nucleodur 100-C18 Gravity	0.868	0.032	−0.240	0.000	−0.158	0.631	6.6	C_{18}-B
Nucleodur C18 Gravity	1.056	0.041	−0.097	−0.025	−0.080	0.316	11.0	C_{18}-B
EC Nucleosil 100-5 Protect 1	0.544	0.048	−0.411	0.309	-3.213	−0.573	2.7	EPG
MacMod/ACT								
ACE 300 C8	0.786	−0.003	−0.112	0.032	0.145	2.336	1.8	C_8-B
ACE C4	0.674	−0.018	−0.178	0.026	0.090	0.316	2.5	C_4-B
Ace 5 C4-300	0.710	0.014	−0.183	0.039	0.166	0.356	1.3	C_4-B
Ace5 C18	1.000	0.026	−0.095	−0.006	0.143	0.096	7.9	C_{18}-B
ACE 5 C18-300	0.968	−0.024	0.003	0.006	0.232	0.208	3.1	C_{18}-B
Ace5 C8	0.833	0.008	−0.219	0.024	0.109	0.145	4.9	C_8-B
Ace 5CN	0.409	−0.107	−0.729	−0.008	−0.086	0.441	0.8	Cyano
Ace 5 CN-300	0.460	0.074	−0.165	0.030	0.151	0.856	0.4	Cyano
ACE AQ	0.804	−0.051	−0.129	0.034	0.009	0.167	4.7	EPG
Ace Phenyl	0.638	0.145	−0.305	0.031	0.128	0.461	2.8	Phenyl
Ace Phenyl-300	0.599	0.105	−0.234	0.032	0.164	0.548	1.1	Phenyl
MacMod/Higgins								
Precision CN	0.431	−0.114	−0.485	0.019	−0.041	0.606	1.3	Cyano
PRECISION C18	1.003	0.003	−0.041	−0.009	0.079	0.341	9.5	C_{18}-B
PRECISION C8	0.821	−0.014	−0.180	0.021	0.095	0.241	4.9	C_8-B
Precision C18-PE	0.977	−0.019	−0.070	0.000	0.013	0.175	8.6	EPG
Precision Phenyl	0.587	0.142	−0.304	0.030	0.094	0.504	2.6	Phenyl

Table 13 (*Continued*)

Column[a]	***H***	***S****	***A***	***B***	***C***(2.8)	***C***(7.0)	k_{ref}[b]	Type[c]
Merck								
LiChrosorb RP-18	0.969	−0.057	0.266	−0.048	0.978	1.240	7.1	C_{18}-A
LiChrospher 100 RP-18	1.006	−0.021	0.183	−0.036	0.646	0.896	9.5	C_{18}-A
Chromolith RP18e	1.003	0.028	0.009	−0.014	0.103	0.187	3.1	C_{18}-B
LiChrospher 60 RP-Select B	0.747	−0.060	−0.042	0.006	0.108	1.773	5.1	C_{18}-B
Purospher RP-18	0.585	0.254	−0.560	−1.309	−1.934	1.109	5.7	C_{18}-B
Purospher STAR RP18e	1.003	0.013	−0.069	−0.035	0.018	0.044	10.5	C_{18}-B
Superspher 100 RP-18e	1.030	0.025	−0.028	−0.011	0.352	0.266	9.3	C_{18}-B
Nacalai Tesque								
COSMOSIL AR-II	1.017	0.011	0.128	−0.028	0.116	0.494	8.1	C_{18}-B
COSMOSIL MS-II	1.032	0.041	−0.129	−0.012	−0.117	−0.027	8.1	C_{18}-B
Cosmosil 5-C18-PAQ	0.829	−0.034	−0.342	0.054	−0.343	0.057	5.6	EPG
Nomura								
Develosil C30-UG-5	0.978	−0.038	−0.191	0.015	0.159	0.178	7.8	C_{30}-B
Develosil ODS-HG-5	0.981	0.015	−0.169	−0.007	0.187	0.221	8.1	C_{18}-B
Develosil ODS-MG-5	0.964	−0.039	−0.163	−0.002	−0.012	0.051	11.2	C_{18}-B
Develosil ODS-UG-5	0.997	0.025	−0.145	−0.003	0.150	0.155	8.4	C_{18}-B
Phenomenex								
Bondclone C18	0.825	−0.057	−0.121	0.046	0.080	0.348	4.5	C_{18}-A
Partisil C8	0.750	−0.070	−0.095	0.075	0.037	0.547	4.5	C_8-A
Partisil ODS(3)	0.809	−0.080	−0.008	0.000	0.317	0.902	5.4	C_{18}-A
Sphereclone ODS(2)	0.972	−0.040	0.271	−0.056	0.864	1.324	7.6	C_{18}-A
Jupiter300 C18	0.946	0.030	−0.222	0.009	0.235	0.219	2.9	C_{18}-B
Jupiter300 C4	0.696	0.009	−0.429	0.017	0.151	0.140	1.3	C_4-B
Jupiter300 C5	0.728	0.022	−0.384	0.014	0.128	0.330	1.5	C_5-B
Luna C18	1.018	−0.025	0.072	0.008	−0.361	−0.036	10.9	C_{18}-B
Luna C18(2)	1.003	0.023	−0.121	−0.006	−0.269	−0.173	9.6	C_{18}-B
Luna C5	0.798	0.036	−0.255	0.001	−0.278	0.114	5.9	C_5-B
Luna C8	0.875	−0.037	−0.015	0.024	−0.400	0.133	7.0	C_8-B
Luna C8(2)	0.889	0.042	−0.223	−0.003	−0.299	−0.169	7.2	C_8-B
Prodigy ODS(2)	1.022	−0.032	0.101	0.003	0.051	0.000	7.9	C_{18}-B
Prodigy ODS (3)	1.023	0.024	−0.129	−0.011	−0.195	−0.133	10.1	C_{18}-B
Selectosil C18	0.911	0.054	0.034	−0.009	0.296	0.743	7.0	C_{18}-B
Synergi Max-RP	0.989	0.028	−0.008	−0.013	−0.133	−0.034	9.5	C_{18}-B
Ultracarb ODS (30)	1.114	0.016	0.377	−0.050	−0.311	0.731	18.2	C_{18}-B
Aqua C18	0.979	0.024	0.004	0.005	0.106	0.236	9.0	C_{18}-B
Luna CN	0.452	−0.112	−0.323	−0.024	0.439	1.321	1.3	Cyano
Polaris C18-Ether	0.943	−0.013	−0.122	0.027	0.164	0.553	5.5	EPG
Polaris C8-Ether	0.705	−0.023	−0.312	0.040	0.095	0.269	1.8	EPG
Synergi Hydro-RP	1.032	−0.007	0.193	−0.046	−0.060	0.278	11.3	EPG
Synergi Polar-RP	0.644	−0.144	−0.271	−0.004	0.041	0.762	3.9	EPG
Luna Phenyl-Hexyl	0.775	0.124	−0.284	−0.001	0.001	0.383	5.2	Phenyl
Prodigy Phenyl-3	0.525	0.198	0.051	0.024	0.228	1.465	2.3	Phenyl
Curosil-PFP	0.695	0.079	−0.267	−0.004	0.119	0.379	4.0	Fluoro
Restek								
Ultra AQ C18	0.857	−0.115	0.431	0.001	0.122	1.239	8.7	C_{18}-A
Allure C18	1.115	0.043	0.112	−0.045	−0.048	0.066	15.7	C_{18}-B
Restek Ultra C18	1.055	0.030	−0.068	−0.021	0.008	−0.066	12.6	C_{18}-B
Restek Ultra C8	0.876	0.031	−0.230	0.016	0.043	0.012	7.6	C_8-B
Ultra IBD	0.657	−0.031	−0.022	0.233	−0.512	0.915	3.8	EPG
Allure PFP Propyl	0.732	−0.157	−0.179	−0.037	0.710	1.485	6.8	Fluoro
Ultra PFP	0.501	−0.089	−0.228	−0.003	−0.033	0.588	1.9	Fluoro
SepServe								
UltraSep ES AMID H RP18P	0.751	0.013	−0.101	0.259	−0.527	0.855	4.9	EPG
UltraSep ES PHARM RP18	0.953	0.061	0.435	−0.057	0.593	1.674	8.5	C_{18}-B
SGE								
Exsil C8	0.788	0.069	0.019	0.003	0.614	1.116	4.7	C_8-A
Exsil ODS	0.992	−0.036	0.292	−0.040	0.836	1.229	7.6	C_{18}-A
Wakosil 5C8RS	0.802	−0.008	−0.272	0.001	−0.117	0.097	5.6	C_{18}-B
Wakosil II 5C18AR	0.998	0.075	−0.055	−0.034	0.070	0.010	6.2	C_{18}-B
Wakosil II 5C18HG	1.039	0.036	0.015	−0.023	0.009	0.210	7.1	C_{18}-B
Wakosil II 5C18RS	0.964	−0.008	−0.160	−0.009	−0.070	0.046	9.2	C_{18}-B

Table 13 (*Continued*)

Column[a]	***H***	***S****	***A***	***B***	***C***(2.8)	***C***(7.0)	k_{ref}[b]	Type[c]
Shiseido								
CAPCELL C18 UG120	1.007	−0.036	0.037	−0.012	0.016	0.001	6.9	C_{18}-B
CAPCELL C18 AG120	1.030	−0.060	0.122	−0.065	0.543	0.628	7.2	C_{18}-B
CAPCELL C18 M G	1.005	−0.010	0.042	−0.007	0.079	0.007	10.2	C_{18}-B
CAPCELL C18 SG120	0.987	−0.031	0.093	−0.023	0.121	0.197	6.6	C_{18}-B
CAPCELL C18 A Q	0.867	0.046	−0.068	0.014	−0.093	0.402	7.0	EPG
CAPCELL C18 ACR	1.025	−0.045	0.073	−0.015	0.037	0.111	8.5	C_{18}-B
CAPCELL PAK C8 DD	0.836	−0.020	−0.154	0.015	−0.111	−0.075	5.4	C_8-B
CAPCELL PAK C8 UG120	0.854	−0.037	−0.097	−0.013	−0.046	−0.010	4.3	C_8-B
Imtakt/Silvertone Sciences								
Cadenza CD-C18	1.057	−0.031	0.083	−0.028	0.113	0.042	9.9	C_{18}-B
Supelco								
Discovery BIO Wide pore C18	0.836	0.015	−0.253	0.028	0.121	0.119	3.4	C_{18}-B
Discovery BIO Wide pore C5	0.653	−0.018	−0.308	0.027	0.090	0.219	1.1	C_5-B
Discovery BIO Wide pore C8	0.839	0.018	−0.225	0.033	0.205	0.194	2.2	C_8-B
Discovery C18	0.985	0.026	−0.126	0.005	0.176	0.154	4.8	C_{18}-B
Discovery C8	0.832	0.012	−0.237	0.029	0.119	0.143	3.3	C_8-B
Discovery CN	0.404	−0.111	−0.709	−0.009	−0.029	0.491	0.8	Cyano
Discovery Amide C16	0.758	−0.016	−0.560	0.225	−0.042	0.026	4.0	EPG
Discovery HS PEG	0.305	0.023	−0.739	0.158	−0.559	0.360	0.7	EPG
Supelcosil LC-18	1.019	−0.046	0.185	0.158	1.599	1.756	5.9	C_{18}-A
Supelcosil LC-18-DB	0.981	−0.026	0.054	0.116	0.484	0.534	5.7	C_{18}-A
Supelcosil LC-8	0.833	−0.047	−0.029	0.081	1.117	1.094	3.6	C_8-A
Supelcosil LC-8-DB	0.821	−0.037	−0.064	0.145	0.449	0.557	3.4	C_8-A
Discovery HS F5	0.631	−0.166	−0.325	0.023	0.709	0.940	4.0	Fluoro
Thermo/Hypersil								
Thermo CN	0.397	−0.110	−0.615	−0.002	−0.035	0.513	0.6	Cyano
Aquasil C18	0.795	−0.110	0.244	0.016	0.214	1.634	7.4	EPG
Hypersil 100 C18	1.033	0.013	−0.006	−0.023	0.338	0.638	8.7	C_{18}-A
Hypersil BDS C18	0.993	0.017	−0.095	−0.009	0.336	0.280	5.6	C_{18}-A
Hypersil Elite	0.958	0.031	0.151	−0.010	0.314	0.739	6.5	C_{18}-A
Hypersil ODS	0.974	−0.027	−0.124	0.017	0.912	0.973	5.5	C_{18}-A
Hypersil ODS-2	0.985	0.018	0.137	−0.012	0.254	0.370	5.6	C_{18}-A
Hypersil PAH	0.946	−0.060	0.226	−0.029	1.439	1.724	5.3	C_{18}-A
Hypersil Beta Basic-18	0.993	0.032	−0.097	0.003	0.163	0.126	6.4	C_{18}-B
Hypersil Beta Basic-8	0.834	0.016	−0.247	0.029	0.111	0.115	4.2	C_8-B
Hypersil BetamaxNeutral	1.098	0.036	0.067	−0.031	−0.039	0.011	17.0	C_{18}-B
BetaBasic CN	0.426	0.043	−0.453	0.014	0.014	0.904	0.8	cyano
BetaMax Acid	0.635	−0.057	−0.597	0.376	-2.064	−0.510	5.8	EP
BetaMax Base	0.470	0.060	−0.391	0.010	0.014	1.146	2.2	CN
Hypersil Bio Basic-18	0.975	0.025	−0.098	0.008	0.253	0.217	3.3	C_{18}-B
Hypersil Bio Basic-8	0.821	0.012	−0.233	0.028	0.230	0.210	1.8	C_8-B
Hypersil GOLD	0.881	−0.002	−0.017	0.036	0.162	0.479	3.9	C_{18}-B
Hypurity C18	0.981	0.025	−0.089	0.004	0.192	0.168	5.5	C_{18}-B
HyPurity C4	0.713	0.000	−0.291	0.028	0.121	0.252	1.9	C_4-B
Hypurity C8	0.833	0.010	−0.201	0.034	0.157	0.161	3.5	C_8-B
Hypurity Cyano	0.451	0.049	−0.492	0.021	−0.016	0.839	0.7	Cyano
Hypersil Prism C18 RP	0.692	0.066	−0.350	0.312	−2.903	−0.674	4.8	EPG
Hypersil Prism C18 RPN	0.706	−0.021	0.001	0.235	−0.508	0.661	3.4	EPG
Hypurity Advance	0.406	−0.088	−0.119	0.183	−1.309	0.922	1.6	EPG
Fluophase PFP	0.675	−0.129	−0.311	0.065	0.817	1.375	4.5	Fluoro
Fluophase RP	0.698	0.028	0.103	0.039	1.034	1.417	3.4	Fluoro
BetaBasic Phenyl	0.571	0.167	−0.422	0.054	0.099	0.753	1.7	Phenyl
Betasil Phenyl-Hexyl	0.693	0.054	−0.323	0.021	0.038	0.341	4.3	Phenyl
Varian								
OmniSpher 5 C18	1.055	0.050	−0.033	−0.029	0.121	0.057	10.8	C_{18}-B
Polaris C18-A	0.929	0.007	−0.227	0.062	0.149	0.160	5.2	EPG
Polaris C8-A	0.601	−0.008	−0.609	0.104	−0.074	0.209	2.2	EPG

Table 13 (*Continued*)

Column[a]	***H***	***S****	***A***	***B***	***C***(2.8)	***C***(7.0)	k_{ref}[b]	Type[c]
Waters								
MicroBondapak C18	0.798	−0.076	−0.030	0.016	0.285	0.854	4.6	C_{18}-A
Nova-Pak C18	1.048	0.005	0.096	−0.029	0.545	0.562	6.5	C_{18}-A
Nova-Pak C8	0.897	−0.027	−0.098	0.003	0.609	0.619	3.9	C_8-A
Resolve C18	0.961	−0.121	0.316	−0.064	1.918	2.141	7.9	C_{18}-A
Spherisorb C8	0.763	−0.090	−0.032	0.052	0.736	1.141	4.9	C_8-A
Spherisorb ODS-1	0.680	−0.180	0.318	0.010	0.844	1.299	4.6	C_{18}-A
Spherisorb ODS-2	0.962	−0.074	0.070	0.033	0.908	1.263	8.3	C_{18}-A
Spherisorb S5 ODSB	0.975	0.027	0.240	0.384	−0.642	1.680	6.9	C_{18}-A
Atlantis dC18 b	0.918	−0.032	−0.191	0.003	0.036	0.087	8.1	C_{18}-B
DeltaPak C18100A	1.028	0.018	−0.017	−0.010	−0.051	0.024	9.0	C_{18}-B
DeltaPak C18300A	0.955	−0.014	−0.103	0.016	0.236	0.287	3.0	C_{18}-B
J'Sphere H80	1.132	0.060	−0.023	−0.067	−0.242	−0.161	13.3	C_{18}-B
J'Sphere L80	0.763	−0.039	−0.214	0.000	−0.399	0.346	5.8	C_{18}-B
J'Sphere M80	0.927	−0.027	−0.121	−0.003	−0.293	0.140	9.1	C_{18}-B
Symmetry 300 C18	0.985	0.031	−0.050	0.004	0.228	0.202	3.5	C_{18}-B
Symmetry 300 C4	0.658	−0.015	−0.431	0.013	0.100	0.183	1.4	C_4-B
Symmetry C18	1.053	0.062	0.020	−0.020	−0.302	0.124	9.8	C_{18}-B
Symmetry C8	0.894	0.047	−0.204	0.020	−0.507	0.284	7.0	C_8-B
Xterra MS C18	0.985	0.012	−0.141	−0.014	0.133	0.051	6.4	C_{18}-B
Xterra MS C8	0.803	0.006	−0.294	−0.006	0.057	−0.010	3.7	C_8-B
YMC Basic	0.821	−0.006	−0.235	0.028	0.070	0.093	3.3	C_{18}-B
YMC Hydrosphere C18	0.937	−0.022	−0.129	0.006	−0.139	0.157	6.8	C_{18}-B
YMC ODS-AQ	0.965	−0.036	−0.135	0.004	−0.068	0.100	8.6	C_{18}-B
YMC Pack Pro C18 RS	1.114	0.057	−0.061	−0.056	−0.176	−0.224	12.7	C_{18}-B
YMC Pro C18	1.015	0.013	−0.117	−0.006	−0.154	−0.005	8.7	C_{18}-B
YMC Pro C8	0.890	0.014	−0.214	0.007	−0.322	0.020	6.5	C_8-B
Nova-Pak CN HP 60A	0.362	−0.165	0.100	0.000	0.691	1.175	0.4	Cyano
Symmetry Shield C18	0.877	0.007	−0.344	0.096	−0.689	0.175	7.3	EPG
Symmetry Shield C8	0.750	−0.024	−0.505	0.108	−0.592	0.169	5.7	EPG
Xterra C18 RP	0.770	−0.055	−0.430	0.106	−0.155	−0.157	4.3	EPG
Xterra C8 RP	0.660	−0.057	−0.617	0.107	−0.186	−0.197	3.1	EPG
Xterra Phenyl	0.690	0.076	−0.374	−0.003	0.102	−0.033	2.6	Phenyl
MicroBondapak Phenyl	0.580	−0.156	−0.252	0.024	0.356	0.976	2.1	Phenyl
Nova-Pak Phenyl	0.700	−0.162	−0.304	0.016	0.765	0.812	2.5	Phenyl
ZirChrom								
ZirChrom-EZ	1.110	0.100	−0.770	−0.070	2.170	2.170	1.1	Zr
ZirChrom-PBD	1.340	0.140	−0.210	−0.020	2.260	2.260	1.0	Zr
ZirChrom-PS	0.644	−0.284	−0.303	0.089	1.823	1.820	0.3	Zr

See Appendix A for details.

[a] Source or supplier shown first, then individual columns from that source follow.

[b] Value of *k* for ethylbenzene.

[c] Type of column; EPG, embedded or end-capped polar group; phenyl, phenylpropyl or phenylhexyl column; cyano, cyanopropyl column; fluoro, per-fluoro alkyl or phenyl-column; Zr, bonded zirconia column; in case of alkyl-silica columns, ligand length is indicated (C_8, C_{18}, etc.), and type-A or -B silica is also noted.

and -B alkyl-silica columns using mobile phases of near-neutral-pH, the available evidence implies a more important role for slow desorption (b) as a cause of peak tailing. Slow desorption is expected to be more pronounced with increasing silanol ionization (or a related increase in metal contamination of the silica), suggesting increased tailing for larger values of ***C*** at higher pH. In fact, such a correlation has been noted (Table 8 of [10]) for a mobile-phase pH 6.0: "low" tailing for $\boldsymbol{C}(6.0) < 0.1$, "moderate" tailing for $\boldsymbol{C}(6.0) \approx 0.5$, and "high" tailing for $\boldsymbol{C}(6.0) \approx 1.1$. The avoidance of peak tailing with higher-pH mobile phases therefore seems favored for columns with smaller values of ***C***.

4. Conclusions

The hydrophobic-subtraction model reviewed in this paper provides a comprehensive and detailed treatment of separation selectivity in reversed-phase liquid chromatography (RP-LC) as a function of the sample and column. Retention can be described quantitatively by the relationship:

$$\log \alpha \equiv \log\left(\frac{k}{k_{EB}}\right) = \underset{(i)}{\eta'\boldsymbol{H}} - \underset{(ii)}{\sigma'\boldsymbol{S}^*} + \underset{(iii)}{\beta'\boldsymbol{A}} + \underset{(iv)}{\alpha'\boldsymbol{B}} + \underset{(v)}{\kappa'\boldsymbol{C}} \quad (2)$$

Terms (i)–(v) of Eq. (2) represent contributions to retention and column selectivity from various solute–column interac-

tions (illustrated in the cartoons of Fig. 2): hydrophobicity (i), steric resistance (ii), hydrogen bonding of basic (iii) or acidic (iv) solutes to, respectively, acidic or basic column sites, and ion-interaction or ion-exchange (v). Values of η', σ', β', α' and κ' measure the contribution of the solute to retention, while the corresponding bolded parameters measure column hydrophobicity $\boldsymbol{H}$, steric resistance to penetration into the stationary phase $\boldsymbol{S}^*$, hydrogen-bond acidity $\boldsymbol{A}$ and basicity $\boldsymbol{B}$, and negative charge on the column $\boldsymbol{C}$ (or ion-exchange capacity). Values of $\boldsymbol{H}$, $\boldsymbol{S}^*$, $\boldsymbol{A}$ and $\boldsymbol{B}$ can be regarded as approximately independent of separation conditions (mobile phase composition, temperature), while $\boldsymbol{C}$ varies in a predictable way with mobile phase pH.

Eq. (2) has been tested for 150 solutes of widely different molecular structure and for several hundred RP-LC columns which include C_1–C_{30} alkyl-silica (both type-A and -B), embedded-polar group, polar-end-capped, cyano, and most other commonly used column types. For a given column type, Eq. (2) can predict values of α with an average accuracy of ±1–3% (comparisons to date with >7000 experimental measurements of α). These results indicate that all significant solute–column interactions have been accounted for, and values of the column-selectivity parameters $\boldsymbol{H}$, $\boldsymbol{S}^*$, etc. therefore provide a complete and reliable characterization of column selectivity. For retention on phenyl and fluoro-substituted columns, the application of Eq. (2) to retention data for certain solutes suggests that two additional solute–column interactions must be taken into account. In the case of phenyl columns, π–π interactions result in increased retention of π-bases such as nitro-substituted aromatic hydrocarbons. Similarly, variable dispersion interactions (not recognized by Eq. (2)) become important for both phenyl and fluoro-substituted columns, due to large differences in their polarizability (or refractive index) versus other column types. Qualitative predictions can nevertheless be made regarding the effects of the latter solute–column interactions on separation selectivity as a function of sample composition and column type.

Values of the solute (η', σ', etc.) and column ($\boldsymbol{H}$, $\boldsymbol{S}^*$, etc.) parameters appear consistent with our physico-chemical understanding of the interactions represented by each of the five terms of Eq. (1). Thus, values of η', σ', etc. can be related to solute molecular structure, and values of $\boldsymbol{H}$, $\boldsymbol{S}^*$, etc. can be rationalized with column properties such as ligand length and concentration, pore diameter, end-capping and silica acidity (type-A versus type-B). Furthermore, values of $\boldsymbol{H}$, $\boldsymbol{S}^*$, etc. for columns of different type (alkyl-silica, embedded-polar-group, cyano, phenyl, etc.) can be reconciled with the known chemical properties of these different columns. Eq. (2) therefore appears to represent physical reality, as well as providing a reliable measure of column selectivity and a better understanding of the basis of column selectivity as a function of column properties and functionality.

Values of $\boldsymbol{H}$, $\boldsymbol{S}^*$, etc. for more than 300 RP-LC columns of various kinds have now been measured (Table 13), which allows quantitative comparisons of column selectivity for these columns. Several practical applications of Eq. (2) are possible (Section 3), including the selection of columns of (a) equivalent or (b) very different selectivity. Equivalent columns may be required when a replacement column for a RP-LC procedure is no longer available, while columns of very different selectivity can be useful in method development for the separation of previously overlapping peaks. Columns of very different selectivity are also useful for the development of orthogonal separations, where pronounced changes in separation selectivity can be used to verify an absence of overlapped peaks in an original separation. Successful examples of column selection for several previously developed, routine RP-LC separations are summarized in this paper, based on Eq. (2) and values of $\boldsymbol{H}$, $\boldsymbol{S}^*$, etc.

5. Nomenclature

a	stationary phase hydrogen bond basicity (Eq. (1))
A	"type-A" column made from metal-containing silica
$\boldsymbol{A}$	relative column hydrogen-bond acidity, related to number, acidity and accessibility of silanol groups in the stationary phase (Eq. (2))
$\boldsymbol{A}_b$	average value of $\boldsymbol{A}$ for type-B alkyl-silica columns (Eq. (13))
b	stationary phase hydrogen bond acidity (Eq. (1))
B	"type-B" column made from pure silica; also, %B refers to %(v/v) of the B-solvent in the mobile phase
$\boldsymbol{B}$	relative column hydrogen-bond basicity (Eq. (2))
$\boldsymbol{B}_b$	average value of $\boldsymbol{B}$ for type-B alkyl-silica columns (Eq. (13))
$\boldsymbol{C}$	relative column cation exchange activity, related to number and accessibility of ionized silanols in stationary phase (Eq. (2))
$\boldsymbol{C}$(2.8)	value of $\boldsymbol{C}$ for pH 2.8 (Eq. (12))
$\boldsymbol{C}$(7.0)	value of $\boldsymbol{C}$ for pH 7.0 (Eq. (12))
$\boldsymbol{C}_b$	average value of $\boldsymbol{C}$ for type-B alkyl-silica columns (Eq. (13))
C_L	ligand concentration (μmoles/m^2)
d_p	pore diameter (nm)
EPG	embedded polar group
F_s	column matching function (Eq. (15))
F_s^*	value of F_s corrected for absence of acids or bases (Eq. (16))
$\boldsymbol{H}$	relative column hydrophobicity (Eq. (2))
$\boldsymbol{H}_b$	avg. value of $\boldsymbol{H}$ for type-B alkyl-silica columns (Eq. (13))
k	retention factor, equal to $(t_R - t_0)/t_0$
k_{EB}	value of k for ethylbenzene (reference solute in Eq. (2))
k_1, k_2	values of k for solutes 1 and 2, respectively
$k_{2.8}$, $k_{7.0}$	values of k for berberine at pH 2.8 and 7.0, respectively (Eq. (12))
L	molecular length; the number of atoms (excluding hydrogen) in the longest connected series that does not double back on itself

$P_{o/w}$ octanol–water partition coefficient (Eq. (6))
r stationary phase excess molar refraction (Eq. (1)); also, correlation coefficient
R_2 solute excess molar refraction (Eq. (1))
RP-LC reversed-phase liquid chromatography
s dipolarity/polarizability parameter for stationary phase (Eq. (1))
$\boldsymbol{S}$ equal to $-\boldsymbol{S}^*$; values of $\boldsymbol{S}$ were used in early papers [4,5,10,12], instead of values of $\boldsymbol{S}^*$
$\boldsymbol{S}^*$ relative steric resistance to insertion of bulky solute molecules into the stationary phase; as $\boldsymbol{S}^*$ increases, bulky solute molecules experience greater difficulty in penetrating the stationary phase and being retained (Eq. (2)); $\boldsymbol{S}$ as defined previously (and referred to as "steric interaction") is equal to $-\boldsymbol{S}^*$
$\boldsymbol{S}^*_b$ average value of $\boldsymbol{S}^*_b$ for type-B alkyl-silica columns (Eq. (13))
S.D. standard deviation
t_0 column dead time (min)
t_R retention time (min)
TEA triethylamine
V_x solute molar volume (Eq. (1))
x_B, x_C correction factors in Eq. (16)
ZrO_2 bonded-zirconia column

Greek letters
α separation factor for two solutes; also, k/k_{ref} (Eq. (2))
α' relative solute hydrogen-bond acidity (Eq. (2))
α_2^H solute hydrogen-bond acidity in solution (Eq. (1))
$\alpha_{A/P}$ ratio of k-values for benzylamine/phenol; 30% methanol/water, 40 °C
α_{CH_2} methylene selectivity; equal to ratio of k-values for successive homologs; 80% methanol/water, 40 °C
$\alpha_{C/P}$ ratio of k-values for caffeine/phenol; 30% methanol/water, 40 °C
$\alpha_{TBN/BaP}$ ratio of k-values for tetrabenzonaphthalene/benzo(a)pyrene [19]
$\alpha_{T/O}$ ratio of k-values for triphenylene/*o*-terphenyl; 80% methanol/water, 40 °C
β' relative solute hydrogen-bond basicity (Eq. (2))
β_2 solute hydrogen-bond basicity in solution (Eq. (1))
$\delta \log k$ contribution to $\log k$ other than hydrophobicity; see Fig. 3 and related text
$\delta\sigma'$ contributions to σ' other than from solute length; Eq. (8)
η' relative solute hydrophobicity (Eq. (2))
κ' effective charge on solute molecule (positive for cations, negative for anions) (Eq. (2))
κ'_1, κ'_2 values of κ' for solutes 1 and 2
π_2^H dipolarity/polarizability parameter for solute (Eq. (1))
σ' relative steric resistance of solute molecule to penetration into stationary phase (σ' is larger for more bulky molecules) (Eq. (2))
ν free energy to create a cavity in the stationary phase (Eq. (1))

Acknowledgement

It is appropriate to acknowledge the help of a number of different people and institutions, in the completion of the present 6-year study. First, 24 active participants in this project can be identified as the co-authors of eleven previous papers [4,5,10–12,30–33,72,75]. Second, almost every major column company has donated columns to this project for the measurement of values of $\boldsymbol{H}$, $\boldsymbol{S}^*$, etc.; their names are provided in Table 13. Third, a major part of the funding required for the work described in papers [4,5,10–12,30–33,72,75] was provided by Small Business Innovative Research (SBIR) grants from the National Institutes of Health. Fourth, we are much indebted to the Product Quality Research Institute and its membership for carrying out inter-laboratory comparisons of our column characterization procedure [30], for examples of its application to practical assay procedures [72], and for ongoing studies involving the selection of columns of greatly differing selectivity for use in orthogonal separations. Fifth, the coordination of early studies among different groups was supported by Nan Wilson of BASi, while Jonathan Gilroy of BASi has filled a similar critical role in later studies. Finally, we are indebted to Uwe Neue (Waters Corp.), Colin Poole (Wayne State University), Daniel Marchand and Ken Croes (University of Wisconsin, River Falls), and David McCalley (University of the West of England) for their help with the present paper.

Appendix A. Values of $\boldsymbol{H}$, $\boldsymbol{S}^*$, etc. for different columns

Table 13 summarizes values of $\boldsymbol{H}$, $\boldsymbol{S}^*$, etc. for more than 300 different RP-LC columns. All values were measured as described in [10,30] (50% acetonitrile/buffer, 35 °C), using the 16-solute test procedure with test solutes of Table 6. Table 13 includes both previously reported [10,11,31–33] and subsequent unpublished data. These values of $\boldsymbol{H}$, $\boldsymbol{S}^*$, etc. are also included in commercially-available software (Column Match; Rheodyne LLC, Rohnert Park, CA), which will include data for additional columns as they become available.

References

[1] W.R. Melander, Cs. Horváth, in: Cs. Horváth (Ed.), High-Performance Liquid Chromatography. Advances and Perspectives, vol. 2, Academic Press, New York, 1980, p. 113.
[2] P.W. Carr, D.E. Martire, L.R. Snyder, J. Chromatogr. A 656 (1993) 1.
[3] W. Melander, J. Stoveken, Cs. Horvath, J. Chromatogr. 199 (1980) 35.

[4] N.S. Wilson, M.D. Nelson, J.W. Dolan, L.R. Snyder, R.G. Wolcott, P.W. Carr, J. Chromatogr. A 961 (2002) 171.
[5] N.S. Wilson, J.W. Dolan, L.R. Snyder, P.W. Carr, L.C. Sander, J. Chromatogr. A 961 (2002) 217.
[6] K. Kimata, K. Iwaguchi, S. Onishi, K. Jinno, R. Eksteen, K. Hosoya, M. Araki, N. Tanaka, J. Chromatogr. Sci. 27 (1989) 721.
[7] L.C. Sander, S.A. Wise, J. Chromatogr. A 656 (1993) 335.
[8] C.F. Poole, S.K. Poole, J. Chromatogr. A 965 (2002) 263.
[9] E. Cruz, M.R. Euerby, C.M. Johnson, C.A. Hackett, Chromatographia 44 (1997) 151.
[10] J. Gilroy, J.W. Dolan, L.R. Snyder, J. Chromatogr. A 1000 (2003) 757.
[11] J.J. Gilroy, J.W. Dolan, P.W. Carr, L.R. Snyder, J. Chromatogr. A 1026 (2004) 77.
[12] N.S. Wilson, M.D. Nelson, J.W. Dolan, L.R. Snyder, P.W. Carr, J. Chromatogr. A 961 (2002) 195.
[13] L.C. Tan, P.W. Carr, M.H. Abraham, J. Chromatogr. A 752 (1996) 1.
[14] W.J. Lambert, J. Chromatogr. A 656 (1993) 469.
[15] J.G. Dorsey, M.G. Khaledi, J. Chromatogr. A 656 (1993) 485.
[16] W.W. Yau, J.J. Kirkland, D.D. Bly, Modern Size-Exclusion Chromatography, Wiley-Interscience, New York, 1979. Chapter 2.
[17] M.F. Vitha, P.W. Carr, J. Phys. Chem. 104 (2000) 5343.
[18] J.P. Larmann, J.J. DeStefano, A.P. Goldberg, R.W. Stout, L.R. Snyder, M.A. Stadalius, J. Chromatogr. 255 (1983) 163.
[19] Certificate of Analysis, SRM 869a, Column Selectivity Test Mixture for Liquid Chromatography (Polycyclic Aromatic Hydrocarbons), National Institute of Standards and Technology, Gaithersburg, MD, 1998.
[20] L.C. Tan, P.W. Carr, J.M.J. Frechet, V. Smigol, Anal. Chem. 66 (1994) 450.
[21] J. Nawrocki, J. Chromatogr. A 779 (1997) 29.
[22] M.A. Stadalius, J.S. Berus, L.R. Snyder, LC-GC 6 (1988) 494.
[23] S.M.C. Buckenmaier, D.V. McCalley, M.R. Euerby, Anal. Chem. 74 (2002) 4672.
[24] Y. Sudo, J. Chromatogr. A 813 (1998) 239.
[25] J.J. Kirkland, J.L. Glajch, R.D. Farlee, Anal. Chem. 61 (1988) 2.
[26] M.S. Cypryk, J. Organometall. Chem. 483 (1997) 545.
[27] A. Mendez, E. Bosch, M. Roses, U.D. Neue, J. Chromatogr. A 986 (2003) 33.
[28] U.D. Neue, C.H. Phoebe, K. Tran, Y.-F. Cheng, Z. Lu, J. Chromatogr. A 925 (2001) 49.
[29] F. Gritti, G. Guiochon, J. Chromatogr. A 1041 (2004) 63.
[30] L.R. Snyder, A. Maule, A. Heebsch, R. Cuellar, S. Paulson, J. Carrano, L. Wrisley, C.C. Chan, N. Pearson, J.W. Dolan, J.J. Gilroy, J. Chromatogr. A 1057 (2004) 49.
[31] N.S. Wilson, J. Gilroy, J.W. Dolan, L.R. Snyder, J. Chromatogr. A 1026 (2004) 91.
[32] D.H. Marchand, K. Croes, J.W. Dolan, L.R. Snyder, J. Chromatogr. A (2004) doi:10.1016/j.chroma.2004.11.015.
[33] D.H. Marchand, K. Croes, J.W. Dolan, L.R. Snyder, R.A. Henry, K.M. R. Kallury, S. Waite, P.W. Carr, J. Chromatogr. A 2004 doi:10.1016/j.chroma.2004.11.014.
[34] U.D. Neue, E. Serowik, P. Iraneta, B.A. Alden, T.H. Walter, J. Chromatogr. A 849 (1999) 87.
[35] U.D. Neue, Y.-F. Cheng, Z. Lu, B.A. Alden, P.C. Iraneta, C.H. Phoebe, K. Van Tran, Chromatographia 54 (2001) 169.
[36] B. Buszewski, R. Gadzala-Kopciuch, R. Kaliszan, Anal. Chem. 69 (1997) 3277.
[37] J.E. O'Gara, B.A. Alden, T.H. Walter, J.S. Petersen, C.L. Niederlander, U.D. Neue, Anal. Chem. 67 (1995) 3809.
[38] J.J. Kirkland, J.W. Henderson, J.D. Martosella, B.A. Bidlingmeyer, J. Vasta-Russell, J.B. Adams Jr., LCGC North Am. 17 (1999) 634.
[39] A. Sandi, L. Szepesy, J. Chromatogr. A 818 (1998) 1.
[40] U.D. Neue, B.A. Alden, T.H. Walter, J. Chromatogr. A 849 (1999) 101.
[41] P.E. Antle, L.R. Snyder, LC Mag. 2 (1984) 840.
[42] P.E. Antle, A.P. Goldberg, L.R. Snyder, J. Chromatogr. 321 (1985) 1.
[43] J.L. Glajch, J.C. Gluckman, J.G. Charikofsky, J.J. Minor, Kirkland, J. Chromatogr. 318 (1985) 23.
[44] W.T. Cooper, L.-Y. Lin, Chromatographia 21 (1986) 335.
[45] M.C. Pietrogrande, F. Dondi, G. Blo, P.A. Borea, C. Bighi, J. Liq. Chromatogr. 10 (1987) 1065.
[46] L.R. Snyder, J.J. Kirkland, J.L. Glajch, Practical HPLC Method Development, second ed., Wiley-Interscience, New York, 1997.
[47] N. Tanaka, Y. Tokuda, K. Iwaguchi, M. Araki, J. Chromatogr. 239 (1982) 761.
[48] T. Hanai, J. Hubert, J. Chromatogr. 291 (1984) 81.
[49] J.L. Glajch, J.C. Gluckman, J.G. Charikofsky, J.M. Minor, J.J. Kirkland, J. Chromatogr. 318 (1985) 23.
[50] G. Thevenon-Emeric, A. Tchapla, M. Martin, J. Chromatogr. 550 (1991) 267.
[51] J. Leon, E. Reubsaet, R. Vieskar, J. Chromatogr. A 841 (1999) 147.
[52] G.E. Berendsen, K.A. Pikaart, L. De Galan, C. Olieman, Anal. Chem. 52 (1980) 1990.
[53] H.A.H. Billiet, P.J. Schoenmakers, L. De Galan, J. Chromatogr. 218 (1981) 443.
[54] A. Haas, J. Kohler, H. Hemetsberger, Chromatographia 14 (1981) 341.
[55] P.C. Sadek, P.W. Carr, J. Chromatogr. 288 (1984) 25.
[56] P.C. Sadek, P.W. Carr, M.J. Rugio, Anal. Chem. 59 (1987).
[57] M.R. Euerby, A.P. McKeown, P. Petersson, J. Sep. Sci. 26 (2003) 295.
[58] J. Nawrocki, M.P. Rigney, A. McCormick, P.W. Carr, J. Chromatrogr. A 657 (1993) 229.
[59] M.R. Buchmeiser, J. Chromatrogr. A 918 (2001) 233.
[60] J.H. Park, Y.K. Ryu, J.H. Lim, H.S. Lee, J.K. Park, Y.K. Lee, M.D.D. Jang, J.K. Suh, P.W. Carr, Chromatographia 49 (1999) 635.
[61] A. Bolk, A.K. Smilde, in: R.M. Smith (Ed.), Retention and Selectivity in Liquid Chromatography, Elsevier, Amsterdam, 1995, p. 403.
[62] B.A. Olsen, G.R. Sullivan, J. Chromatogr. A 692 (1995) 147.
[63] L.A. Lopez, S.C. Rutan, J. Chromatogr. A 965 (2002) 301.
[64] M.R. Euerby, P. Pettersson, LC-GC Eur. 13 (2000) 665.
[65] H.A. Claessens, Trends Anal. Chem. 20 (2001) 563.
[66] D. Visky, Y. Vander Heyden, T. Ivanyi, P. Baten, J. De Beer, Z. Kovacs, B. Noszai, E. Roets, D.L. Massart, J. Hoogmartens, J. Chromatogr. A 977 (2002) 39.
[67] E. Van Gyseghem, M. Jimidar, R. Sneyers, D. Redlich, E. Verhoeven, D.L. Massart, Y. Vander Heyden, J. Chromatogr. A 1042 (2004) 69.
[68] M.R. Euerby, P. Petersson, J. Chromatogr. A 994 (2003) 13.
[69] J.C. Fetzer, The Chemistry and Analysis of the Large Polycyclic Aromatic Hydrocarbons, John Wiley and Sons, New York, 2000.
[70] C.M. Bell, L.C. Sander, J.C. Fetzer, S.A. Wise, J. Chromatogr. A 753 (1996) 37.
[71] J.C. Fetzer, Separation of Fullerenes by Liquid Chromatography, Royal Society of Chemistry, Cambridge, UK, 1999, p. 25.
[72] J.W. Dolan, A. Maule, L. Wrisley, C.C. Chan, M. Angod, C. Lunte, R. Krisco, L.R. Snyder, J. Chromatogr. A, submitted.
[73] J.W. Dolan, L.R. Snyder, N.M. Djordjevic, D.W. Hill, D.L. Saunders, L. Van Heukelem, T.J. Waeghe, J. Chromatogr. A 803 (1998) 1.
[74] J.W. Dolan, L.R. Snyder, N.M. Djordjevic, D.W. Hill, L. Van Heukelem, T.J. Waeghe, J. Chromatogr. A 857 (1999) 1.
[75] C.F. Poole, The Essence of Chromatography, Elsevier, Amsterdam, 2003.
[76] H. Cortes (Ed.), Multidimensional Chromatography: Techniques and Applications, Marcel Dekkerm, New York, 1990.
[77] D.H. Marchand, L.A. Williams, J.W. Dolan, L.R. Snyder, J. Chromatogr. A 1015 (2003) 53.